CRANFIELD UNIVERSITY

MARIA ROYO BONO

INTEGRATION OF GAS TURBINE PERFORMANCE MODEL WITH DIESEL ENGINE PERFORMANCE MODEL FOR MARINE APPLICATION

SCHOOL OF AEROSPACE TRANSPORT AND MANUFACTURING
Thermal Power

MSc
Academic Year: 2016 - 2017

Supervisor: Suresh Sampath
August 2017

CRANFIELD UNIVERSITY

SCHOOL OF AEROSPACE TRANSPORT AND MANUFACTURING
Thermal Power

MSc

Academic Year 2016 - 2017

MARIA ROYO BONO

INTEGRATION OF GAS TURBINE PERFORMANCE MODEL WITH DIESEL ENGINE PERFORMANCE MODEL FOR MARINE APPLICATION

Supervisor: Suresh Sampath
August 2017

This thesis is submitted in partial fulfilment of the requirements for the degree of Thermal Power
(NB. This section can be removed if the award of the degree is based solely on examination of the thesis)

© Cranfield University 2017. All rights reserved. No part of this publication may be reproduced without the written permission of the copyright owner.

ABSTRACT

The design of a marine propulsion system for naval application is challenging, since the high-performance requirements to accomplish a certain mission, usually do not agree with an efficient operation. For this reason, the development of alternative propulsion systems, such as the combination of different prime movers emerged. One of the most efficient arrangement is the CODAG configuration, which combines the use of diesel engines and gas turbines. In this way, the operating profile of a particular vessel can be optimised for high performance and low consumption.

This project involves the development of a CODAG propulsion system model in order to optimise the operating profile of a specific vessel. The required power for a particular scenario has been obtained using a Matlab code. It integrates the performance of two high speed diesel engines and an aero-derivative gas turbine based on the GE-LM2500. A matching methodology has been generated to couple the prime movers and the vessels propulsive device. In addition, Turbomatch simulations have been executed to understand the influence of ambient temperature on the gas turbine performance and therefore, on the performance of the CODAG propulsion system. In the same way, the degradation of the gas turbine has been analysed.

As a result, it has been built a tool that integrates the above-mentioned features capable of assessing the vessel's fuel consumption for a given operating profile. The developed tool exhibits a great potential to optimise the performance of vessels with a CODAG propulsion system. Depending on the vessel requirements, the optimization could be among a wide range of possibilities. Also, different CODAG configurations, such as adding another gas turbine, or removing one diesel engines can be analysed.

Keywords:

CODAG, Diesel engine, Gas turbine, Fuel consumption, Integration, Engines-propeller matching

ACKNOWLEDGEMENTS

My family for the psychological support throughout this intense year. Their encouragement gave me the strength to overcome all the difficulties that I have faced during my entire life.

My family in Cranfield for all the shared moments, this year would not have been the same without having known all of you.

My supervisor, Doctor Suresh Sampath, and his colleague, Amit Batra, for giving me the opportunity and help to develop my research project.

TABLE OF CONTENTS

ABSTRACT i
ACKNOWLEDGEMENTS ii
LIST OF FIGURES v
LIST OF TABLES viii
LIST OF EQUATIONS ix
NOMENCLATURE xi
1 INTRODUCTION 1
1.1 Aim and objectives 2
1.2 Thesis structure 2
2 LITERATURE REVIEW 4
2.1 Marine propulsion plants evolution through history 4
2.2 Marine propulsion system selection 6
2.2.1 Marine propulsion system main components 6
2.2.2 Marine propulsion system classification depending on the prime mover type 8
2.2.3 Factors that influence on the propulsion plant selection 9
2.3 Combined power plants 10
2.3.1 COSAG: Combined steam turbine and gas turbine 11
2.3.2 COGAS: Combined gas turbine and steam turbine 12
2.3.3 CODAD: Combined diesel engine and diesel engine 13
2.3.4 CODOG: Combined diesel engine or gas turbine 13
2.3.5 CODAG: Combined diesel engine and gas turbine 14
2.3.6 COGOG: Combined gas turbine or gas turbine 16
2.3.7 CODLAG: Combined electric-diesel engine and gas turbine 16
2.3.8 Combined propulsion plant comparison 17
2.4 CODAG propulsion system prime movers 20
2.4.1 Diesel engine 20
2.4.2 Gas turbine 21
2.4.3 Prime movers comparison: diesel engine and gas turbine 24
2.5 Marine gas turbine degradation 26
2.5.1 Recoverable and non-recoverable degradation 27
2.5.2 Degradation mechanisms 27
3 METHODOLOGY 30
3.1 CODAG propulsion plant configuration 30
3.1.1 Diesel engine 30
3.1.2 Gas turbine 31
3.2 Marine vessel power prediction model 32
3.2.1 Marine vessel selection 34
3.2.2 Hull resistance module 35
3.2.3 Wake, thrust deduction and relative rotative efficiency 40

3.2.4 Screw propeller module 42
3.2.5 Shaft losses 46
3.2.6 Gearbox losses 46
3.3 Turbomatch gas turbine model 48
4 ENGINES-PROPELLER MATCHING 51
4.1 Diesel engine-propeller matching 52
4.2 Gas turbine-propeller matching 54
5 OVERALL MARINE POWER PLANT PERFORMANCE 59
5.1 Theoretical background 60
5.2 Ambient temperature effect 63
5.2.1 Ambient temperature effect on the marine propulsion plant 70
5.3 Gas engine degradation effect 73
5.3.1 Components degradation 74
5.3.2 Overall degradation effect 80
5.3.3 Degradation effect on the marine propulsion plant 84
5.4 Ambient temperature and engine degradation combined effect on the marine propulsion plant 87
5.5 Simulation of a vessel's operating profile 91
6 CONCLUSIONS AND RECOMENDATIONS 92
6.1 Recommendations 95
REFERENCES 96
APPENDICES 99

LIST OF FIGURES

Figure 2-1. Chronological line of marine propulsion systems evolution 6

Figure 2-2. COSAG components distribution 12

Figure 2-3. COGAS components distribution 13

Figure 2-4. CODAD components distribution 13

Figure 2-5. CODOG components distribution 14

Figure 2-6. CODAG components distribution 15

Figure 2-7. COGOG components distribution 16

Figure 2-8. CODLAG components distribution 17

Figure 2-9. Propulsion systems comparison investment [1] 18

Figure 2-10. Components diagram of a simple cycle and an intercooled recuperated cycle 22

Figure 2-11. Comparison of the specific fuel consumption curves against the load for different gas turbines cycles [3] 23

Figure 3-1. Power layout along propulsion system 32

Figure 3-2. Block diagram of power engine prediction model 34

Figure 3-3. Effective power as a function of the vessel's speed 40

Figure 3-4. Procedure followed to obtain the thrust that the propeller delivers at a certain propeller's rotational speed 45

Figure 3-5. Propeller thrust coefficient, torque coefficient and open water efficiency 46

Figure 3-6. Comparison between the effective power and the power that the diesel engines must generate 47

Figure 3-7. Comparison between the effective power and the power that the gas turbine must generate 48

Figure 3-8. Marine gas turbine engine scheme 49

Figure 4-1. Propeller Law 51

Figure 4-2. Basic concept of engine-propeller matching 52

Figure 4-3. Performance map of diesel engine 53

Figure 4-4. Diesel engine-propeller matching curves 54

Figure 4-5. Iterative process followed to obtain the free power turbine's work for different turbine rotational speeds. 57

Figure 4-6. Free turbine performance when fuel flow and rotational speed variate 58

Figure 5-1. Influence of ambient temperature on diesel and gas turbine engines [24] 59

Figure 5-2. Operating point displacement on compressor's map due to an increase of the output work..... 62

Figure 5-3. Inlet mass flow variation as a function of the ambient temperature for a constant power output 64

Figure 5-4. Fuel flow and compressor rotational speed as a function of ambient temperature for a constant power output..... 65

Figure 5-5. Operating point displacement on compressor's map due to an increase of the ambient temperature 66

Figure 5-6. Compressor pressure ratio as a function of the ambient temperature for a constant power output 66

Figure 5-7. Thermal efficiency and specific fuel consumption as a function of the ambient temperature for a constant power output 67

Figure 5-8. Turbine entry temperature as a function of ambient temperature for a constant power output 68

Figure 5-9. Maximum power supplied by the gas engine over propeller's law for different ambient temperatures..... 72

Figure 5-10. Degradation of the gas engine's performance due to fouling 75

Figure 5-11. Degradation of the compressor efficiency and compressor and turbine temperatures 76

Figure 5-12. Degradation of the power output, thermal efficiency and specific fuel consumption due to compressor fouling 77

Figure 5-13. Variation of different engine parameters due to turbine erosion... 78

Figure 5-14. Degradation of the power output, thermal efficiency and specific fuel consumption due to turbine erosion..... 79

Figure 5-15. Engine parameters evolution as a function of the degradation for a constant power output of 25 MW 81

Figure 5-16. Thermal efficiency and specific fuel consumption evolution as a function of the degradation for a constant power output of 25 MW..... 82

Figure 5-17. Maximum power supplied by the gas engine over propeller's law for different levels of degradation..... 86

Figure 5-18. Thermal efficiency as a function of the ambient temperature and the engine’s degradation for the whole gas turbine speed range 89

Figure 5-19. Specific fuel consumption as a function of the ambient temperature and the engine's degradation for the whole gas turbine speed range 90

Figure 5-20. Typical warship operating profile and fuel consumption distribution 91

LIST OF TABLES

Table 2-1. Combined propulsion plants acronyms 11

Table 2-2. Comparison CODAG/CODLAG 6000-ton ship [1] 19

Table 2-3. CODAG prime movers density power [4] [5] [6] [7] 25

Table 2-4. Comparison between diesel and gas turbine engines 26

Table 2-5. Classification of diverse ways of performance deterioration [8] 27

Table 3-1. Diesel engine characteristics [3] 31

Table 3-2. Gas turbine characteristics [10] [11] 31

Table 3-3. Watercraft parameters used in the developed model [14] 35

Table 3-4. C_{stern} parameter value for different hull shapes [22] 41

Table 3-5. Types of propeller 43

Table 3-6. Propeller design parameters 43

Table 3-7. Gas turbine parameters used in the simulations 50

Table 5-1. Performance parameter results for different power outputs when the ambient temperature increases 69

Table 5-2. Engine's maximum performance as ambient temperature rises 71

Table 5-3. Fuel savings due to the use of different operational modes as ambient temperature increases 73

Table 5-4. Engine performance for different degradation levels when the demanded power output is 10 MW 83

Table 5-5. Engine performance for different degradation levels when the demanded power output is 15 MW 83

Table 5-6. Engine performance for different degradation levels when the demanded power output is 25 MW 84

Table 5-7. Engine's maximum performance as degradation progresses 85

Table 5-8. Fuel savings due to the use of different operational modes as degradation progresses 87

Table 5-9. Typical warship operating profile 92

LIST OF EQUATIONS

(3-1)..... 32
(3-2)..... 33
(3-3)..... 33
(3-4)..... 36
(3-5)..... 37
(3-6)..... 37
(3-7)..... 37
(3-8)..... 37
(3-9)..... 37
(3-10)..... 37
(3-11)..... 37
(3-12)..... 37
(3-13)..... 38
(3-14)..... 38
(3-15)..... 38
(3-16)..... 38
(3-17)..... 38
(3-18)..... 38
(3-19)..... 38
(3-20)..... 38
(3-21)..... 39
(3-22)..... 39
(3-23)..... 39
(3-24)..... 40
(3-25)..... 40
(3-26)..... 40
(3-27)..... 40
(3-28)..... 41

(3-29)..... 41
(3-30)..... 42
(3-31)..... 42
(3-32)..... 43
(3-33)..... 43
(3-34)..... 44
(3-35)..... 44
(3-36)..... 44
(3-37)..... 44
(3-38)..... 44
(3-39)..... 44
(3-40)..... 44
(3-41)..... 45
(3-42)..... 46
(4-1)..... 55
(4-2)..... 55
(4-3)..... 56
(4-4)..... 56
(4-5)..... 56
(4-6)..... 56
(5-1)..... 60
(5-2)..... 61
(5-3)..... 63
(5-4)..... 63
(5-5)..... 75
(5-6)..... 79

NOMENCLATURE

A_E/A_O	Blade area ratio
A_T	Projected front area of the above watercraft
B	Breadth
C_A	Correlation allowance resistance coefficient
C_{AA}	Air resistance coefficient
C_{APP}	Appendage resistance coefficient
C_B	Block coefficient
C_F	Friction coefficient
CO_2	Carbon dioxide
CODAD	Combined Diesel engine and Diesel engine
CODAG	Combined Diesel and Gas turbine
CODLAG	Combined electric-diesel engine and gas turbine
CODOG	Combine Diesel or Gas turbine
COGAS	Combined Gas and Steam turbine
COGOG	Combined Gas turbine or Gas turbine
COSAG	Combined Steam and Gas turbine
C_P	Prismatic coefficient
c_p	Specific heat capacity
C_R	Residual resistance coefficient
C_V	Viscous resistance coefficient
D_P	Screw diameter
FCV	Fuel calorific value
F_n	Froude number
ISA	International standard atmosphere
J	Advance ratio
k	Shape factor
K_T	Thrust coefficient
K_Q	Torque coefficient
L	Length between perpendiculars
LBC	Longitudinal centre of buoyancy
LCC	Life cycle costing

L_{fn}	Reference length for Froud number calculation
L_{OS}	Length over surface
L_{WL}	Length water line
$\dot{m}$	Mass flow
N_{Boss}	Number of bossings
N_{Brac}	Number of brackets
NO_x	Nitrogen oxides
N_{Rud}	Number of rudders
N_s	Propeller rotational speed
N_{Thr}	Number of side thrusters
P	Pitch angle
P_{in}	Inlet pressure
P_E	Effective power
P_D	Delivered power
P_{out}	Outlet pressure
P_{PM}	Prime mover power
PR	Pressure ratio
P_T	Thrust power
R	Resistance, Ideal gas constant
R_A	Correlation allowance resistance
R_{AA}	Air resistance
R_{APP}	Appendage resistance
R_F	Friction resistance
R_n	Reynolds number
R_R	Residual resistance
rpm	Revolutions per minute
R_{TS}	Total ship resistance
S	Wetted surface
SFC	Specific fuel consumption
t	Thrust deduction fraction
T	Thrust, draft
T_A	Aft draft
t/c	Thickness to chord length ratio

TET	Turbine entry temperature
T_F	Fore draft
T_{in}	Inlet temperature
T_{out}	Outlet temperature
V	Ship velocity
V_a	Average speed of flow into the propeller
Z	Number of blades
γ	Adiabatic index

η_c	Compressor isentropic efficiency
η_{GB}	Gearbox efficiency
η_{hull}	Hull efficiency
η_o	Open water efficiency
η_R	Relative rotative efficiency
η_S	Shaft transmission efficiency
η_t	Turbine isentropic efficiency
η_{th}	Thermal efficiency
ρ	Sea water density
ω_T	Taylor wake fraction

1 INTRODUCTION

More than a century has passed since Rudolf Diesel invented the thermodynamic cycle that carries his name. Since then, the diesel engine has been successfully integrated into diverse fields, becoming the most popular prime mover in the marine propulsion industry. Different diesel engine configurations have been used in all types of watercrafts, from simple boats and yachts to huge cargo and commercial vessels, even in warships. The basic configuration consists of a diesel engine coupled to a propulsion shaft, by means of a series of reduction gears, which in turn drives the propeller that thrusts the vessel. The number and types of diesel engines installed in a watercraft may vary depending on the power demand and the required speed. Other common configuration, especially used for high speed passenger ferries consists of a waterjet driven by a diesel engine. Regarding the naval application, during the last decades, innovative configurations based on the combination of diesel engines and other types of prime movers such as steam and gas turbines have been arising. The purpose of these power plants is to take advantage of the benefits that different type of propulsion systems present. For instance, the CODAG propulsion system is a combination of diesel and gas turbine engines, which depending on the velocity requirement employs one or the other prime mover. Usually, for low speeds, the diesel engines drive the propeller by means of reduction mechanisms and when higher speeds are demanded, the gas turbines are the ones in charge of propelling the vessel. Besides, if an additional power is demanded both engines are used in conjunction. It is well known that the diesel engine success comes from its low specific fuel consumption, although it is a voluminous and heavy machine. Whereas the gas turbine is characterised by high power densities in exchange of high specific fuel consumption. Therefore, the total contribution can be summarised in high installed power, space savings and optimised fuel consumption. Which, for naval purposes represents more space for ammunitions, more efficient cruise operations at part loads and very high speeds when it is required. Examples of this particular propulsion system are installed in the F124 (German Navy), MILGEM Corvette (Turkish Navy) or the NSC Deepwater (US Coast Guard) [1].

1.1 Aim and objectives

The purpose of this project is to study the performance of a propulsion system that integrates a diesel engine and a gas turbine for marine application. In order to achieve the aim of this thesis the following objectives have been proposed:

- Description of a methodology for preliminary CODAG propulsion system design
- Development of a Matlab code capable of predicting required power for considered operating modes according to the defined methodology
- The development of a matching methodology between the propeller and each the diesel engine and the gas turbine engine
- The estimation of the required power by the prime movers in order to assess the performance of the whole propulsion system.
- study of ambient temperature and engine degradation effects on the performance of the gas turbine and the integrated marine propulsion plant
- The assessment of a vessel's fuel consumption operating profile by means of the built tool.

As a result, it has been built a tool capable of assessing the vessel's fuel consumption for a given operating profile. The developed tool exhibits a great potential to optimise the performance of vessels with a CODAG propulsion system. Depending on the vessel requirements, the optimization could be among a wide range of possibilities.

1.2 Thesis structure

The structure of this thesis is organised into six chapters and the main content of each section is summarised below.

Chapter 1: introduces the topic by giving a brief explanation about CODAG propulsion systems application, followed by the aims and the potential contribution of the work develop on this thesis.

Chapter 2: provides a revision of the current state of the art of the combined propulsion plants for marine application, states the main factors that influence on

the propulsion system selection focusing on the CODAG power plants. In addition to a theoretical section concerning marine gas turbine engines degradation.

Chapter 3: presents the methodology followed to build the model of a CODAG propulsion system, as well as, the gas turbine model set for Turbomatch simulations in order to study the degradation of the engine.

Chapter 4: details the integration of the two prime movers with the propeller, to do so a brief theoretical introduction is given followed by the procedures used to match both engines with the propeller.

Chapter 5: displays the results obtained from the temperature and degradation studies and provides a discussion about the influence of these two parameters on the propulsion plant performance. Moreover, it is shown the potential of the developed tool by means of an example of a vessel's operating profile.

Chapter 6: summarises the conclusions obtained throughout the thesis and provides suggestions for future work.

2 LITERATURE REVIEW

The marine propulsion consists in the displacement of a watercraft from one point to another, over a water surface in opposition to the forces that act against this movement. Mainly, these resisting forces are, the water friction caused by the submerged hull and the air friction caused by the afloat structure.

Moreover, vessel's displacement should heed to certain facets such as craft's speed, manoeuvrability, autonomy, hull's and propeller's designs, as well as, propulsion plant operation safety. Naval designers must accomplish the requisites demanded by the craft for the least resistance possible in a safe and economical way. In addition, the watercraft must be capable of operating in diverse geographical areas and under different weather conditions.

These factors are usually opposed ones with the others. On the one hand, if a fast craft is required, the range and autonomy are essential. Whereas, when maximising the autonomy is the priority, other concerns as fuel consumption, storage, operation and installation cost must be taken into consideration. In any case the designed propulsion system must be safe, flexible and easy to operate. The most challenging aspect is to achieve the right balance between the technical aspects and operational capabilities required for a specific mission. This principle has defined naval propulsion systems evolution through the history.

2.1 Marine propulsion plants evolution through history

Naval propulsion development commenced with simple row systems, which consisted of manually operated oars. Soon after, this system was enhanced by aligning several oars in a row, in this way it was possible to increase the power, speed and dimensions of the watercraft. Later on, in order to leverage the wind power, sails were installed as an additional propulsion system.

During the ancient period, oars and sails were utilized combined or independently by Egyptians, Phoenicians, Romans and Vikings until the evolution of the riggings, the new navigation tools and the need of higher watercraft autonomy terminated with galleys and rowing boats. Both propulsion systems were

dependent on sea conditions, wind or tides, uncontrollable factors, which limited their use to certain geographical areas and weather conditions.

At earliest of the XIX century, sailing technology had reached its maturity, huge vessels equipped with triangular sails which enhanced the sailing technique increasing the speed and manoeuvrability. Around this period the steam engine became popular and the interest in introducing it in the naval sphere started growing. However, it is not until 1824, when Sadi Carnot presented the thermodynamics' second law, that consolidated the steam cycle, and made possible the development of the steam propulsion power plants.

In 1894, Charles Parson introduced a more efficient machine than the steam engine, the steam turbine. Such an invention was installed for the first time in the *Turbinia*, a torpedo boat capable to reach 30 knots. After such a success, sailing boats finally gave place to steam vessels propelled by screw propellers.

In the same period, Rudolf Diesel, developed the thermodynamic cycle of an engine based on the internal combustion inside a cylinder, using a petroleum derivative as fuel. And eventually, the Diesel engine became a harsh competitor among the existing prime movers, limiting steam power plants to certain applications.

The World War II was an agent of progress on diverse technological fields, new advances were blossomed such as radar, sonar, nuclear fission and fusion or reaction engines. Regarding the naval sector, high powerful nuclear power plants were developed. However, the installations costs and the technological difficulties associated to nuclear propulsion, in addition to the new naval strategic concepts that caused a change in the trend of the warships power systems. A new concept was born from the evolution of gas turbines and modern Diesel engines for marine application, known as, combined propulsion plants, which are characterised by taking advantage of the different propulsion systems such as, steam turbines, Diesel engines, gas turbines and electric-Diesel engines, becoming a very efficient propulsion system.

Below Figure 2-1 summarises the chronological evolution of the marine propulsion systems for war application along with relevant events that mark a milestone in the naval context.

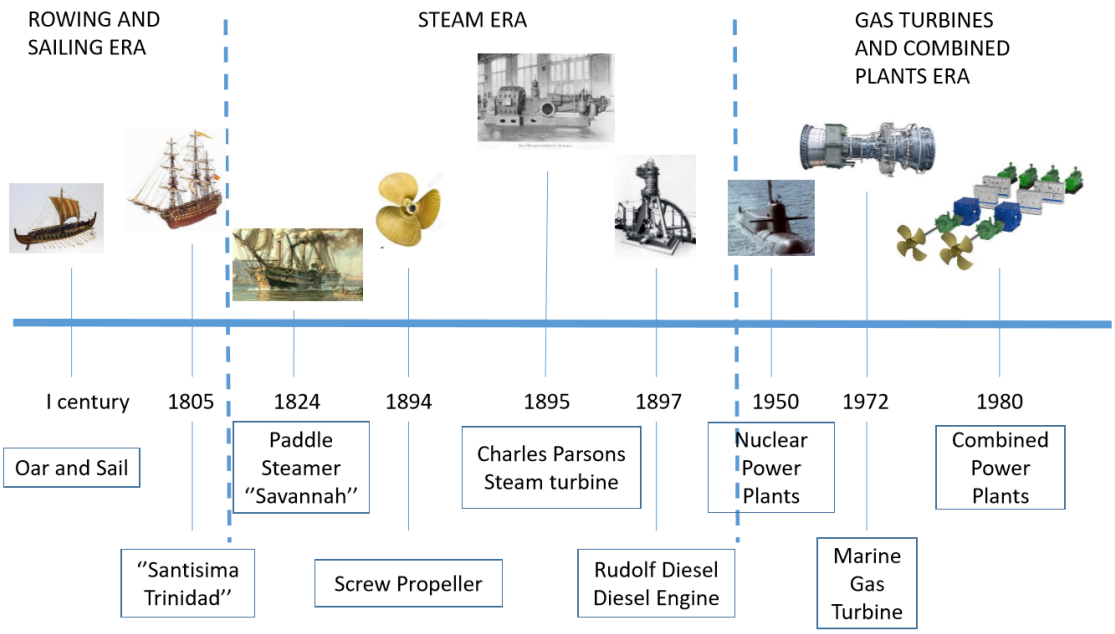

Figure 2-1. Chronological line of marine propulsion systems evolution

2.2 Marine propulsion system selection

With the purpose of providing a judgement capacity about the selection of the suitable propulsion system for a determined vessel, in this section is given a general knowledge about the main factors that influence in the choice. The discussed subjects are the main components of a propulsion system, the type of prime movers and the elements that finally determine the appropriate power system.

2.2.1 Marine propulsion system main components

Every marine propulsion system is designed to transform different energy forms into mechanical work utilized for the vessel's propulsion; for instance, steam power plants convert chemical energy, obtained from the burned fuel in the boilers, into calorific energy, which turns water into steam. This steam is sent through pipes to the turbine, where it is transformed into mechanical energy. This mechanical energy moves the shaft transmitting the movement to the screw

propeller, which in turn, converts this movement into thrust and eventually the displacement of the vessel is produced.

To manage efficiently the energy during the transformation process from the storage source to the production of the required thrust, it is needed a whole system, composed by different subsystems, whose functions are specific and complementary among them. In a warship, this whole system is named power plant and its main subsystems are the followings:

Engine

Component in charge of transforming the chemical energy into mechanical energy to drive the propeller. The most common engines are gas turbine, steam turbine, Diesel engine, electric engines or a combination of themselves (combined plants).

Gearbox, clutches

Their main objective is to reduce the engine revolutions in concordance with the suitable propeller's rotational speed. Additionally, they couple and decouple the engine to the shaft, and in some ocassions they invert the spinning direction of the engine in order to change the vessel's course.

Transmission shafts

Their mission is to communicate the gearbox and clutches with the propeller lengthwise the vessel. Shafts are borne by bearings that absorb all kind of vibrations besides axial and radial loads.

Propeller

Its principal function is to convert the mechanical energy, delivered as torque, into effective thrust. The most common type is the screw propeller, which generates thrust accelerating a water column in the opposite direction to the ship's advance. The two kinds of screw propellers are fix pitch propeller or controllable pitch propeller.

Additionally, there are other auxiliary subsystems necessary to make the complete system work. For instance, the energy management system that supplies the electricity for the on board consume and the control of the propulsion plant.

2.2.2 Marine propulsion system classification depending on the prime mover type

Relying upon the type of engine used as prime mover to drive the propeller, the marine propulsion systems can be classified according to the following typology.

Steam turbines power plants

The steam is generated by boilers and introduced in a turbine which produces mechanical energy to drive the propeller. The number of boilers, turbines and shafts depends on the power plant configuration and the vessel's application.

Gas turbines power plants

In this kind of propulsion plant, all forms of energy transformation occur inside the gas turbine; where a mix of fuel and air is burned obtaining a great volume of exhaust gases that finally move a power turbine. The power turbine generates mechanical work used to drive the shaft. Typically, these engines are used in the combined power plants.

Diesel engine power plants

These power plants are characterised because the energy conversion befalls inside the diesel engine. At the same time, there different types of diesel engine depending on many aspects, such as the power, size, piston velocity or the cylinders distribution among others.

Combined power plants

These power plants integrate diverse prime movers in different configurations. Mainly, the prime movers are gas turbines, diesel engines and lately diesel-electric combined engines. The purpose of this combination is to reach higher performance impossible to achieve when the engines are operating alone.

Unconventional power plants

In this group are included all the power plants whose operating principle or technological development has not been globally spread.

2.2.3 Factors that influence on the propulsion plant selection

The propulsion plant selection depends on the vessel's mission requirements. These requirements mark the technical and operational factors that define the suitable propulsion system for a particular watercraft.

- Among the technical factors, the followings can be highlighted.

Specific fuel consumption

It represents thermal machine ability to convert a certain amount of fuel into mechanical work. This parameter is provided in the nominal specifications of the engine and shows the energetic efficiency of the propulsion plant. The specific fuel consumption defines in some way the ship's autonomy.

Fuel type

It indicates the flexibility of the propulsion power plant in using more than one type of fuel. This feature is related with the storage ease and the on-board fuel management, as well as, the operation cost.

Installation cost

It is referred to the cost that implies the installation of a propulsion power plant to generate one power unit, considering as well, the related auxiliary subsystems.

Power limitations

Depending on the prime mover type, the number of engines and the configuration, the maximum power output may variate. In order to make use of the propulsion plant possibilities it is essential to know the maximum power that the prime mover is capable to supply.

- Regarding the operational factors, the followings can be highlighted.

Speed

Directly related with the power delivered by the propulsion power plant by an exponential function. Vessel's speed must be studied according to the mission specifications, considering that fuel consumption and the cost of the propulsion power plant increase with the rise of the maximum speed.

Autonomy

It exhibits the ships capacity to execute prolonged missions far from the operational base. Regarding to the design and the type of power plant, the vessel's autonomy depends on the specific fuel consumption and its storage capacity.

Power to weight ratio

Represents the weight and the volume that the propulsive installation requires to generate a power unit. This factor is extremely important for small and medium crafts, since the better propulsion plant's power to weight ratio, the greater the autonomy and the room available for carrying extra payload.

2.3 Combined power plants

As previously mentioned, there are diverse types of prime movers capable to deliver the demanded power used to overcome the resistance to motion at a certain speed. Each of them presents different advantages, but at the same time, some drawbacks associated with the efficiency, operability and maintenance of the propulsion power plant.

The combination of different types of engines in a single plant, arranged in such a way that they can operate simultaneously or sequentially, is denominated combined power plants or hybrid power plants.

This kind of power plants represent an ingenious solution to enhance the benefits of each prime mover and at the same time lessen its disadvantages, obtaining an efficiency improvement for the whole velocity range, power and fuel consumption. During cruise, efficient engines are employed economising fuel consumption, and

when high speeds are required, powerful engines are used. Thus, this power plants offer a great versatility and flexibility that reduce the cost of vessel's operation widening its performance.

Combined propulsion plants are essentially destined for warship application, since these vessels operate at maximum power only during the 5% of its entire life [2]. Therefore, it is a waste to utilise a propulsion plant design to delivered great amounts of power, when most of the craft's life, it operates at medium and low velocities and the system's efficiency is not optimised for that operation. Nevertheless, the final selection of a combined power plant depends on the operational requirements of the vessel.

Hybrid power plants are named by acronyms which indicate the utilised propulsion systems and if these systems operate simultaneously or sequentially. The most common acronyms are the presented in Table 2-1.

Table 2-1. Combined propulsion plants acronyms

CO	**Co**mbined
D	**D**iesel engine
A/O	**A**nd / **O**r
G	**G**as turbine
S	**S**team turbine

2.3.1 COSAG: Combined steam turbine and gas turbine

This propulsion system consists of a combination of steam and gas turbines, which deliver power to the shaft connected to the propeller. It is required the installation of reduction mechanisms, gearboxes and clutches in order to control if the turbines must operate individually or simultaneously. The propulsion plant scheme is represented in Figure 2-2.

The main advantages that the steam turbine presents are the reliability and the high efficiency during cruise operation. Meanwhile the gas turbine provides a fast acceleration, an instantaneous starter and a good power to weight ratio. The first generation of vessels propelled by gas turbines used a COSAG configuration.

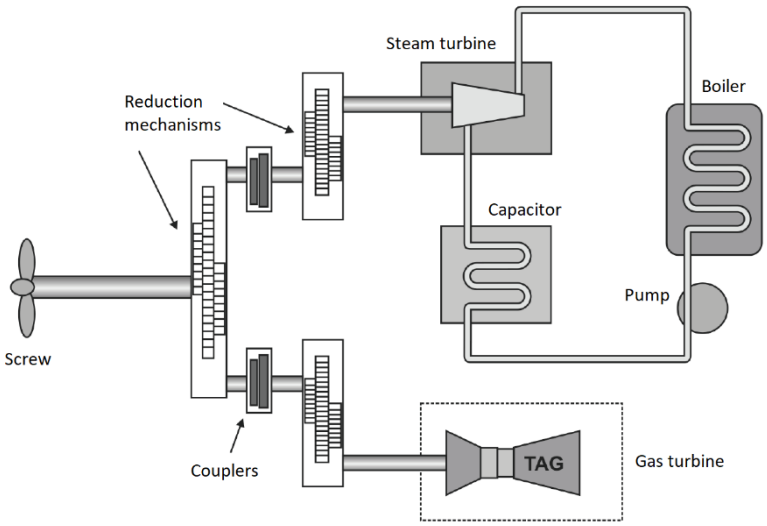

Figure 2-2. COSAG components distribution

2.3.2 COGAS: Combined gas turbine and steam turbine

As in the previous configuration, steam and gas turbines are employed. In this case, it is used a combined cycle, in which, the exhaust gases from the gas turbine feed the steam turbine by means of a heat exchanger. In this way, the energy extracted from the exhaust gases is not wasted, the specific fuel consumption decreases and the efficiency of the whole system increases. Currently, this system is not used anymore in marine propulsion power plants, but in the industrial power generation.

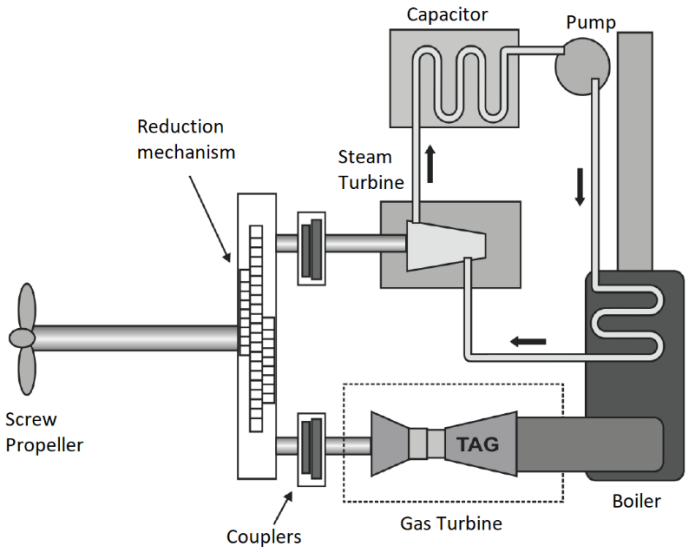

Figure 2-3. COGAS components distribution

2.3.3 CODAD: Combined diesel engine and diesel engine

This system combines more than one Diesel engine. Depending on the craft's speed demand, the power requirement will be different, and one or more engines will be coupled through a series of clutches and transmission mechanisms to the shaft that drives the propeller. The main benefit is that for lower speeds the use of small engines reduces the fuel consumption.

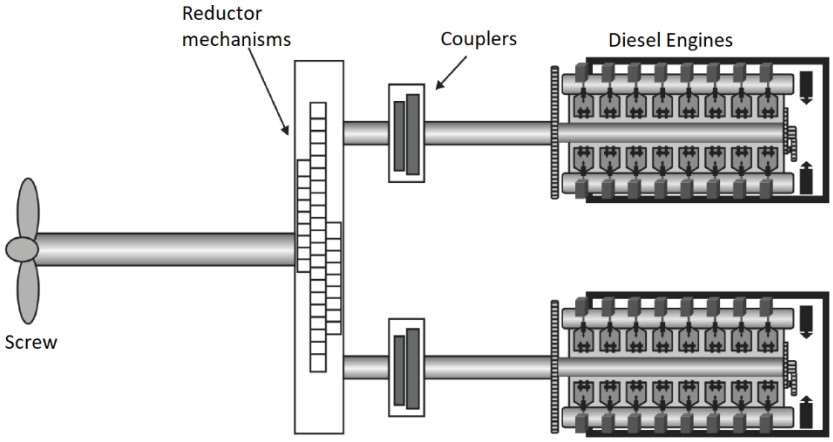

Figure 2-4. CODAD components distribution

2.3.4 CODOG: Combined diesel engine or gas turbine

This configuration presents two diesel engines and two gas turbines mechanically coupled to two independent shafts. In other words, one diesel and one turbine

per shaft. In this case both type of engines cannot operate simultaneously; during cruise diesel engines drive the propellers, and when higher power is required diesel engines are disconnected and the gas turbines generate the thrust.

Compared to other combined plants the transmission system is simpler, however, more powerful turbines are needed for the same power. Generally, this power plants are installed in vessels that require more superior top speed than cruise speed, such as frigates, destroyers or corvettes.

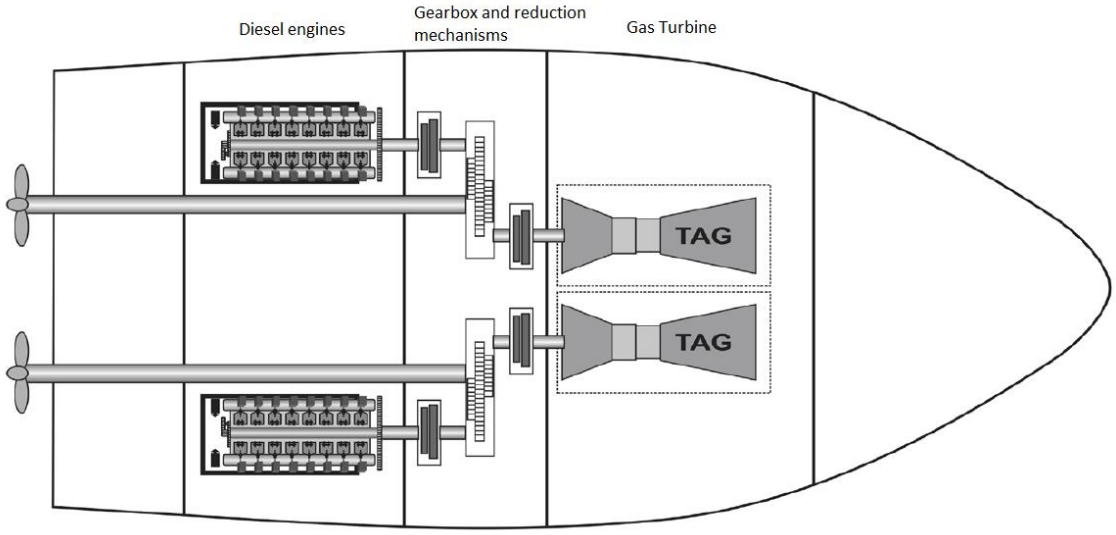

Figure 2-5. CODOG components distribution

2.3.5 CODAG: Combined diesel engine and gas turbine

This configuration combines diesel engines and gas turbines. In this case both engines can operate simultaneously; during cruise, diesel engines drive the propellers, and when higher power is required it is possible to increment the power by adding the gas turbine contribution.

The power difference between the mode in which the diesel engine is driving the propeller and the mode in which diesel and gas turbine engines drive together the propeller, is so large that multi speed gearboxes are required to not interrupt diesel engine's operation. Therefore, more complex transmission systems are employed compared to CODOG configuration.

CODAG configuration presents a satisfactory power to weight ratio and takes less room than an equivalent power system using only diesel engines. This is due to the fact that smaller diesel engines are employed and the compactness of gas turbine and its corresponding transmissions.

These plants take advantage of the high efficiencies that the diesel engines supply during low speed and cruise until velocities of 20 knots roughly; gaining autonomy and reducing the operational cost compared with the solely use of gas turbines. Nevertheless, the transmission mechanisms are heavier and more complex.

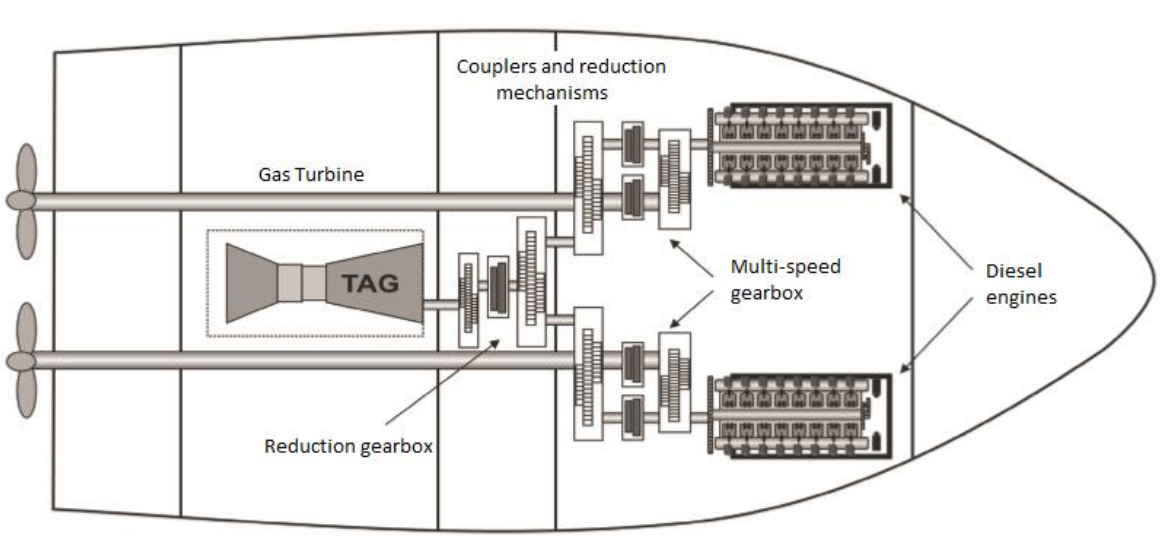

Figure 2-6. CODAG components distribution

There are some CODAG variations in which diesel engines and gas turbines have independent shafts to avoid complex transmission mechanisms. However, more propellers are needed, this reduces the efficiency of the thrust device causing turbulence and side forces.

A particular variation known as CODAG WARP, CODAG water jet and refined propeller, is a power plant composed by a CODAG system with and hydro-jet and a screw as propellers. The Diesel engines drive the screw propellers in a CODAD configuration and the hydro-jet is propelled by the gas turbine. In this way, while the gas turbine is not operating there is no turbulence generation and screw's efficiency does not fall.

2.3.6 COGOG: Combined gas turbine or gas turbine

In this propulsion system, energy generation is obtained just by means of gas turbines. There is a low power gas turbine efficient for cruise speeds, and a high power turbine with acceptable efficiency for high speeds. This system includes a series of couplers and clutches that allow the selection of one turbine but not both simultaneously.

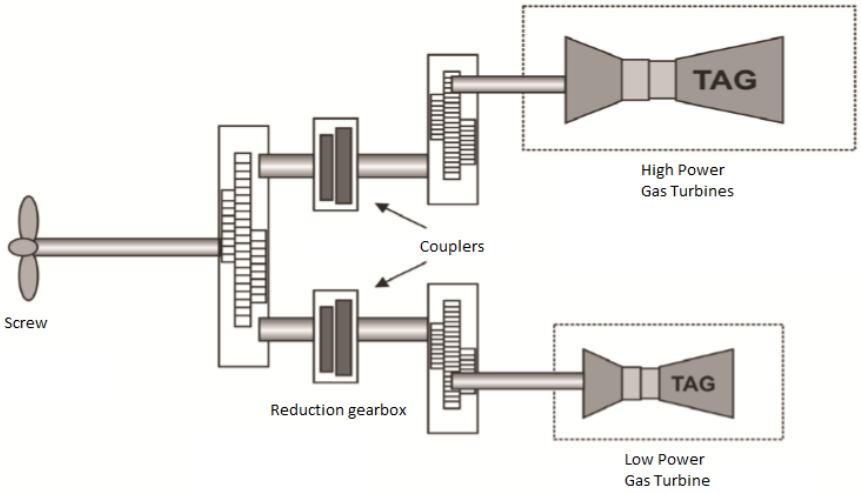

Figure 2-7. COGOG components distribution

The main COGOG's interest is the usage of compact systems such as gas turbines. Moreover, it is a simple design, that does not require complex transmission mechanisms and preserves and excellent power to weight ratio, in exchange of higher fuel consumption.

2.3.7 CODLAG: Combined electric-diesel engine and gas turbine

CODLAG systems are the state of art of warship combined power plants. Basically, two electric engines fed by diesel generators are connected to two shafts. These engines supply enough power for port manoeuvres and low speeds; when higher speed is required a gas turbine is used and thus, power is increased. One advantage regarding the others combined power plants is the reduced operational cost, due to the reduction in the number of diesel engines. The same engines that propel the craft are used to generate the energy supply.

In addition, electric engines are efficient for a wider range of velocities and can be connected directly to the shafts, without the need of using reduction mechanisms. On the other hand, maintenance inspections are less frequent and simpler than with the other type of power plants. Other advantage of the electric-diesel system is that the electric engines can be placed at the aft of the craft, reducing the length of the propulsion shaft. Currently CODLAG systems are mostly installed in submarines, though some floating watercrafts such as anti-submarine vessels.

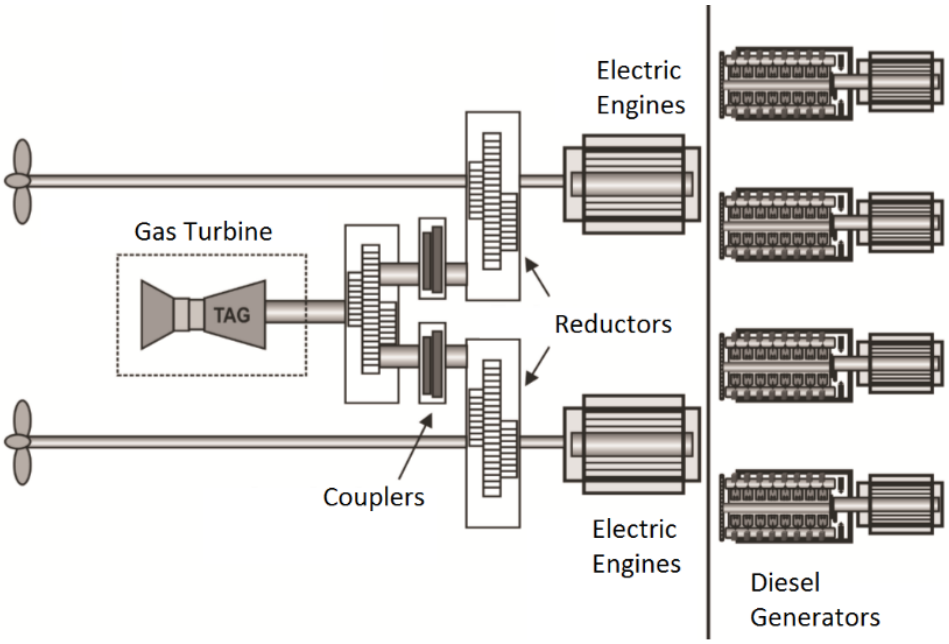

Figure 2-8. CODLAG components distribution

2.3.8 Combined propulsion plant comparison

From the reasons mentioned previously, it can be stated that the combined propulsion systems are the most suitable power plants for modern naval vessels. Due to the naval application, the selection criteria of the type of propulsion plant depends mostly on the ship speed requirements, the shock capability, the noise reduction or the infrared signature. Other relevant aspects are the change in the operation requirements, the ability of reaching a greater speed range, the mission flexibility, the fact of being longer periods away from the base with smaller crews and, the production of cleaner emissions.

Below it is done a comparison between different combined propulsion plants supported by current information extracted from the Application Center Governmental Naval.

Regarding diesel engine combined plants, an economic study about the investment cost and life cycle costing shows the expenses that each propulsion system means. The compared power plants are: two diesel engines driven directly the propellers, a CODOE, a CODOD and a CODAD power plants. The CODOE configuration is a hybrid combination between a diesel engine and an electric system composed by a generator, a frequency converter and an electrical motor. Whereas the CODOD configuration is a combination of two different diesel engines, one of them used during cruise and the other, more powerful, for high speed demand.

Figure 2-9 presents a comparison of the costs of the four propulsion plants. The column in blue represents the investment cost that includes the cost of the engines, gearboxes, shafts, propellers, gensets, electrical motors and frequency converters. And the column in orange represents the life cycle costing, which includes the fuel consumption and the lubricating oil. The results have been calculated assuming that every engine operates 2000 hours per year.

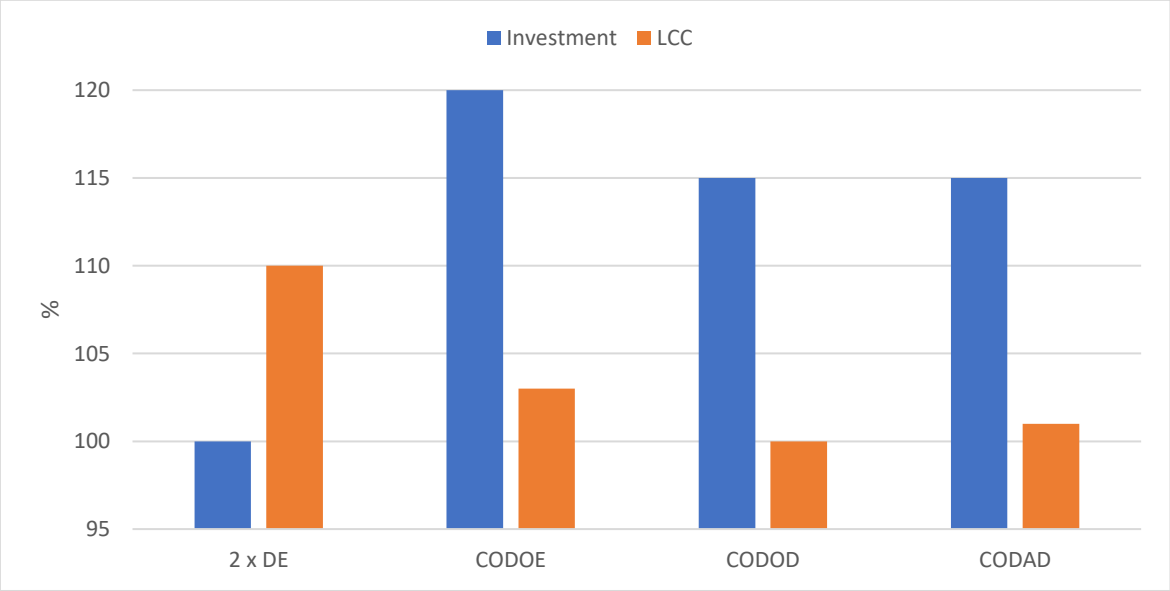

Figure 2-9. Propulsion systems comparison investment [1]

Another study compares the volume and the weight of the components belonging to two 6000-ton ships with different propulsion plants: CODAG and CODLAG. From the values of the Table 2-2, it can be seen how the CODLAG system requires more and heavier components than the CODAG system. For example, the diesel engines of the CODAG configuration are lighter and occupy less volume than the electrical motors, that are their equivalents, in the CODLAG configuration. Moreover, the gas turbine required in the CODLAG system weights more than the one of the CODAG system, the reason for this is that the electrical propulsion systems need more power to achieve same ship speed compared to mechanical systems.

Table 2-2. Comparison CODAG/CODLAG 6000-ton ship [1]

	Volume (m^3)		Weight (tons)	
	CODAG	CODLAG	CODAG	CODLAG
Main Switch-Board 6,6 kV	0	240	0	18
Xfrm & Converter 6,6 kV	0	675	0	52
Gearbox	630	630	160	173
Shaft + Propeller	-	-	165	175
Main Diesel Engines	378	0	122	0
Electrical Motors	0	540	0	140
Gas Turbines	300	300	37	43
Generator Sets	648	1200	96	225
Summary	1956	3585	580	826

As it can be appreciated even if the CODLAG propulsion systems guarantee higher operational efficiencies and better fuel consumptions, the weight and the volume required is quite higher than for a CODAG configuration. If both vessels present the same weight, and the CODAG configuration is lighter, this means that more space will be available for carrying additional payload. And thus, depending on the vessel's priorities it will be more convenient to operate at higher efficiencies or to carry extra payload.

2.4 CODAG propulsion system prime movers

One of the thesis aims is to study the performance of integrating a diesel engine with a gas turbine for marine application, for this reason a CODAG propulsion system has been selected and below a detailed explanation about their prime movers is given.

2.4.1 Diesel engine

The diesel engine is the most common prime mover for marine application. The key of its success has been the wide power range that it covers, from few kilowatts to 100 megawatts, and the very low fuel consumptions compared to the other engines. As its name suggests, this engine operates using the diesel cycle, which ignites the combustion by compressing a fuel-air mixture. This combustion befalls intermittently inside a cylinder.

According to the rotational speed, diesel engines can be classified in: slow, medium and fast engines.

Generally, slow engines are huge 2-stroke engines that present a maximum rotational speed of 180 rpm. Besides the very low fuel consumption, the reduce rotational speed allows to directly couple the engine to the shaft, that drives the propeller, enhancing the propulsive efficiency. On the other hand, medium and fast diesels, are 4-stroke engines, which rotational speeds variate from 300 to 800 rpm and from 1000 to 2000 rpm, respectively. Therefore, reduction mechanisms and gears are required, in order to match the engine with the propeller.

The power output produced by the diesel engine is proportional to the rotational speed, this fact leads to the problem of matching the engine and the propeller. As time passes, the resistance will increase due to fouling and for the same reason more thrust will be required. Therefore, to maintain the same speed the load on the engine will increase. This requires during the design process the selection of an appropriate gear ratio between the prime mover and the propeller, so that later, the engine will not become overloaded.

Compared to the other technologies, the diesel engines are directly reversible and a lot more efficient when they operate at partial load. In addition, the employed fuel ensures a high storage security which is essential for naval application.

Nevertheless, the intermittent movement of these engines generates vibrations and low frequency noise that is widely propagable and easily detectable by passive sonars. In order to avoid it, the engines are installed in capsules with antivibration bearings and noise isolating systems, becoming a heavier system. As a matter of fact, diesel engines present a low power to weight ratio with regard to the gas engines. Moreover, as a great number of the engine components are submitted to all this vibration, frequent inspections are necessary, increasing the operational and maintenance cost.

2.4.2 Gas turbine

The gas engines are one the latest type of prime movers integrated in the naval propulsion. Initially, these gas turbines were uniquely employed in the propulsion of aircrafts, and that is the reason for the current marine gas turbines to come from an aero-gas turbine that has been adapted for the marine application. Basically, the difference between the turbojets and marine turbines relies on the way of exploiting the energy stored in the exhaust gases. Meanwhile the turbojet produces thrust by means of a nozzle, ejecting a jet flow that propels the aircraft due to the action-reaction principle; the marine turbine presents a power turbine, instead of a nozzle. This turbine is only linked aerodynamically with the gas generator. Thus, the free power turbine is assembled in an independent shaft that is connected through a series of reduction mechanisms to the propulsion shaft that drives the screw propeller.

Marine gas turbines are internal continuous combustion engines that operate on the Brayton cycle. Over the years, noteworthy progress has been made in increasing the thermal efficiency. As a matter of fact, since the first generation of marine gas turbines in the sixties, thermal efficiency has risen from 25% at the rated power to efficiencies over 40%. In addition, the simple cycle has been modified leading to different configurations in order to enhance the engines part

load operation and optimise the fuel consumption by improving even more the thermal efficiency. For instance, the part load performance can be enhanced by using an intercooled recuperated cycle, which injects the exhausted gases at the inlet of the combustor, in order to heat the fresh air and reduce the fuel consumption. This technique was introduced by Rolls-Royce in the gas turbine model WR-21, reaching a 42% in the thermal efficiency across the 80% of the operating range [3]. Figure 2-10 shows the components diagram of a simple cycle and an intercooled recuperated cycle.

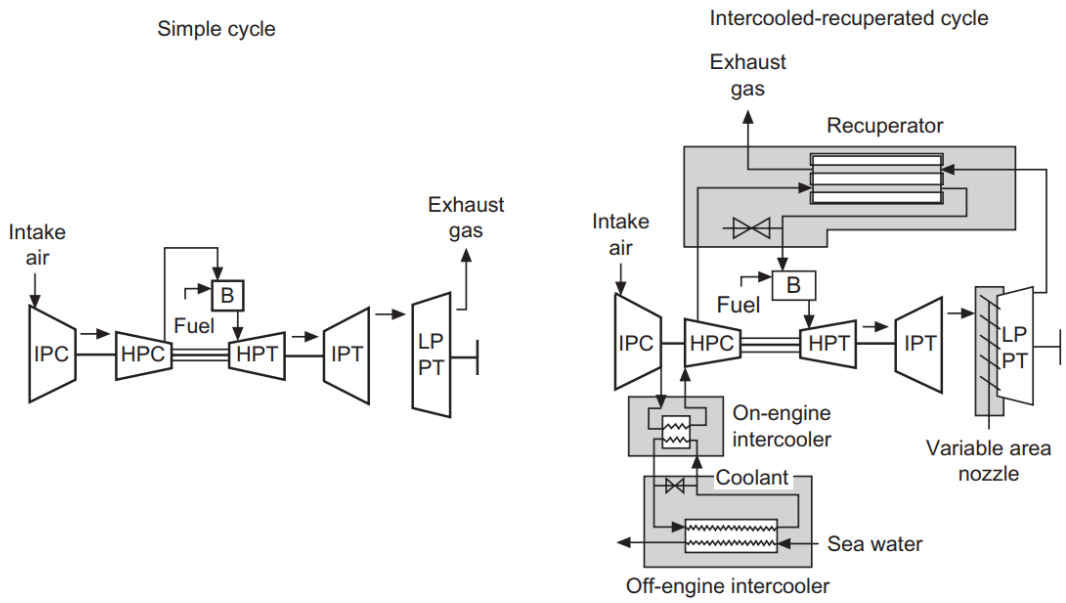

Figure 2-10. Components diagram of a simple cycle and an intercooled recuperated cycle

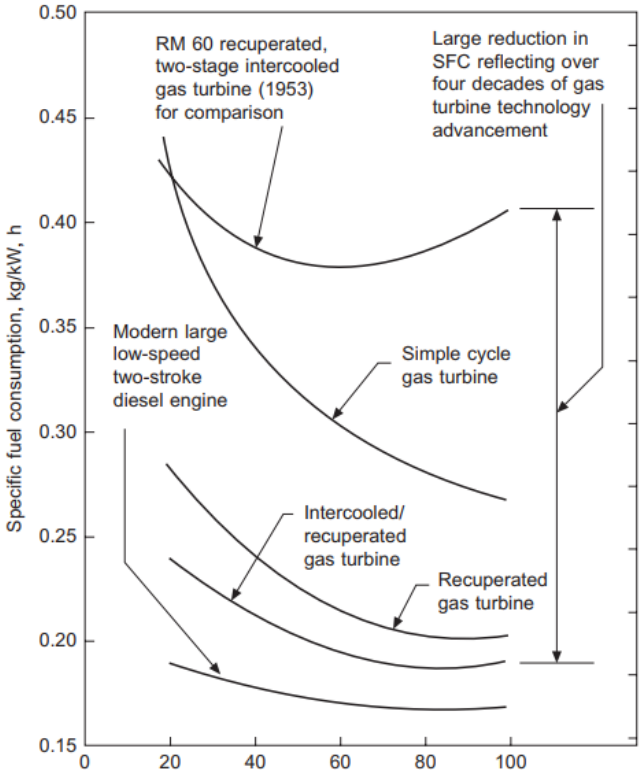

Figure 2-11. Comparison of the specific fuel consumption curves against the load for different gas turbines cycles [3]

Figure 2-11 shows a comparison of the specific fuel consumption curves against the load for different gas turbines cycles, besides the curve of a modern large low speed two-stroke diesel engine.

Among the different cycle configurations, the combined cycle option produces the highest efficiencies and power outputs, as a result of presenting the lower pressure ratio above the other configurations, including the simple cycle. This configuration consists of a gas engine combined with a bottoming steam cycle.

Its main disadvantage is the demanded space and the weight increase due to the heat recovery steam generator, which makes this configuration inappropriate for marine application. According to Mitsubishi Heavy Industries studies, the intercooled recuperated cycle is the best option for marine application, since it presents the highest thermal efficiencies after the combined cycle and the flattest specific fuel consumption curve (Figure 2-11). Nevertheless, the cost and the size

of the employed recuperator must be reduced to make this system appropriated for marine propulsion.

Compared to the other prime movers, marine gas turbines present the best power to weight ratio in exchange of higher specific fuel consumptions above all at part load operation. The simple design and the absence of different components moving intermittently, reduce the lubrication oil consumption and the balance problems, enhancing the operation reliability. At the same time, lower noise and vibration levels are produced which is beneficial from a strategic point of view. Both reasons increase the length between maintenance inspections reducing the operating cost of the engine, although the investment cost is quite higher compared to other prime movers.

Another great advantage is the fast response of the engine, providing higher speeds and reducing the time of manoeuvring for large vessels. Moreover, gas engines are capable to operate at full load without a long warming up period, and the engine starter requires few minutes instead of hours.

2.4.3 Prime movers comparison: diesel engine and gas turbine

Once the main characteristics of the two prime movers integrated in a CODAG propulsion system have been analysed, a brief comparison is given in order to summarise the benefits of this combined power plants for marine application.

The main advantage of gas turbines engines is the high power density, in order to illustrate it, Table 2-3, indicates the power density of different gas turbines and diesel engines for marine application. According to the values, gas turbine engines show a superior density power.

Table 2-3. CODAG prime movers density power [4] [5] [6] [7]

	ENGINE	POWER DENSITY (MW/tons)
Gas Turbine Engine	General Electric - LM500	4,96
	General Electric - LM2500	5,36
	General Electric - LM6000	5,40
	Rolls Royce - MT30	5,54
Diesel Engine	MAN Diesel & Turbo - 6L32/40	0,079
	MAN Diesel & Turbo - 18V32/40	0,106
	WÄRTSILÄ - 6L46F	0,074
	WÄRTSILÄ - 16V46F	0,082

Other relevant characteristic is the power demand that a vessel requires to complete a certain mission. As a matter of fact, different engine requirements will be needed for different kind of vessels, and this will condition the selection of the appropriate propulsion system.

Depending on the application the space requirement is another determining factor. For instance, military vessels seek for fast vessels characterised for having slim hulls, and therefore, a high power density systems are necessary. However, commercial and cargo vessels tend towards efficient diesel engine, which low consumptions compensate the disadvantages of heavy and voluminous propulsion systems.

Regarding the specific fuel consumption, the diesel engine superiority is due to the higher efficiencies that the operating cycle provides compared to the gas turbine cycle.

Finally, a resume of the advantages and drawbacks of each kind of engine is presented in Table 2-4, in order to show the potential benefits of integrating both in a unique propulsion system.

Table 2-4. Comparison between diesel and gas turbine engines

	Diesel Engine	Gas Turbine
Weight		**OK**
Size		**OK**
Investment Cost	**OK**	
Maintenance Cost		**OK**
Fuel Consumption	**OK**	
Fuel Cost		**OK**
Part-load operation	**OK**	
Transient response		**OK**
NOx emissions	**OK**	
CO_2 emissions		**OK**

2.5 Marine gas turbine degradation

In general gas turbine engine's performance is influenced by environmental conditions. These conditions are harsher in marine application due to the salt contained in the air. The performance degradation of the gas turbine affects the engine's life, the power output and the fuel consumption. Therefore, it is paramount to understand which mechanisms are responsible for engine degradation and if the performance deterioration is recoverable or not.

Gas turbine deterioration can be produced by diverse phenomena; however, this section is focused on the degradation mechanisms that the effect of sea salt causes. Sea salt accumulates over compressor blades, reducing the space available between them. In addition, the erosion provoked by the salt advance distorts blade profiles. Then, the outgoing air is introduced in the burner, where the combustion takes place and in presence of salt it leads to sulfidation. This process accelerates corrosion appearance and it is detrimental for turbine performance. After prolonged operation under this condition, both compressor and turbine are said to be fouled.

2.5.1 Recoverable and non-recoverable degradation

Gas turbine deterioration can be classified into recoverable, non-recoverable and permanent degradation. However, the distinction between them is somewhat confusing, since the recoverable effort is very different depending on the kind of deterioration. For instance, the recovery action could be as simple as injecting water or detergent during gas turbine operation or on the contrary require a component replacement in overhaul, bringing the performance of the system back to its initial state. Table 2-5 displays diverse ways of performance deterioration classified according to the different types of degradation.

Table 2-5. Classification of diverse ways of performance deterioration [8]

Recoverable degradation		
· Compressor fouling · Turbine section fouling · Inlet/Outlet Δp increase		
Unrecoverable degradation		
· Flow path damage · Surface erosion · Airfoil roughness · Corrosion	· Hot section corrosion · Tip clearance increases · Seal clearance increases · Non-recoverable axial fouling effects	· Drift of control calibration · Compressor bleed valve malfunctions · IGV or VGV misschedule · Nozzle deflection
Permanent degradation		
· Casing distortion · Distortion of airfoil platforms · Airfoil untwist		

2.5.2 Degradation mechanisms

2.5.2.1 Fouling

Fouling is produced by the adherence of particles to the components surface, modifying the roughness and the shape of the blade profiles. The presence of oil

or simply moist air favours the fouling degradation and it can be prevented by using by means of air filters. The most usual fouling deposits that remain attached on the compressor surfaces are: salts, heavy hydrocarbons, carbon dirt and other types of dirt. [9] In order to remove the attached deposits and restore the efficiency of the component periodic compressor washing is required.

2.5.2.2 Corrosion

Corrosion is the loss of material due to chemical reactions produced by the interaction between the metal and the environment. Some types of corrosion are more propitious to appear in the hot section of the gas engine. Corrosion befalls either by pollutants present in the air or by fuel, water and combustion derived contaminants. Among the different types the corrosion the most important mechanisms are oxidation, hot corrosion and sulfidation.

The oxidation of a metal is produced by the loss of one or more electrons, transforming the metal into a positively charged ion. Consequently, a surface of metal oxide is created. This layer can act as a protective barrier or on the contrary, can accelerate the deterioration of the material mechanical properties.

Other type of corrosion is the hot corrosion, as its name indicates it occurs when the chemical reactions happen at high temperatures. The main drawback is the prediction of the oxidation due to its rapid development. The presence of salt deposits favours this type of degradation.

When the interaction is between a metal and a sulphur in the presence of an oxidizing atmosphere, the deterioration mechanism is known as sulfidation. In the same way as the other corrosion mechanisms, a rapid oxidation causes the degradation of the material due to the loss of the protective layer.

The compressor is not likely to suffer from corrosion during operation since the component remains dry. Nevertheless, during shutdowns when the condensation of water over the compressor surface, can produce a corrosive liquid by absorbing chemical species such as salts and sulphurs.

2.5.2.3 Erosion

Erosion is the wearing away of the material due to the impact of abrasive particles. Only a 10 μm diameter particle can erode the rotating pieces, worsening the performance of the component. This kind of degradation is quite expensive since its damage is not recoverable, and the only solution is to replace the piece or recoating it.

2.5.2.4 Damage

Damage is a kind of erosion, however on another level due to the large size of the objects that impact against the engine surfaces. These objects can be products of broken pieces, carbon accumulation from the fuel nozzles or pieces of ice coming from the inlet.

2.5.2.5 Abrasion

In order to respect the clearances, engines use abradable surfaces, which could allow a certain degree of friction during engines operation. In general, removal of materials would lead to increase in seal or tip gaps. The means of engines cleaning or washing would be helpful to eliminate some of these effects, on the other hand, other maintenance methods, such as the adjustment, repair, or replacement of components could be adopted.

3 METHODOLOGY

This section presents the description of the methodology followed to build the model of a CODAG propulsion system, as well as, the gas turbine model set for Turbomatch simulations in order to study the degradation of the engine.

3.1 CODAG propulsion plant configuration

The studied propulsion plant is a CODAG type, thus it presents three different operational modes, in which different engines configurations are operating.

- Loiter and cruise mode: one 4-stroke diesel engine connected mechanically to each propeller, thus two reciprocating engines in total. In this mode, the vessel's speed range covers from 0 to 21 knots, therefore it is used for port manoeuvres and mainly cruise.
- High speed: an aero-derivative gas turbine, with similar performance to model GE LM2500 it is used to boost the craft from 21 knots to 28 knots.
- Top speed: CODAG configuration is used in this mode, both kind of engines supply power to the propellers at the same time. An extra thrust is achieved for very special operations that require considerable high speed, although its durability is brief since the components are working close to their limit. Top speed is approximately 30 knots.

3.1.1 Diesel engine

The diesel engines employed are based on PAXMAN (MAN DIESEL) model 18VP185. This engine accomplishes the demanded requirements for the loiter and cruise mode. In Table 3-1 an overview of engine's characteristics is presented.

Table 3-1. Diesel engine characteristics [3]

Parameter	Value
Bore (mm)	185
Mean effective pressure (bar)	25.3
Mean piston speed (m/s)	12.8
Cylinders (-)	V18
Maximum Power Rate (kW)	4000
Speed at Maximum Power Rate (rpm)	1950
Continuous Power Rate (kW)	3300
Two-stage turbocharging arrangement with intercooling and aftercooling	

3.1.2 Gas turbine

The gas turbine employed is based on the marine gas turbine LM2500. The basic configuration of this engine consists of a single-rotor gas turbine and an aerodynamically coupled power turbine. It presents a six-stage, axial flow design compressor, an annular combustion chamber with 30 fuel nozzles, a two-stage high pressure turbine, and a six-stage high efficiency power turbine. For the non-aero application, the nozzles are coated with CODEP and the blades are coated with platinum-aluminide to improve resistance to erosion, corrosion and oxidation. In Table 3-2 an overview of engine's characteristics is presented. [10]

Table 3-2. Gas turbine characteristics [10] [11]

Parameter	Value
Inlet mass flow (kg/s)	68.96
Fuel flow (kg/s)	1.581
Overall pressure ratio (-)	18
Exhaust gas temperature (K)	836.26
Power output (MW)	25.05
Rotational speed (rpm)	3600
Thermal efficiency (%)	0.37

3.2 Marine vessel power prediction model

Before expanding on the modelling of the power prediction of a CODAG propulsion system, a brief explanation of power loss along ship's power plant is given.

Initially, to reach a certain velocity, vessel's power plant must supply enough power to overcome the resistance faced by the ship and to maintain the desired speed. Nevertheless, since the prime movers deliver the power until the propellers leverage this power to convert it into thrust, some losses may occur. Therefore, prime movers must supply higher powers to guarantee that the propellers receive sufficient power to accomplish the mission requirements.

¡Error! No se encuentra el origen de la referencia. shows the power layout of t he propulsion system. To understand the relationship between different powers, they will be defined from the propeller to the prime mover.

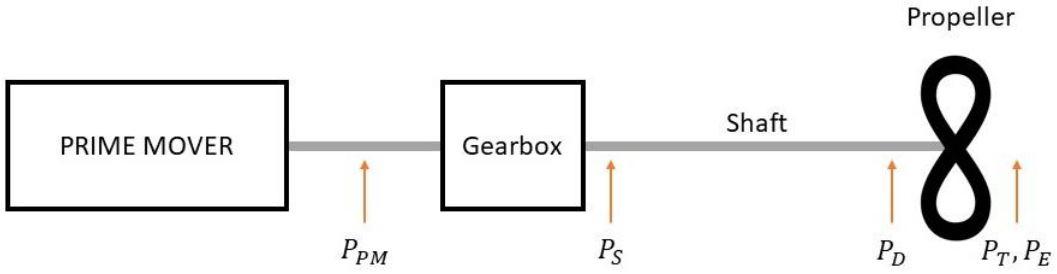

Figure 3-1. Power layout along propulsion system

The ratio of the work done on the ship to that done by the screw is called hull efficiency and relates the effective power and the thrust power. The first corresponds to the power required to move a ship at a set velocity against its resistance. Whereas the second is defined as the power required to deliver certain thrust at a specific speed of advance. Equation (3-1) shows this relation, which reflects the integration level between the screw and the hull.

$$\eta_{hull} = \frac{P_E}{P_T} = \frac{R\,V}{T\,V_a} \tag{3-1}$$

Occasioned by propeller's performance part of the power is lost and therefore, the needed power to drive the propeller must be higher. The relation between thrust power and delivered power is called propeller efficiency and it is composed by the open water efficiency and the relative rotative efficiency.

$$\frac{P_T}{P_D} = \eta_o \eta_R \tag{3-2}$$

The open water efficiency [12] provides the reduction of thrust power absorbed by the propeller operating without a hull attached, i.e. in open water. Whereas, the relative rotative efficiency adjusts the open water performance of the propeller to its performance behind the hull.

Other sources of loss are due to the transmission efficiency, both shaft and gearbox consume part of the power delivered by the prime movers, ending up with an outgoing value a lot higher than the effective power.

$$P_E = \eta_{hull}\, \eta_o\, \eta_R\, \eta_s\, \eta_{GB}\, P_{PM} \tag{3-3}$$

In this section, an explanation of the process followed to obtain the different efficiencies and powers is given. According to the operational mode, different gearboxes will be used and thus, the losses and the way of obtaining the prime move power will differ. [13]

The developed model to predict marine vessel's power meets the block diagram presented in Figure 3-2. The model above calculates the demanded power from the prime movers to move a defined vessel at a specified velocity.

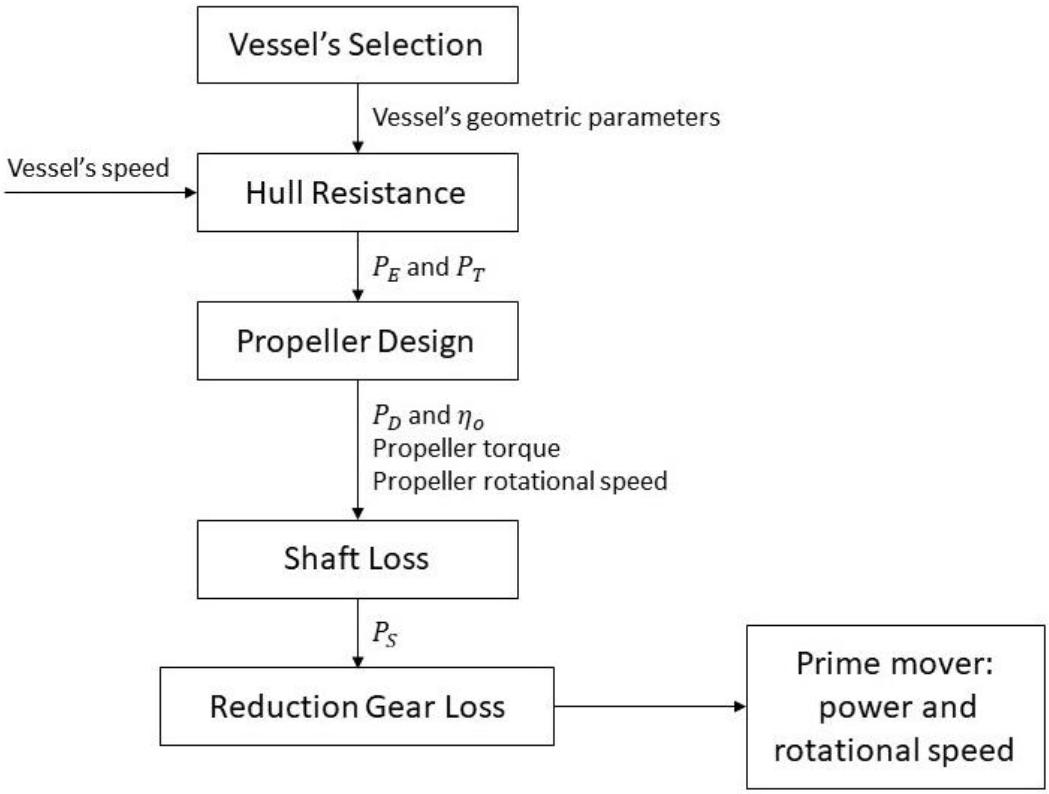

Figure 3-2. Block diagram of power engine prediction model

3.2.1 Marine vessel selection

This section includes a description of an existing marine vessel that has been used as a reference for building the power prediction model.

This vessel is the last generation naval vessel Type 45 Destroyer. The reason of having selected this craft is its power plant similarity to a CODAG propulsion system. Type 45 Destroyer presents an integrated electric propulsion system, where two 4-stroke high speed diesel engines, rated at roughly 2 MW for port manoeuvring and low cruising speeds. In addition to two Rolls-Royce WR-21 gas turbines engines, rated 21 MW for high vessel's performance.

Initially, only geometrical parameters are required to develop the first module, the hull resistance calculation. In Table 3-3 an exhibition of the demanded parameters is presented.

Table 3-3. Watercraft parameters used in the developed model [14]

Parameter	Value
Length between perpendiculars (m)	147
Breadth at the water line (m)	18
Mean draft (m)	5.1
Displacement (tons)	7350
Wetted surface (m^2)	2829.5
Prismatic coefficient (-)	0.58
Block coefficient (-)	0.5
Transversal immersed area (m^2)	20

Although most of the parameters are simple vessels measurements, others such as the prismatic and the block coefficient are unknown for someone that is not a naval expert. For this reason, both coefficients are briefly explained below.

- Prismatic coefficient: ratio of the displacement volume to the volume of a prism, which dimensions are the length on the waterline, the mean draft and the breadth at the water line. [15]
- Block coefficient: ratio of the submerged volume of a ship to the volume of a rectangular block, which dimensions are the length between perpendiculars, the mean draft and the breadth at the water line. [15]

3.2.2 Hull resistance module

In order to obtain the power that the prime movers must deliver to achieve a certain speed, first, it is necessary to know the resistance caused by the movement of the ship. There are diverse statistical methods used to calculate hull resistance, but usually, they require a great level of detail regarding vessel parameters and since the application is a warship, it is hard to find these data in published literature. In this section, it is explained the followed procedure to calculate hull resistance. It is a combination of diverse naval architecture methods.

The data of the vessel used to calculate the hull resistance is presented in Table 3-3. In order to proceed with the calculation, some assumptions are taken into consideration.

- The length between the aft end of design waterline and most forward point of the ship below design, waterline named length over the surface, is considered to be equal to the length between perpendiculars.
- It is assumed a sea water density of 1025 kg/m^3.

The total resistance, experimented by the vessel, is defined by different sources of resistance, such as,

- Residual resistance: energy loss caused by the hydrodynamic effect that the waves generate when they get in contact with the hull.
- Friction resistance: created by the hull sliding on a viscous fluid, the sea water.
- Correlation allowance resistance: related to the roughness of the hull, takes into consideration the difference between a new refined hull and a deteriorated hull's surface.
- Air resistance: due to vessel's movement across the air, it is generated by the structure that remains above the water line of the craft.
- Appendage resistance: due to attachments on the ship hull under the water, such as rudders, side thrusters, bossings, brackets…

3.2.2.1 Residual resistance

The residual resistance has been calculated using Hollenbach's method [16], which uses a series of experimental coefficients. The main advantages are that it requires few vessel parameters and provides a precision of 10% [17], which is sufficient for preliminary design. Equation (3-4) is used to calculate the residual resistance.

$$R_R = C_{RH} \frac{\rho}{2} V^2 B T \frac{1}{10} \quad \textbf{(3-4)}$$

Where all the parameters are known except for C_{RH} which is calculated in the following way:

$$C_R = C_{RH}\, B\, T \frac{1}{10\, S} \tag{3-5}$$

To obtain C_R previously it is necessary to estimate $C_{R,standard}$, $C_{R,Fnkrit}$ and k_L using equations (3-6), (3-7), (3-8) and (3-9).

$$C_R = C_{R,Standard}\, C_{R,Fnkrit}\, k_L\, (T/B)^{a1}\, (B/L)^{a2}\, (L_{os}/L_{wl})^{a3}\, (L_{wl}/L)^{a4}\, (D_P/T_A)^{a6}\, (1 + (T_A - T_F)/L)^{a5} (1 + N_{Rud})^{a7} (1 + N_{Brac})^{a8} (1 + N_{Boss})^{a9} (1 + N_{Thr})^{a10} \tag{3-6}$$

$$C_{R,Standard} = b_{11} + b_{12}\, F_n + b_{13}\, F_n^2 + C_B\, (b_{12} + b_{22}\, F_n + b_{23}\, F_n^2) + C_B^2 (b_{31} + b_{32}\, F_n + b_{33}\, F_n^2) \tag{3-7}$$

$$C_{R,Fnkrit} = max\left[1, \left(F_n/F_{n,krit}\right)^{c1}\right] \tag{3-8}$$

$$k_L = e_1 L^{e_2} \tag{3-9}$$

As it can be observed apart from the experimental coefficients provided in Appendix 6.1A.1. Froude's number (3-11) is required to complete the calculation. To obtain it, a characteristic length that depends on the length between perpendiculars must be calculated.

$$L_{fn} = \begin{cases} L_{os} & for\ L_{os}/L < 1 \\ L + 2/3\, (L_{os} - L) & for\ 1 \le L_{os}/L < 1.1 \\ 1.0667\, L & for\ 1.1 \le L_{os}/L \end{cases} \tag{3-10}$$

$$F_n = \frac{V}{\sqrt{g\, L_{fn}}} \tag{3-11}$$

Also, the critical Froude number:

$$F_{n,krit} = d_1 + d_2 C_B + d_3\, C_B^2 \tag{3-12}$$

3.2.2.2 Friction resistance

The friction resistance (3-13) has been calculated following IITC-1957 method [17]. It is a model ship correlation line, that even though entails some

contemporary modelling errors it is still in use. As it can be seen depends on Reynolds number (3-15), which in turn depends on ship velocity.

$$R_F = \frac{1}{2}\,\rho_S\,S\,V^2 C_F \tag{3-13}$$

$$C_F = \frac{0.075}{(\log_{10} Re - 2)^2} \tag{3-14}$$

$$Re = \frac{L\,V}{1.19 \cdot 10^{-6}} \tag{3-15}$$

3.2.2.3 Correlation allowance resistance

As in friction resistance, the correlation allowance resistance has been obtained multiplying the dynamic pressure times a determined resistance coefficient (3-16). This coefficient has been calculated with Holtrop's formula [18].

$$R_A = \frac{1}{2}\,\rho_S\,S\,V^2 C_A \tag{3-16}$$

$$C_A = 0.006\,(L+100)^{-0.16} - 0.00205 + 0.003\sqrt{\frac{L}{7.5}}\,C_B^4\,c_2(0.04 - c_4) \tag{3-17}$$

$$c_4 = \begin{cases} T_F/L & T_F/L \le 0.04 \\ 0.04 & T_F/L > 0.04 \end{cases} \tag{3-18}$$

As T_F/L is higher than 0.04, the last term of equation (3-17) cancels out.

3.2.2.4 Air resistance

The calculation of the resistance of the air is based on academic and published literature. [19]

$$R_{AA} = \frac{1}{2}\,\rho_S\,S\,V^2 C_{AA} \tag{3-19}$$

$$C_{AA} = \frac{A_T}{1000\,S} \tag{3-20}$$

Where the air resistance coefficient is a thousandth part of the ratio between projected front area of the above watercraft and the wetted surface.

3.2.2.5 Appendage resistance

The calculation of the resistance of the air is based on academic and published literature [19]. As it is shown in equation (3-21) appendages resistance can be calculated as a percentage of the addition of residual resistance, friction resistance and air resistance.

$$R_{APP} = \frac{1.5}{100}\,(R_R + R_F + R_A) \tag{3-21}$$

3.2.2.6 Total resistance

Once all the resistances have been individually obtained, the summation forms the whole resistance experimented by the craft moving at certain speed. The product of the total resistance times the ship's velocity gives the effective power, necessary to estimate the power that the prime movers must supply to reach a certain speed. Figure 3-3 shows the effective power as a function of the vessel's speed.

$$R_T = R_F + R_R + R_{AA} + R_A + R_{APP} \tag{3-22}$$

$$P_E = R_T\, V \tag{3-23}$$

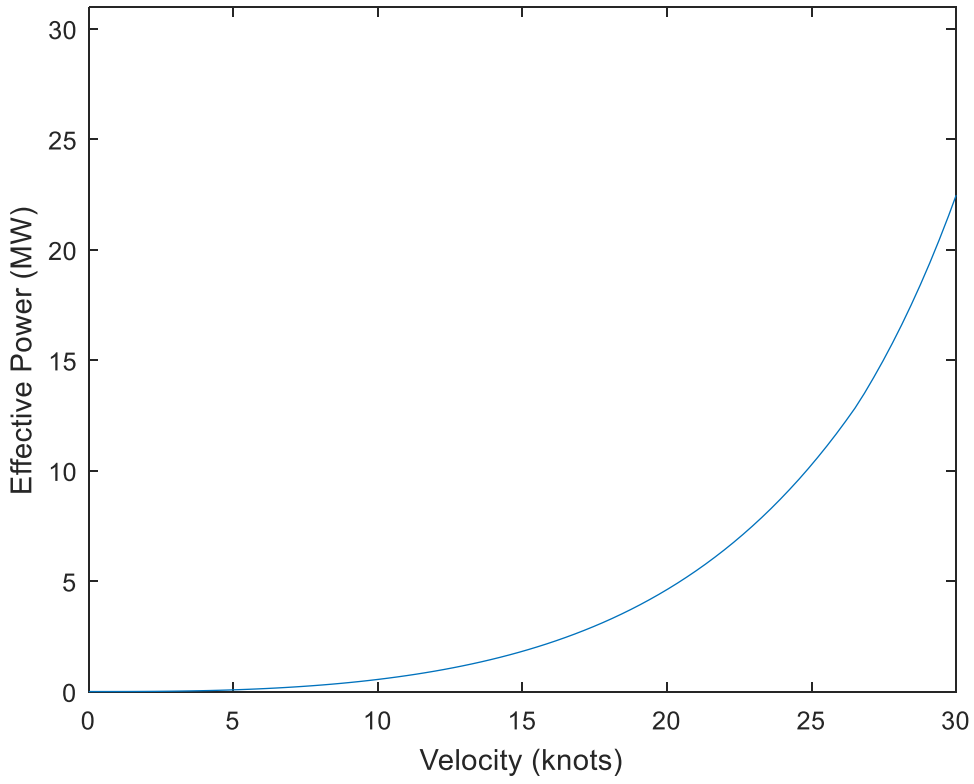

Figure 3-3. Effective power as a function of the vessel's speed

3.2.3 Wake, thrust deduction and relative rotative efficiency

The propulsion device performance is affected by the presence of the hull, which influences the propulsion efficiency and thus, the design of the propulsion device. This interaction is the addition of wake, thrust deduction and the relative rotative efficiency.

3.2.3.1 Wake fraction

Hull's presence distorts the flow into the propeller. Therefore, the average speed of flow into the propeller, V_a, is dissimilar from the speed of advance of the vessel, V. It is common to name this velocities difference in relation to the vessel speed as the Taylor wake fraction ω_T. (3-24)

$$\omega_T = \frac{V_s - V_a}{V_s} \tag{3-24}$$

For twin-propeller vessels, the following equation (3-25) is suggested to calculate the wake factor, based on Holtrop wake data regression analysis. [20]

$$\omega_T = 0.3095\ C_B + 10\ C_V\ C_B - \frac{D}{\sqrt{B\ T}} \tag{3-25}$$

Where all the parameters are known except for the viscous resistance coefficient, whose expression corresponds to equation (3-26):

$$C_V = (1 + k)C_F + C_A \tag{3-26}$$

To obtain C_v it is necessary to calculate first the shape factor (k) of the hull. In order to simplify calculations, appendage shape factor has not been taken into consideration.

$$(1 + k) = 0.93 + 0.487118\ (1 + 0.011\ C_{stern})(B/L)^{1.06806}(T/L)^{0.46106}(L_{WL}/L_R)^{0.121563}(L_{WL}^3/\nabla)^{0.36486}(1 - C_P)^{-0.604247} \tag{3-27}$$

Where all the parameters are known except for the length of the run (L_R) and the C_{stern} parameter, which depends on the hull's shape. Equation (3-28) shows how

to calculate L_R. Considering that the vessel presents a V hull shape, C_{stern} can be obtained from Table 3-4.

$$L_R = L_{WL}\left(1 - C_P + \frac{0.06\ C_P\ LCB}{4\ C_P - 1}\right) \quad \textbf{(3-28)}$$

In addition, LBC is the longitudinal centre of buoyancy and its value is a percentage of the length between perpendiculars. A positive value indicates that centre is shifted forwards, whereas a negative value indicates the opposite. For this particular craft LBC is -0.8%. [21]

Table 3-4. C_{stern} parameter value for different hull shapes [22]

Afterbody form	C_{stern}
Pram with gondola	-25
V-shaped sections	-10
Normal section shape	0
U-shaped sections with Hogner stern	10

3.2.3.2 Thrust deduction

The propeller accelerates the flow ahead of itself, increasing the pressure resistance and the frictional resistance of the hull. Moreover, if separation befalls after the hull without a propulsion device installed, the effect of the propeller could eliminate the separation by reducing the unfavourable pressure gradient over the afterbody. Therefore, the thrust generated by the propeller will exceed hull resistance. This difference between forces in relation to the thrust delivered by the propeller is named the thrust deduction factor. (3-29)

$$t = \frac{T - R}{T} \quad \textbf{(3-29)}$$

For twin-propeller vessels, the following equation (3-30) is suggested to calculate the wake factor, based on Holtrop [20] thrust data regression analysis.

$$t = 0.325\ C_B - 0.1885 \frac{D}{\sqrt{B\ T}} \quad \textbf{(3-30)}$$

3.2.3.3 Relative rotative efficiency

The relative rotative efficiency has been already defined at the beginning of chapter 3. As it can be seen in equation (3-31) the relative rotative efficiency depends on hull shape and the pitch to diameter ratio, which are known for the selected vessel. [18]

$$\eta_R = 0.9737 + 0.111\ (C_P - 0.0225\ LCB) - 0.06325\ P/D \quad \textbf{(3-31)}$$

3.2.4 Screw propeller module

The propeller module is based on the open water characteristics of the Wageningen B-series propellers [23]. The purpose is to obtain for a specific advance ratio (J), which is related to vessel's speed, the corresponding thrust coefficient, torque coefficient and thus, the corresponding open water efficiency. Thereby, it is possible to calculate the power remaining after propellers' performance. The action of propeller cavitation and partial submergence have been neglected.

Wageningen B-series propeller method presents some limitations regarding design propeller parameters, such as: [23]

- Maximum craft's velocity is between 30 and 35 knots.
- The number of propeller blades varies between 2 and 7.
- The propeller's blade area ratio varies between 0.3 and 1.05.
- The propeller's pitch to diameter ratio varies between 0.4 and 1.4.

The chosen propulsion device is a twin-screw propeller with fix pitch angle due to performance simplification. This configuration provides a better propulsion efficiency rather than a single propeller since lower propeller's rotational speeds are achieved for the same power. Basically, propellers can be divided into two main groups (Table 3-5):

Table 3-5. Types of propeller

Fixed Pitch Propeller	Controllable Pitch Propeller
• Cast in one block • Pitch angle is constant and it does not change in operation • Simple mechanism • Ships that not require high degree of manoeuvrability	• Larger hub to allocate the hydraulic mechanism for pitch control • Propeller performance curves can be changed in operation • Expensive • Ships that require high degree of manoeuvrability

Propeller design parameters based on academic literature [21] are shown in Table 3-6:

Table 3-6. Propeller design parameters

Propeller design parameter	Value
Number of blades (-)	5
Propeller's blade area ratio (-)	0.751
Propeller's blade pitch to diameter ratio (-)	1.254
Propeller diameter (m)	4.1

Expressions (3-32) and (3-33) show thrust and torque coefficients parameters dependence. Either of them is a function of the advance ratio, pitch to diameter ratio, blade area ratio, the number of blades, Reynolds number and thickness to chord length ratio.

$$K_T = f_1(J, P/D, A_E/A_O, Z, Rn, t/c) \quad \textbf{(3-32)}$$

$$K_Q = f_2(J, P/D, A_E/A_O, Z, Rn, t/c) \quad \textbf{(3-33)}$$

Thrust and torque coefficients are calculated by means of the equations (3-34) and (3-35). Where $C_{Ts,t,u,v}$, $C_{Qs,t,u,v}$ and the superscripts s, t, u and v [23] are shown in 6.1A.2.

$$K_T = \sum_{s.t.u.v} \left[C_{T_{s,t,u,v}} (J)^s \, (P/D)^t \, (A_E/A_O)^u \, (Z)^v \right] \quad \textbf{(3-34)}$$

$$K_Q = \sum_{s.t.u.v} \left[C_{Q_{s,t,u,v}} (J)^s \, (P/D)^t \, (A_E/A_O)^u \, (Z)^v \right] \quad \textbf{(3-35)}$$

This method applies the following coefficient corrections for Reynold's numbers higher than 2x10^6. [18]

$$K_{T-cor} = K_T + \Delta C_D 0.3 \frac{P \, c_{0.75} Z}{D^2} \quad \textbf{(3-36)}$$

$$K_{Q-cor} = K_Q + \Delta C_D 0.25 \frac{P \, c_{0.75} Z}{D^2} \quad \textbf{(3-37)}$$

Where the difference in the drag coefficient of the propeller's profile section presents the following expressions (3-38) and (3-39).

$$\Delta C_D = (2 + 4(t/c)_{0.75}) \left[0.003605 - \left(1.89 + 1.62 \, \log\left(c_{0.75}/k_p \right) \right)^{-2.5} \right] \quad \textbf{(3-38)}$$

$$(t/c)_{0.75} = (0.0185 - 0.00125Z) D/c_{0.75} \quad \textbf{(3-39)}$$

Where $c_{0.75}$ is the chord length of the propeller's blade at 75% of the radius.

$$c_{0.75} = 2.073 (A_E/A_O) D/Z \quad \textbf{(3-40)}$$

In order to obtain the propeller rotational speed, required to produce the necessary thrust to move the vessel at a certain speed, an iterative process has been carried out as the block diagram shows in Figure 3-4:

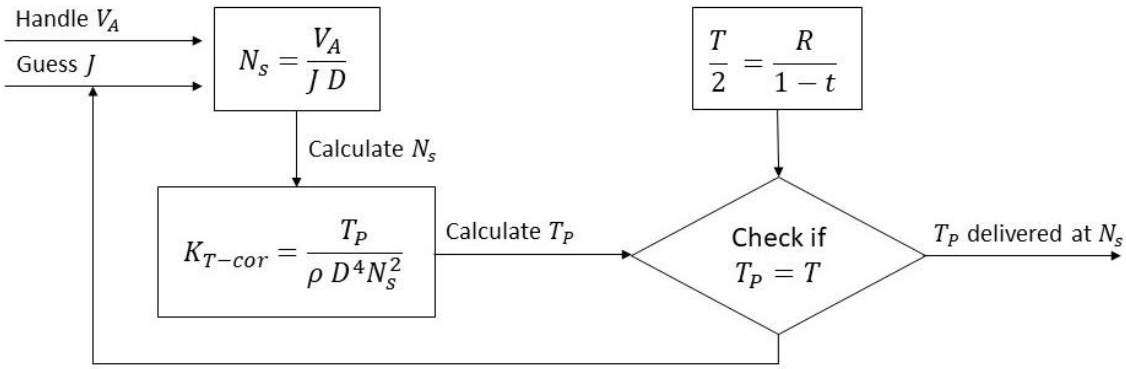

Figure 3-4. Procedure followed to obtain the thrust that the propeller delivers at a certain propeller's rotational speed

For a known speed and a guessed advanced ratio, the propeller's rotational speed can be calculated. Then, through thrust coefficient expression, as all the parameters are known, thrust can be calculated. Finally, this thrust is compared to the resistance obtained at that advanced speed, by means of the thrust deduction coefficient. The thrust delivered by the propeller is half of the thrust required to move the vessel due to the twin screw configuration. This procedure is repeated for different advance coefficient until the required thrust and the delivered thrust match.

In addition, the open water efficiency is calculated using equation (3-41).

$$\eta_{OWE} = \frac{J K_{T-cor}}{2\pi K_{Q-cor}} \quad \textbf{(3-41)}$$

Figure 3-5 shows how the thrust coefficient, torque coefficient and the open water efficiency change as a function of the advance ratio for the chosen fix control propeller.

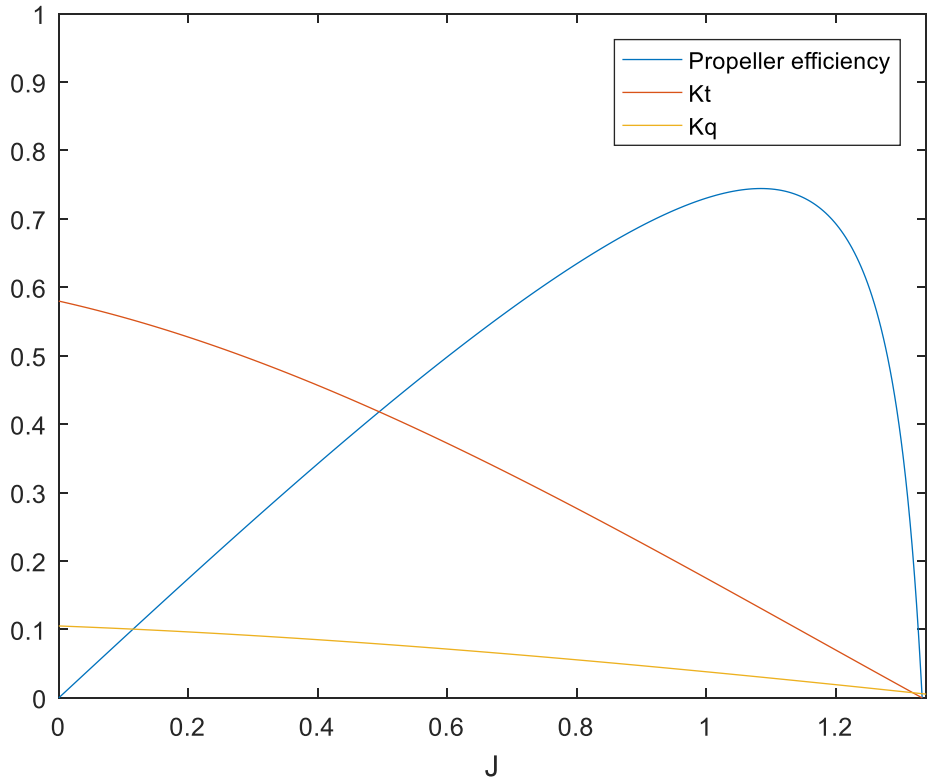

Figure 3-5. Propeller thrust coefficient, torque coefficient and open water efficiency

Once both the open water efficiency and the relative rotative efficiency are known, it is possible to calculate the delivered power by means of equation (3-42). Since the propeller could not absorb all delivered energy from the shaft.

$$P_D = \frac{P_T}{\eta_o \eta_R} \tag{3-42}$$

3.2.5 Shaft losses

Shaft losses are due to the friction between the bearings and the shaft. The model provides the possibility of introducing the loss law that regulates the mechanical losses. By default, the loss is considered linear increasing with the rotational speed of the shaft.

3.2.6 Gearbox losses

When the vessel is moving at determined speed, the propeller must produce certain thrust to reach that speed. This thrust is associated with a specific

propeller rotational speed and torque. Since, propeller and engine are mechanically coupled, the engine must provide the power required to produce enough thrust at the exact rotational speed that would drive the shaft and thus, the propeller at the rotational speed that would produce the required thrust. Therefore, it is necessary the use of reduction gears to couple the engine shaft and the propeller shaft, which are spinning at different rotational speeds. Depending on the operational mode different losses have been used. The gearbox losses model is similar to the shaft model.

Once the gearbox loss is computed, it is known the power that the engines must supply to reach certain vessel's speed. Depending on the requirements the engines are selected for each operational mode. Figure 3-6 shows the computed power that the engines supply, against the remaining power that propels the vessel to reach certain speed for the first operational mode, loiter and cruise. Figure 3-7 it is the same representation, but for the second operational mode, high speed. Finally, the engines must match the propeller to complete the model (Section 4).

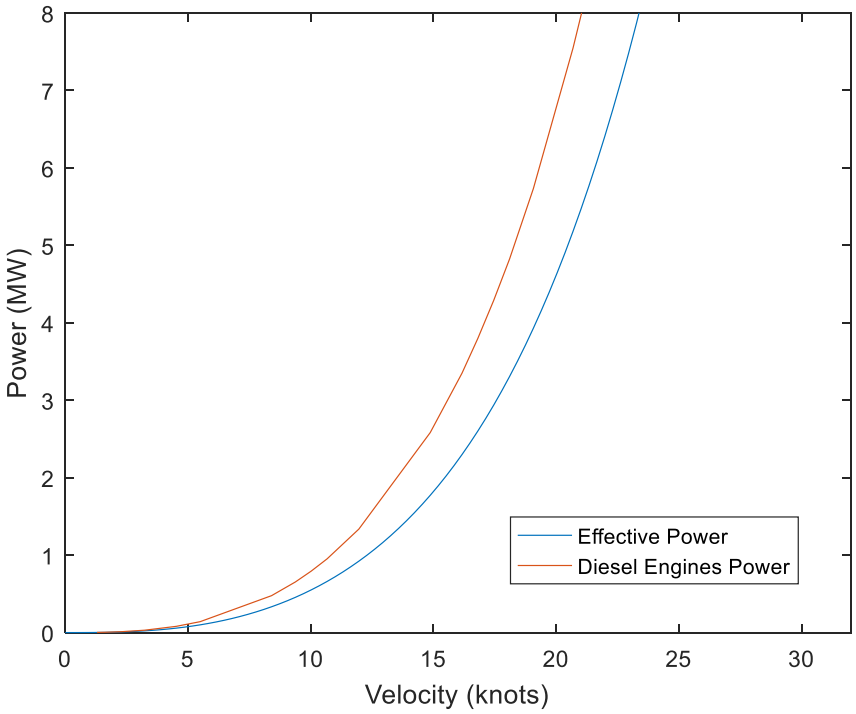

Figure 3-6. Comparison between the effective power and the power that the diesel engines must generate

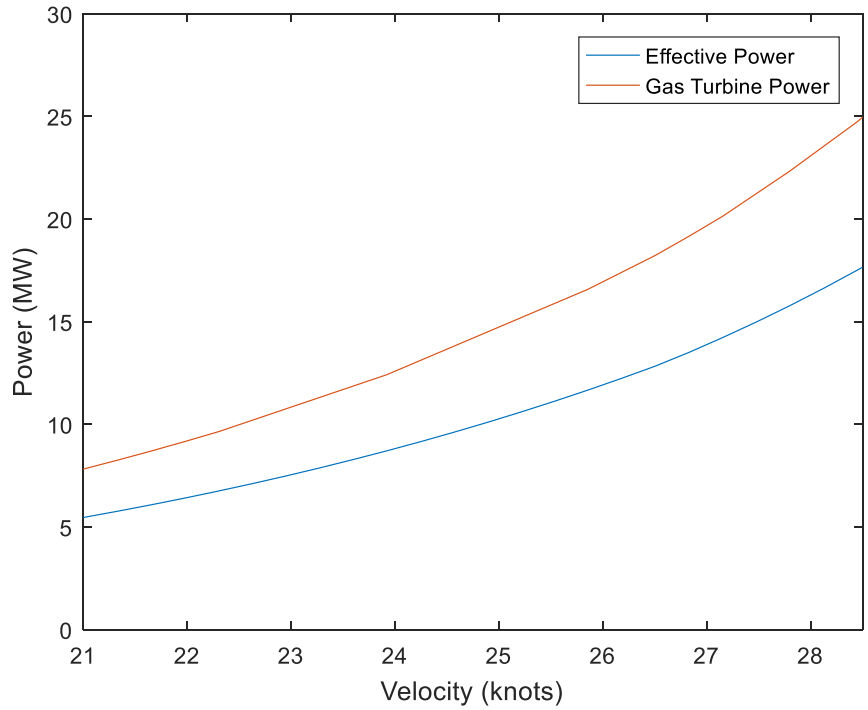

Figure 3-7. Comparison between the effective power and the power that the gas turbine must generate

3.3 Turbomatch gas turbine model

The software used to carry out the simulations of the gas turbine engine is Turbomatch 2.0. Turbomatch is a Fortran code developed in Cranfield University, capable to simulate both steady state, which includes design and off-design performance, and transient state simulations.

The software is composed of several pre-programmed modules, called Bricks. These bricks, for the most part, correspond to engine components, such as compressors, combustion chambers, turbines, nozzles… The programme calls the bricks to simulate different components of the engine considering their particular details and the gas properties at various stations. In addition to its modularity, generic component maps enable the simulation of any gas engine configuration. As a result, thrust, output power or specific fuel consumption are the kinds of parameters given as outputs. The way of interacting with the software is with a text file input, where the gas engine is defined. Likewise, the results are

obtained through a text file output. Matlab codes and Excel sheets have been created to facilitate users postprocess.

The gas engine simulated in Turbomatch is based on the marine gas turbine LM2500. The reason for selecting a similar gas turbine is to perform in the most similar way the behaviour of a real marine gas turbine. Figure 3-8 shows the configuration of the marine gas turbine simulated in Turbomatch.

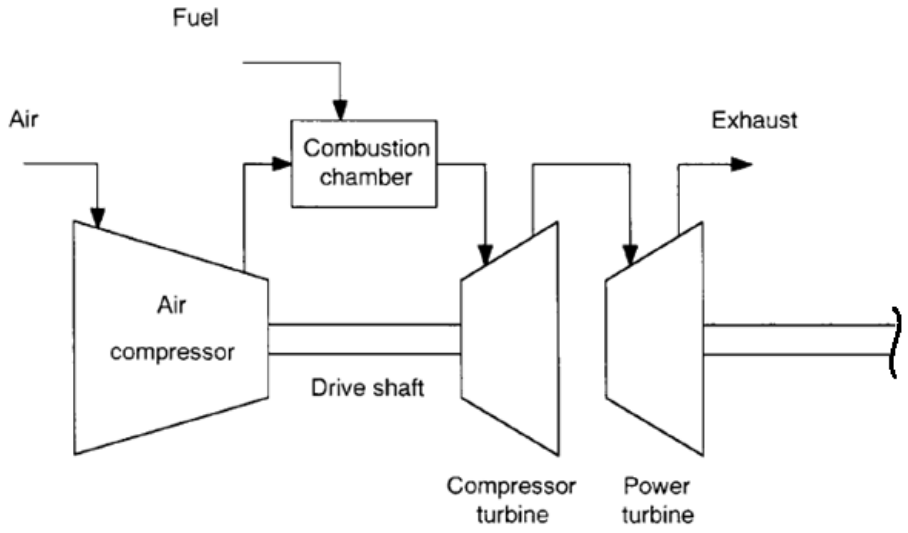

Figure 3-8. Marine gas turbine engine scheme

It is comprised of a gas generator, where a compressor driven by a compressor turbine, increases the pressure of the air, which is burned into the combustion chamber and finally expanded in the compressor turbine; and a free power turbine, which is linked to the gas engine aerodynamically, takes charge of generating the power to drive the propellers.

Even though some parameters have been taken from the engine's manual, others have been assumed, Table 3-7 shows the employed parameters in the simulations.

Table 3-7. Gas turbine parameters used in the simulations

Parameter	Value	Description
Ambient temperature (K)	288.15	Given
Ambient pressure (Pa)	101325	Given
Inlet mass flow (kg/s)	70.86	Assumed
Compressor isentropic efficiency (-)	0.9	Assumed
Compressor pressure ratio (-)	18:1	Given
Fuel flow (kg/s)	1.507	Calculated
Combustor efficiency (-)	0.998	Assumed
Turbine entry temperature	1509.5	Assumed
Turbine isentropic efficiency (-)	0.87	Assumed
Power turbine isentropic efficiency (-)	0.89	Assumed
Exhaust pressure (Pa)	106391,25	Assumed
Power output (MW)	24.9	Calculated

4 ENGINES-PROPELLER MATCHING

As discussed in resistant calculation section, the resistance of the vessel is proportional to the square of the vessel's velocity. Since the effective power is the product of the resistance times the vessel's velocity, the power is proportional to the speed to the power of three. For a craft provided with a fix pitch propeller, the vessel's speed will be proportional to the rotational speed of the propeller. Consequently, the effective power is proportional to the propeller revolutions to the power of three. This is known as propeller's law.

Although propeller's law is usually seen with powers higher than three and it is not valid for different propulsion situations, it is useful for discussions of engine-propeller behaviour. In Figure 4-1, it is represented the rotational speed of a single propeller against the power that it produces. Due to twin propeller configuration, the total power to tow the whole vessel is exactly the double.

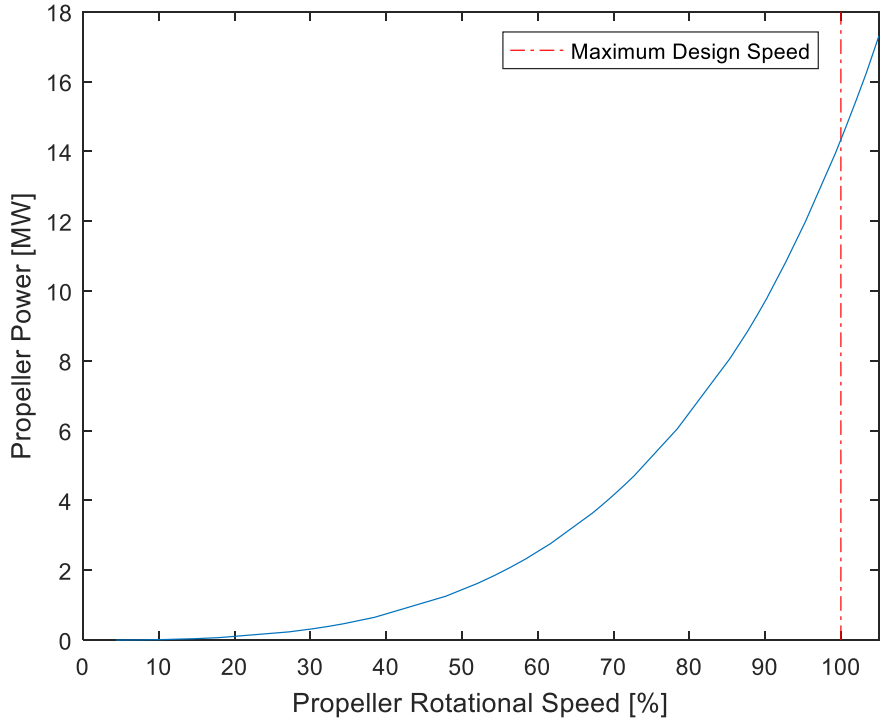

Figure 4-1. Propeller Law

The matching of the engine and the propeller is based on the conservation of the energy. Therefore, the power supply by the engine must equal the power

absorbed by the load, in this case, the load is the propeller. Figure 4-2 is a representation of power-speed characteristics for a propeller and its driving engine. The operating point is the intersection of the two heavy lines, being the only place on the plane where power absorbed by the propeller equals that produced by the engine at common rotational speed.

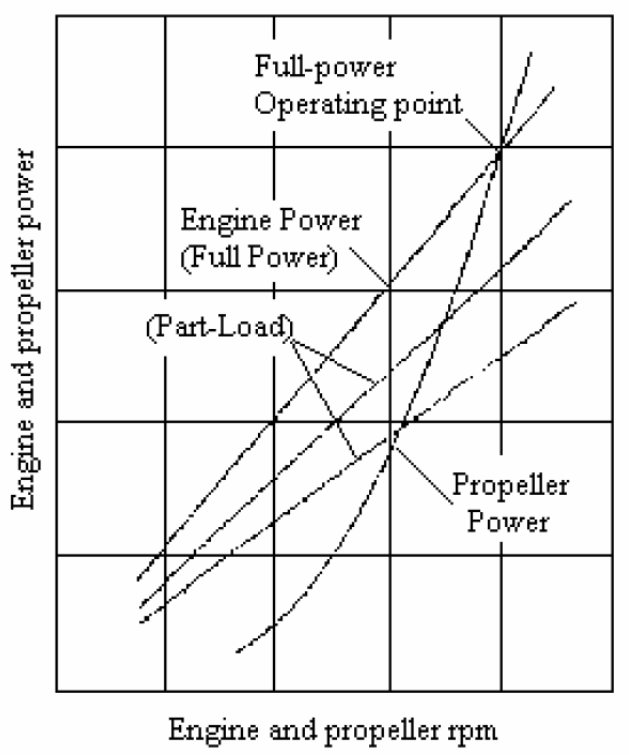

Figure 4-2. Basic concept of engine-propeller matching

4.1 Diesel engine-propeller matching

As previously mentioned, the two Diesel engines must provide sufficient power during the first operational mode, which corresponds to the speed range from 0 to 21 knots. According to Figure 3-6, where engine prime mover power is plotted against the vessel's speed, to reach 21 knots the engines must supply a power of 4000 kW each.

Apart from delivering the required power to reach a certain speed, engines must match the propeller in order to control power plant’s operation. In other words, to achieve a specified speed, propellers must provide a determined thrust, which is obtained by spinning the propeller at a specific rotational speed. Knowing that

diesel engine rotates at higher rotational speeds than a propeller is capable, it is necessary the use of reduction gears. Since the ship designer has some freedom in selecting the gear reduction ratio, this propeller matching problem can usually be solved by selecting a ratio that allows best rpm for both engine and propeller.

In Figure 4-3 it is presented the performance map of the diesel engine, where it can be seen the power obtained for different rotational speeds, as well as, the consumption that this implies. In addition, it has been plotted the propeller law and it can be appreciated that it is inside the performance area of the engine, which means that engine and propeller match.

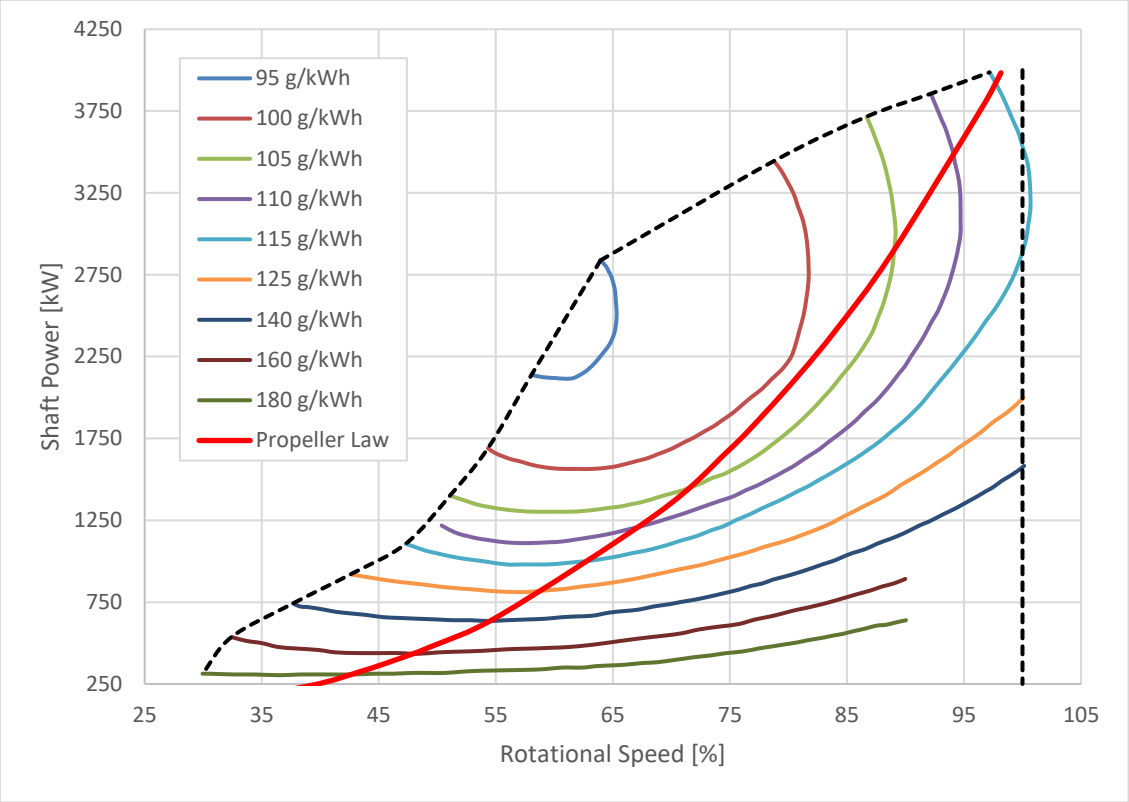

Figure 4-3. Performance map of diesel engine

Moreover, in Figure 4-4 propeller law has been extracted from the performance engine map to show in a simplified way, the operating line used in the first operational mode. It can be seen the power delivered by the engines as a function of the propeller rotational speed and the fuel consumption that each operating point means.

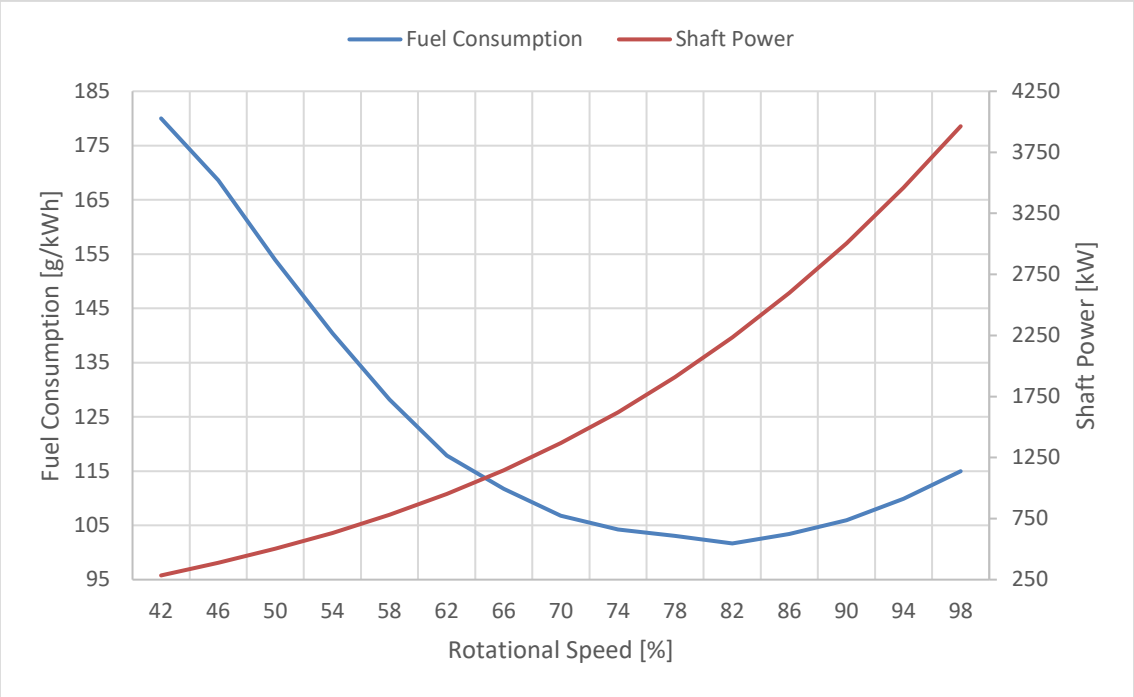

Figure 4-4. Diesel engine-propeller matching curves

4.2 Gas turbine-propeller matching

Unlike diesel engine-propeller matching, the procedure followed to match the gas turbine and the propellers is an iterative process using Turbomatch. This software does not allow to use the rotational speed of the gas engine as a handle, so it is not possible to obtain the required fuel to produce the aimed power and rotational speed, and thus an alternative solution was adopted.

Other inconvenient is that Turbomatch works with relative rotational speeds, which not only depend on the design point but on the turbine inlet temperature as well. Therefore, the developed procedure is based on this relative rotational speed which cannot be directly linked to the rotational speed of the propellers. However, it gives an approximate idea of the behaviour of the gas turbine when fuel and rotational speed are modified.

To analyse the how the gas engine responds to fuel flow and rotational speed variation some facts and assumptions have been taken into consideration:

- As an aero-derivative gas engine, which latest component is a free power turbine instead of a nozzle, the pressure at the outlet of the engine must

correspond to atmosphere pressure taking full advantage of the exhaust mass flow.

- The free power turbine is choked, which means that the mass flow across it cannot increase more. If the free power turbine remains choked, there will not be any significant change in upstream components pressure. Thus, knowing the value of the free turbine inlet pressure and the fact that there is a full expansion, the pressure through the free power turbine is known.
- It has been assumed an ideal gas constant of 287 J/(kgK).
- The specific heat capacity at constant pressure has been calculated for the design point by means of equation (4-1), where all the parameters are known except the c_p:

$$Work_{power\ turbine} = \dot{m} c_p \Delta T_{power\ turbine} \quad \textbf{(4-1)}$$

- Finally, the adiabatic index has been obtained using the relations between c_p and R, as expression (4-2) shows.

$$\gamma = \frac{c_p}{1 - R} \quad \textbf{(4-2)}$$

The followed methodology calculates the power output for a given fuel flow when the rotational speed of the free power turbine variates. To do so, Turbomatch simulations have been performed changing the fuel flow from 0.8 kg/s to 1.8 kg/s every 0.2 kg/s. From each calculated point, the wished parameters are the mass flow, total pressure and temperature at the inlet of the free turbine, besides, the map of the power turbine.

A relevant aspect to consider is that Turbomatch works with relative rotational speeds. Particularly, in the turbine, the parameter used to express the rotational speed is known as CN, which is the ratio between the rotational speed of the turbine divided by the turbine inlet temperature and divided again by the same relation for the design point. Therefore, the dependence of the rotational speed, on the turbine inlet temperature complicates the direct matching between the gas engine and the propeller.

In order to obtain the map of the power turbine, a Matlab code has been generated. This program is able to read the interesting parameters, such as enthalpy's increment divided by the turbine inlet temperature $(\Delta h/T_{in})$, corrected mass flow $\left(\dot{m}\sqrt{T_{in}}/P_{in}\right)$ and efficiency (η_t). Once these values are obtained for each speed line (CN), a scaling factor given in the output file of the Turbomatch simulations may be applied. The reason for this is that Turbomatch works with generic component maps that are the same for different simulations, however, when real values are wanted, those factors convert the generic maps into specific maps related to the values obtained in the simulations.

Once the free power turbine map is known, for a given fuel flow a relative rotational speed is selected and guessing the value of $(\Delta h/T_{in})$ in the turbine's map the corresponding efficiency can be obtained interpolating. Then, by means of the definition of turbine efficiency, equations from (4-3) to (4-6), it is possible to determine the corresponding pressure ratio PR.

$$\eta_t = \frac{T_{in} - T_{out}}{T_{in} - T'_{out}} = \frac{\frac{\Delta T}{T_{in}}}{1 - \frac{T'_{out}}{T_{in}}} \tag{4-3}$$

$$\frac{T'_{out}}{T_{in}} = \left(\frac{P_{out}}{P_{in}}\right)^{\frac{\gamma-1}{\gamma}} = \left(\frac{1}{PR}\right)^{\frac{\gamma-1}{\gamma}} \tag{4-4}$$

$$\Delta h = c_p \Delta T \tag{4-5}$$

$$\eta_t = \frac{\frac{\Delta h}{c_p T_{in}}}{1 - \left(\frac{1}{PR}\right)^{\frac{\gamma-1}{\gamma}}} \tag{4-6}$$

To check that the guessing value of $(\Delta h/T_{in})$ is correct, the pressure ratio is calculated as the ratio between the turbine inlet pressure and the turbine outlet pressure, which due to full expansion is the atmospheric pressure. When both pressure ratios agree, the guessed value is the actual value, and as a result, it has been obtained for the same fuel flow, different $(\Delta h/T_{in})$ when changing the rotational speed of the turbine. Finally multiplying $(\Delta h/T_{in})$ times the turbine inlet

temperature and time the mass flow, the work extracted from the turbine can be calculated. This procedure is summarised in Figure 4-5, where a block diagram represents the followed steps.

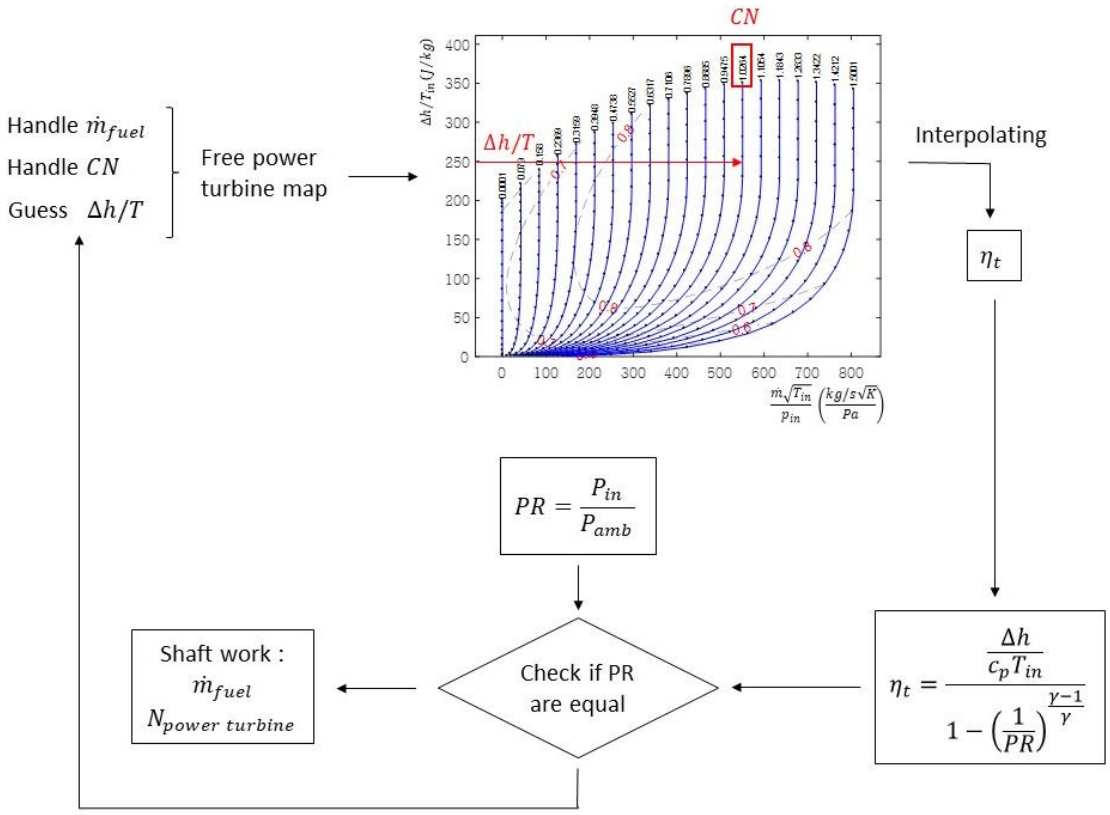

Figure 4-5. Iterative process followed to obtain the free power turbine's work for different turbine rotational speeds.

As a result, Figure 4-6 shows the free power turbine work as a function of the fuel flow for different speed lines.

To verify the accuracy of the process above, the power output of the design point obtained by Turbomatch and by the developed procedure have been compared. A relative error of 2.15% has been obtained. This discrepancy may be addressed to diverse reasons:

- The efficiency used by Turbomatch is not exactly the same as the one obtained interpolating. In addition, to the error introduced when interpolating.

- The assumed ideal gas constant, specific heat capacity at constant pressure and adiabatic index, used to calculate the pressure ratio, are not the same as the ones that Turbomatch uses.

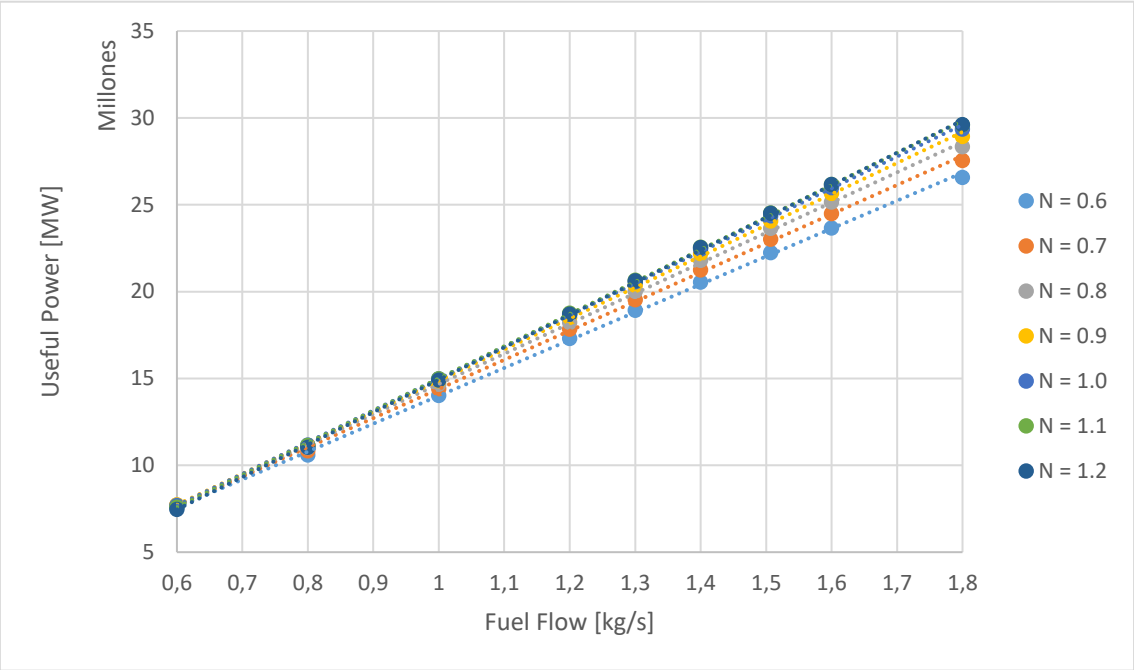

Figure 4-6. Free turbine performance when fuel flow and rotational speed variate

As it can be appreciated in Figure 4-6, as the power output increases the injected fuel differs more depending on the rotational speed of the free turbine. Therefore, the matching between the gas turbine and the propeller becomes more important for a higher power setting.

5 OVERALL MARINE POWER PLANT PERFORMANCE

Once the propulsion power plant is assembled, the next step is to analyse the performance of the different operational modes. This thesis focuses in the second operational mode, where the prime mover is the gas turbine due to diverse reasons are given explicitly in the following section.

On the one hand, a performance study of the ambient temperature has been carried out using Turbomatch software. The reason for doing this is that gas turbines are quite susceptible to ambient temperatures, whereas Diesel engines are barely influenced, as it can be seen Figure 5-1.

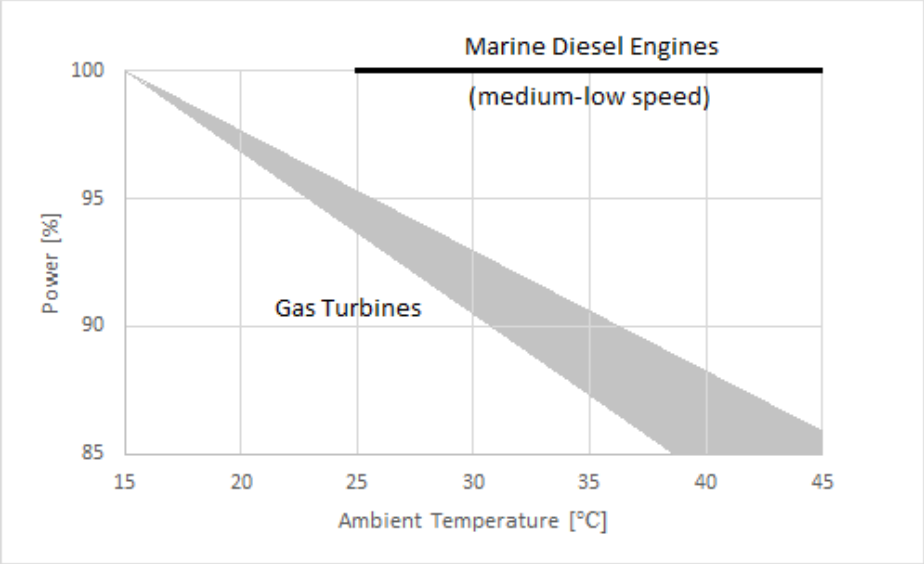

Figure 5-1. Influence of ambient temperature on diesel and gas turbine engines [24]

Since during cruise a vessel may encounter different climatic conditions from place to place, the behaviour of the whole power plant will be affected. Therefore, a study of the gas turbine performance has been carried out varying the temperature from -10 to 40 degrees Celsius.

On the other hand, over time gas turbines engines undergo performance deterioration. This degradation can be produced by diverse phenomena. However, this process is accelerated by the presence of sea salt in the air, thus

for the marine application, it is paramount to consider this performance degradation.

Essentially, sea salt accumulates over compressor blades, reducing the space available for them. Moreover, the erosion provoked by the salt advance distorts the profile of the blades. Then, the outgoing air from the compressor is introduced into the burner, where the combustion takes place. The presence of salt in the air will lead to sulfidation; this process accelerates corrosion appearance and it is detrimental to turbine performance. After prolonged operation under this condition, both compressor and turbine are said to be fouled.

In order to study the influence of the engine degradation over the system's performance, several simulations have been carried out using Turbomatch software.

Both studies, temperature and degradation influence on marine gas turbine performance, show engine's performance at part load and full load operation. In the first case, additional fuel is consumed increasing the cost of the operation. Whereas, for full power, it can be seen how the maximum power is limited with the increase of the temperature or level of degradation, which is translated in a speed reduction.

5.1 Theoretical background

Beforehand analysing the performance of the gas turbine under ambient temperature variation or degradation, a brief explanation is given to understand the engine operation for ideal conditions: constant ambient temperature and no engine degradation.

Initially, the power that feeds the ship propellers is delivered by the free power turbine of the gas engine. This power output is given by equation (5-1).

$$Power\ Output = \left(\dot{m}_{air} + \dot{m}_{fuel}\right) c_{p_{gas}}\, \Delta T_{across\ power\ turbine} \qquad \textbf{(5-1)}$$

To increase the power obtained, the right part of the above equation (5-1) must be increased. In other words, the gas turbine must work harder in order to produce higher amounts of gas at certain temperature and pressure. The higher

the amount of gasses that expand in the free power turbine the higher the power output would be. Thus, the increase of inlet mass flow is necessary. To ingest higher quantities of air, the compressor has to rotate faster and to do so, fuel consumption must increase. Consequently, higher pressure ratio and turbine entry temperature are achieved.

Concerning the pressure ratio increase, it can be seen how as the compressor spins faster, the work transmitted to the working fluid increases and so the temperature at the exit of the component. If the ambient temperature remains constant (T_{in}) it can be appreciated through equation (5-2) that an increase in the outlet temperature of the compressor implies an increase in the pressure ratio.

$$\frac{P_{out}}{P_{in}} = \left(\frac{T_{out}}{T_{in}}\right)^{\frac{\gamma}{\gamma-1}} \quad \textbf{(5-2)}$$

On the other hand, considering that the combustor inlet temperature is higher plus the additional fuel burned to accelerate the compressor, turbine entry temperature will undergo an increase. Which will contribute to the power augmentation, however, temperature rise across the free power turbine will not experiment such an increase since the increase of TET results in an increase of the turbine outlet temperature.

Another way of analysing the same performance is by observing Figure 5-2, which shows a typical compressor map.

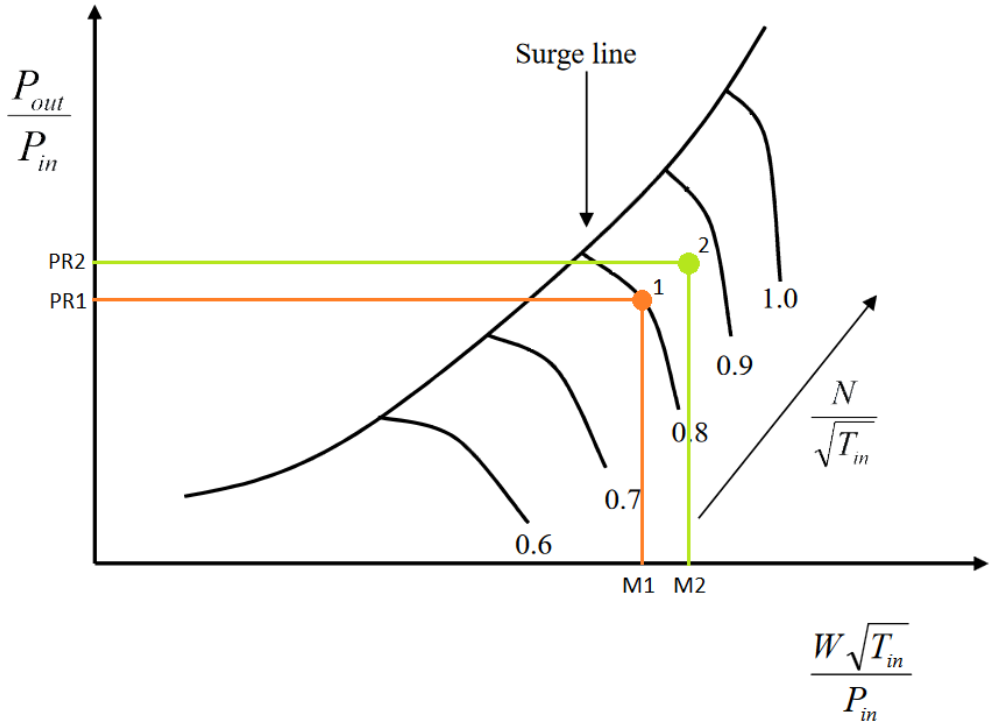

Figure 5-2. Operating point displacement on compressor's map due to an increase of the output work

In Figure 5-2 is plotted the pressure ratio (p_{out}/p_{in}) against the non-dimensional mass flow ($m\sqrt{T_{\text{in}}}/P_{in}$) for many constant rotational speeds ($N/\sqrt{T_{in}}$). Assuming that the compressor is operating at point 1, with a corresponding non-dimensional mass flow ($W\sqrt{T_{in}}/P_{in}$) and pressure ratio (PR_1), at a constant ambient temperature (T_{in}). When higher power output is required, as it has been demonstrated before, compressor rotational speed is increased. Therefore, the operating point of the compressor will shift to point 2, towards higher rotational speeds. As it can be appreciated in the compressor's map and considering that T_{in} remains constant, the new operating point is characterised for presenting a higher mass flow, higher rotational speed and consequently higher pressure ratio.

Regarding the efficiency, it can be demonstrated that when an increase in power output occurs at a constant ambient temperature, the thermal efficiency of the engine will increase as well. Previously, it was made clear that a required increase in power output implies an increase in fuel flow, which in turn increases

the right term of the equation (5-1). But the thermal efficiency of a gas engine with a free power turbine is given by equation (5-3) as shown below:

$$\eta_{th} = \frac{Power\ Output}{Heat\ Input} = \frac{\left(\dot{m}_{air} + \dot{m}_{fuel}\right) c_{p_{gas}}\, \Delta T_{across\ power\ turbine}}{\dot{m}_{fuel}\, FCV} \quad \textbf{(5-3)}$$

Therefore, an increase in power output, which means more fuel, will cause an increase in both terms of the equation (5-3). However, the numerator increases faster than the denominator for higher power setting, resulting in a thermal efficiency rise. The relation between the thermal efficiency and the power output is represented by a curve instead of a straight line since when the power output increases, although the inlet mass flow and the fuel flow increase as well, the temperature difference across the free power turbine decreases. Indeed, this is causing an increase in thermal efficiency but the rate of this increase is slowing down, as more and more power output is required.

Finally, the specific fuel consumption is briefly analysed by means of equation (5-4), as it can be seen the specific fuel consumption of the engine decreases as the power output increases.

$$SFC = \frac{Fuel\ Flow}{Power\ Output} = \frac{\dot{m}_{fuel}}{\left(\dot{m}_{air} + \dot{m}_{fuel}\right) c_{p_{gas}}\, \Delta T_{across\ power\ turbine}} \quad \textbf{(5-4)}$$

As it has been explained above, when the power output is increased, both the numerator and the denominator will increase. Independently of the power output the numerator will be always lower compared to the denominator, therefore the ratio will decrease and thus the SFC will fall as the power output is increased. In the same way, as in the efficiency, this descent is represented by a curve and not a straight line. Owing to the same reasons as before, as the power output increases the temperature difference across the free power turbine reduces.

5.2 Ambient temperature effect

Climate conditions in the sea change constantly and especially the ambient temperature. As it has been stated before, the performance of marine gas turbines is strongly influenced by temperature, and its alteration might have a

positive or negative effect, depending on whether the engine operates at higher or lower ambient temperatures. Therefore, a performance study varying this parameter has been carried out. To do so, the behaviour of the engine has been simulated for the whole power output range, changing only the ambient temperature from -10 up to 40 Celsius degrees. Which corresponds to ISA -25 and ISA +25. Below it has been analysed the engine's response when the ambient temperature variates for a demanded power output.

Essentially, when the ambient temperature rises the air tends to expand, occupying larger volumes and thus, reducing air's density. This means that for the same volume of air ingested by the gas engine, less air mass flow will go through it. In Figure 5-3, where inlet mass flow is plotted against power turbine, it can be appreciated how the increase in ambient temperature reduces the amount of inlet mass flow.

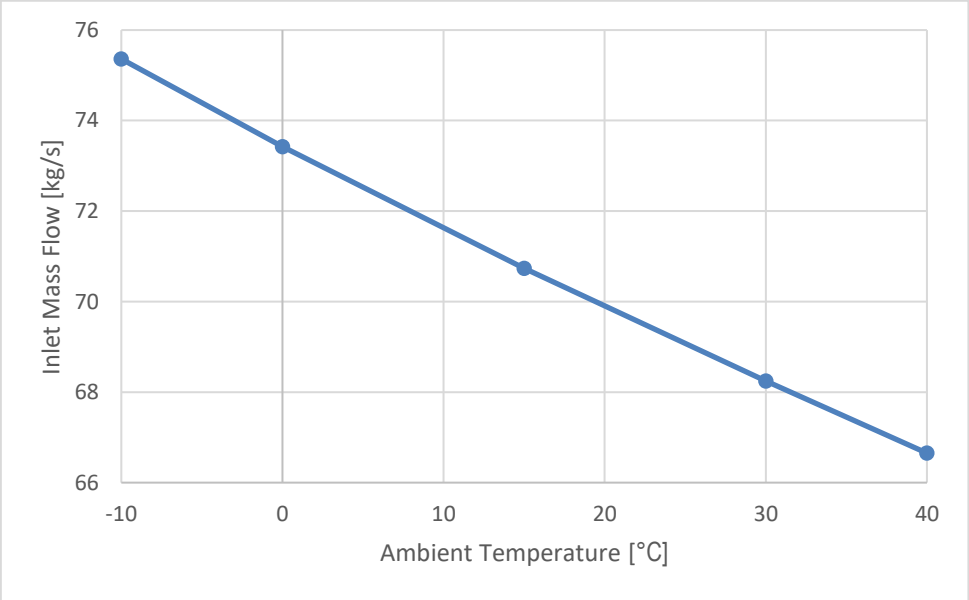

Figure 5-3. Inlet mass flow variation as a function of the ambient temperature for a constant power output

In order to keep the same power output, a higher amount of air must be expanded in the free power turbine and therefore, it is necessary to increase the inlet mass flow. To do so, compressor's rotational speed is augmented by means of higher fuel consumption. The parameter used to represent the rotational speed of the

compressor is the CN, which depends on the compressor inlet temperature and the design point rotational speed as it has been mentioned before. Figure 5-4 demonstrates that both fuel flow and compressor rotational speed, are incremented when the ambient temperature rises.

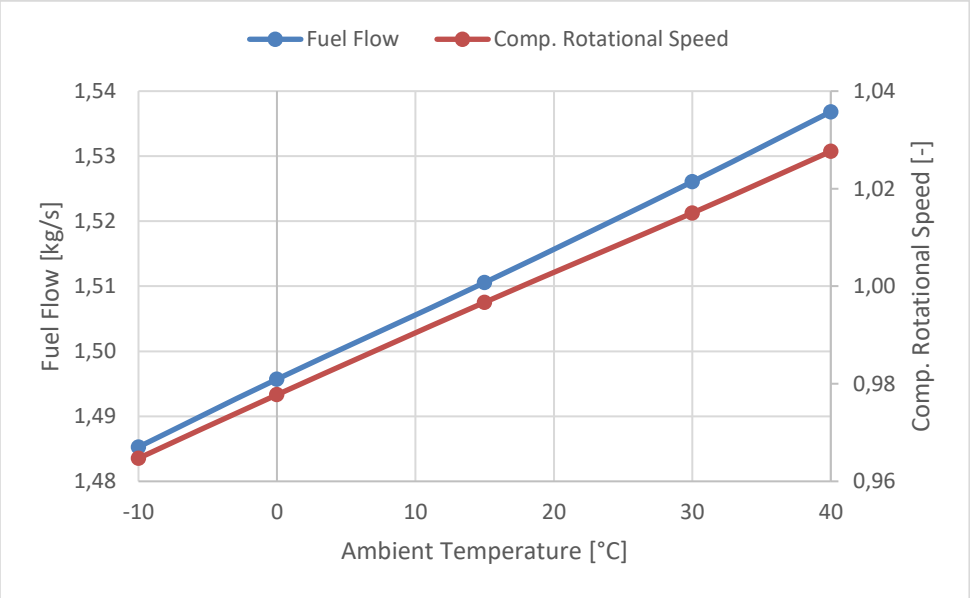

Figure 5-4. Fuel flow and compressor rotational speed as a function of ambient temperature for a constant power output

Another way of analysing the behaviour of the pressure ratio when the ambient temperature increases is by means of the compressor map. Assuming that the engine is operating at point 1 in Figure 5-5, as it has been demonstrated before, a rise of the ambient temperature will reduce the inlet mass flow, therefore the operating point will shift towards the right side of the map. In addition, even though the rotational speed has increased, as the rotational speed lines are represented by means of $N/\sqrt{T_{in}}$, the temperature increase will overcome the increase in rotational speed and the operational point will move towards a lower speed line or downwards in the map. Finally, the new operational point will be represented by a lower inlet mass flow, lower speed line and therefore, by a lower pressure ratio.

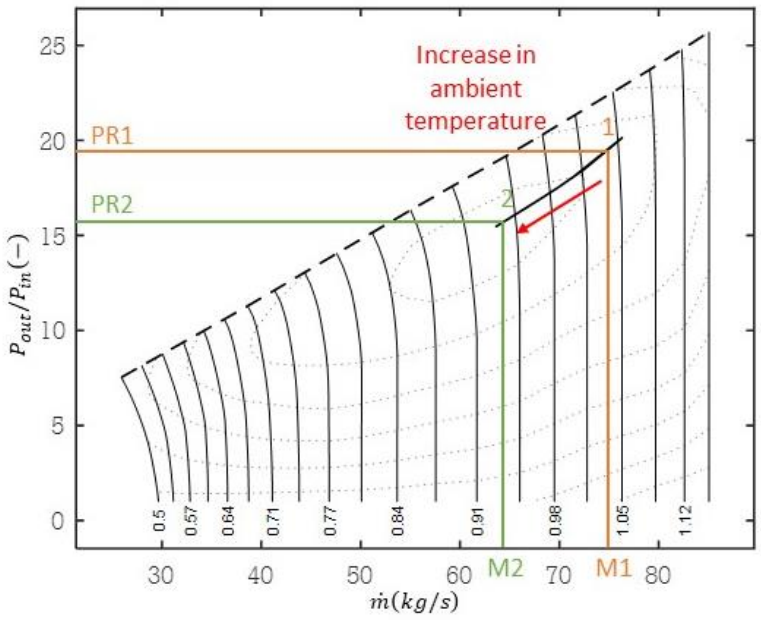

Figure 5-5. Operating point displacement on compressor's map due to an increase of the ambient temperature

According to (5-2), although compressor outlet temperature rises for higher rotational speeds, due to the higher work; the temperature ratio drops and as it has been stated before the pressure ratio as well. Figure 5-6 shows the pressure ratio fall due to the increase in ambient temperature.

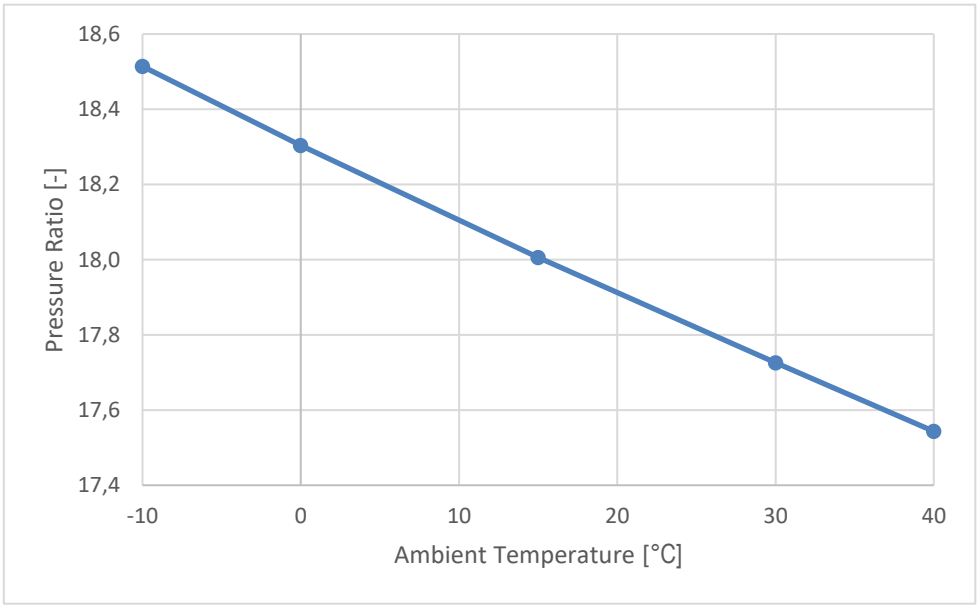

Figure 5-6. Compressor pressure ratio as a function of the ambient temperature for a constant power output

Regarding the thermal efficiency and the specific fuel consumption behaviours, it can be appreciated in Figure 5-7 that as ambient temperature increases the efficiency obtained is lower and the SFC higher. If a constant power output is considered as the ambient temperature increases lower values of efficiency and higher values of SFC are obtained. Basically, it is due to the fuel increase required to compensate the air mass flow lack.

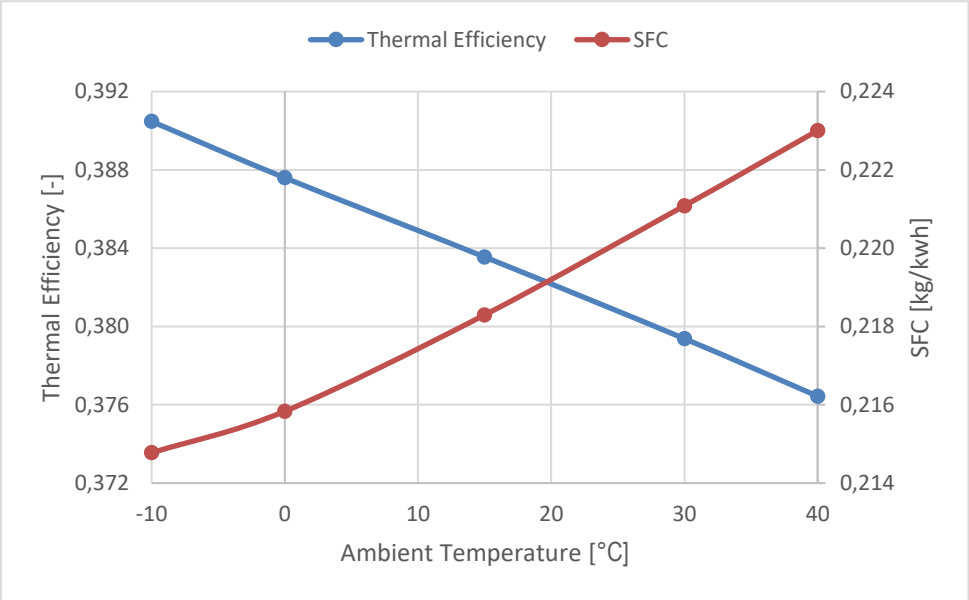

Figure 5-7. Thermal efficiency and specific fuel consumption as a function of the ambient temperature for a constant power output

The operation of the engine under low ambient temperature is desired not only because higher thermal efficiency can be achieved, but also due to lower turbine entry temperatures that are used. When the engine inlet temperature is higher, compressor outlet temperature increases. This in addition to the extra fuel used to augment the compressor rotational speed, leads to higher TET which reduces the engine's working life and augments the frequency of maintenance. Figure 5-8 shows TET behaviour under ambient temperature variation for a constant power output.

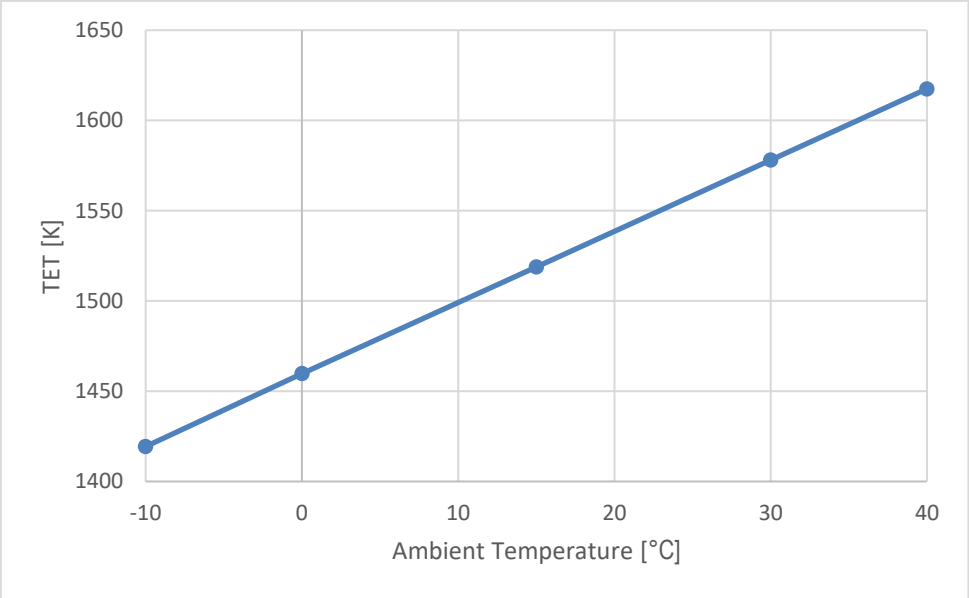

Figure 5-8. Turbine entry temperature as a function of ambient temperature for a constant power output

Herein it is summarised the changes that occur in the engine's performance parameters when a power output is demanded and the ambient temperature increases.

- The inlet mass flow decreases due to density decrease.
- The fuel flow increases in order to increase the rotational speed.
- The pressure ratio falls due to the drop of the temperature ratio across the compressor.
- As a consequence of the previous reasons, the turbine entry temperature increases, the thermal efficiency falls and the specific fuel consumption increases.

With the purpose of showing the quantitative variation of the gas turbine engine performance parameters, a sample of three different power outputs: 10 MW, 15 MW and 25 MW is exhibited in Table 5-1.

Table 5-1. Performance parameter results for different power outputs when the ambient temperature increases

MW	PARAMETER	ISA 0 (15°C)	ISA +25 (40°C)	Variation [%]
10	Inlet Mass Flow (kg/s)	49,40	46,40	-6,06
	Fuel Flow (kg/s)	0,74	0,75	2,30
	Thermal Efficiency (-)	0,316	0,309	-2,02
	Non-Dim. Comp. Rot. Speed (-)	0,81	0,84	3,34
	TET (K)	1207,1	1295,1	7,29
	Pressure Ratio (-)	11,29	10,99	-2,60
	SFC (kg/kWh)	0,264	0,270	2,08
15	Inlet Mass Flow (kg/s)	58,13	54,78	-5,76
	Fuel Flow (kg/s)	1,00	1,02	2,02
	Thermal Efficiency (-)	0,351	0,344	-1,88
	Non-Dim. Comp. Rot. Speed (-)	0,89	0,92	3,40
	TET (K)	1311,02	1402,59	6,98
	Pressure Ratio (-)	13,82	13,48	-2,45
	SFC (kg/kWh)	0,238	0,243	1,97
25	Inlet Mass Flow (kg/s)	70,74	66,65	-5,78
	Fuel Flow (kg/s)	1,51	1,54	1,74
	Thermal Efficiency (-)	0,384	0,376	-1,85
	Non-Dim. Comp. Rot. Speed (-)	1,00	1,03	3,11
	TET (K)	1512,88	1617,51	6,92
	Pressure Ratio (-)	18,01	17,54	-2,57
	SFC (kg/kWh)	0,218	0,223	2,16

5.2.1 Ambient temperature effect on the marine propulsion plant

Previously, in part-load performance, it has been seen that for negative temperature conditions, fuel consumption is increased and engine hot section operating life reduces. Nevertheless, when the gas turbine is operating at maximum power and the ambient temperature is higher than the standard ambient conditions, the delivered power is limited, the engine is not able to reach the same power output as in standard conditions. The reason for this is that the maximum power depends on the highest turbine entry temperature than the materials can stand, and at a certain point, this temperature cannot be overcome since engine integrity is in danger. The engine control system ensures that the maximum TET is not exceeded by cutting out the fuel increase and effectively the propulsive system starts losing power. If the gas turbine cannot provide the required power to reach the demanded velocity, the watercraft speed range lessens. Therefore, warship power plant designers must consider this inconvenient to select a propulsion plant which accomplishes the established requirements for a specific mission independently of the ambient temperature.

Hot section materials work under high thermal loads and thus any temperature rise affects catastrophically engine operating hours, i.e. a 10 K rise of maximum nozzle guide vanes temperature causes blade creep life to decrease 40 % [25]. In order to study the power loss, and therefore the vessel's speed loss, due to high ambient temperatures, it has been assumed that the design point corresponds to the desirable TET and an additional 25 K are set as the maximum operable TET, from which the control system does not increase the fuel rate.

Table 5-2 shows the maximum power that the gas turbine is capable to deliver when ambient temperature increases. This limit has been imposed by the maximum attainable TET, which it has been assumed of 1535 K. In addition to the power, it is represented the power loss relative to the standard atmosphere, the maximum vessel's speed and the vessel's speed loss relative to the standard atmosphere from ISA 0 (15 °C) up to ISA 25 (40 °C), as well as the deterioration of the thermal efficiency and the specific fuel consumption that the engine experiments due to ambient temperature rise.

Table 5-2. Engine's maximum performance as ambient temperature rises

	Maximum Power (MW)	Power Loss (MW)	Variation (%)	Speed (knots)	Speed loss (knots)	Variation (%)
ISA 0	25.740	0.000	0.00	28.34	0.000	0.00
ISA +5	24.795	0.945	3.67	28.28	0.058	0.20
ISA +10	23.867	1.873	7.28	28.01	0.323	1.14
ISA +15	22.933	2.807	10.91	27.74	0.597	2.11
ISA +20	22.022	3.718	14.44	27.46	0.874	3.08
ISA +25	21.129	4.611	17.91	27.18	1.153	4.07

	Thermal Efficiency (-)	Thermal Eff. Loss (-)	Variation (%)	SFC (kg/kWh)	SFC loss (kg/kWh)	Variation (%)
ISA 0	0.384	0.000	0.00	0.217	0.000	0.00
ISA +5	0.382	0.002	0.63	0.217	0.001	0.39
ISA +10	0.379	0.005	1.41	0.219	0.002	1.14
ISA +15	0.375	0.009	2.35	0.221	0.005	2.20
ISA +20	0.372	0.013	3.32	0.224	0.007	3.43
ISA +25	0.368	0.017	4.36	0.227	0.010	4.78

The information given in the Table 5-2, indicates that as ambient temperature increases the power decreases and therefore there is a reduction of the vessel's speed. However, speeds reduction is meaningless compared to the power loss. As a matter of fact, at ISA +25 (40°C), a power loss of 17.91% only implies a speed loss of 4%, which represents a speed reduction of practically a knot. In addition, the engine's performance degrades consuming more fuel and at lower thermal efficiencies. Therefore, as ambient temperature increases, lower maximum power is achieved and although the speed is not relevantly affected the specific fuel consumption increases and the thermal efficiency reduces.

The fact that the vessel's speed does not experiment such a reduction can be explained through the propeller's law. As it has been mentioned in section 4 the propeller law follows a cubic curve, which means that a little increase in speed requires a high amount of power, whereas a large power reduction implies a little speed reduction. Figure 5-9 shows graphically the maximum power and speed attainable, when the maximum TET is reached as a consequence of the ambient pressure rise.

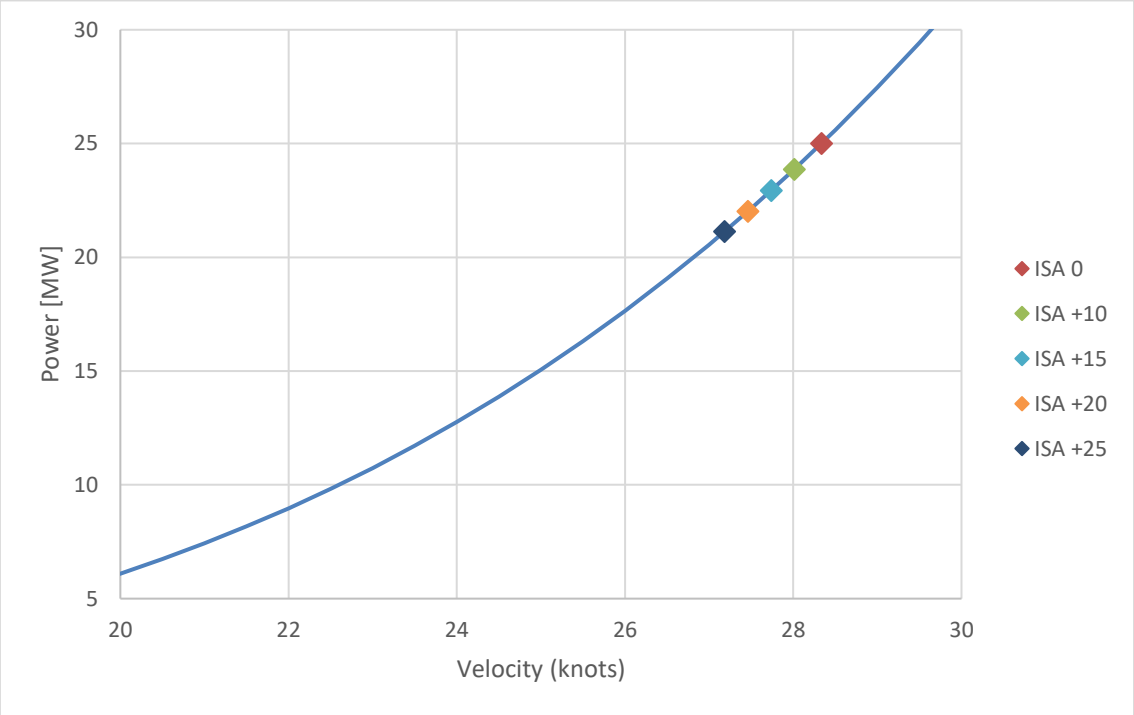

Figure 5-9. Maximum power supplied by the gas engine over propeller's law for different ambient temperatures

Although this power limitation barely modifies the vessel speed ranges for the second operational mode, the fuel consumption loss due to high ambient temperatures is significant and leads to the following idea:

Under a high ambient temperature, when the vessel is sailing at a speed close to the change mode speed, around 21 knots, it could be worthy to reduce vessel's speed in order to use the diesel engines, instead of the gas turbine, and save some fuel, considering that the diesel engines are not affected by the ambient temperature. Depending on the circumstances, the reduction in speed may not

be a problem and from an economical point of view it seems interesting. In order to give an idea of the possible fuel savings, in Table 5-3 it is presented the specific fuel consumption for the first operational mode, when the prime movers are the diesel engines, and for the second operational mode, when the prime mover is the gas engine. As it can be seen below the specific fuel consumption increases with the increment of the ambient temperature for the gas engine mode. Whereas the specific fuel consumption of the diesel engine remains constant since it is unaffected by the ambient temperature.

Table 5-3. Fuel savings due to the use of different operational modes as ambient temperature increases

	Diesel Engines	Gas Turbine	Speed Loss (%)
Speed (knots)	20	21	4.76
Temperature (K)	SFC (g/kWh)	SFC (g/kWh)	Fuel Savings (%)
ISA 0	218.87	295.66	35.09
ISA +5	218.87	297.10	35.75
ISA +10	218.87	298.54	36.40
ISA +15	218.87	299.94	37.04
ISA +20	218.87	301.37	37.70
ISA +25	218.87	302.78	38.34

In spite of the speed loss due to the operating mode change, from the gas turbine utilization to the diesel engine, the fuel savings are sufficient remarkable, between 35% and 38% depending on the ambient temperature. Besides, the gas engine is not working at design point or close to it, which worsens its consumption.

5.3 Gas engine degradation effect

In this section, an independent study of the compressor and turbine has been carried out, in order to appreciate the effects of the different degradation mechanisms that take place in the marine environment. Moreover, it has been analysed the performance of the engine for a constant power setting, the power limitations due to degradation and their consequences over the propulsive plant.

5.3.1 Components degradation

Marine gas turbines are sternly affected by the humid environment and the ingestion of large amounts of sea salt carried in the maritime air. Therefore, as time goes by engine components degrade and their performance decline. Some components are more susceptible to certain mechanisms of performance deterioration than others. For instance, compressor is mainly affected by fouling. This is attributed to the fact that the compressor is the engine's inlet and thus, it behaves as a particle filter retaining air impurities above all at the front stages. Turbines are also influenced by degradation, though in this case other mechanisms are responsible for it, such as erosion and corrosion. The first one, is distinguished by the loss of material due to fuel or air impurities impact, whereas, the second one, is due to the chemical reactions that befall between the component material and the salt present in the air in contact with the sulphur present in the fuel. Other components, such as the combustor or the free power turbine are less exposed to degradation. Combustion efficiency is barely reduced due to degradation, even if combustor outlet temperature profile is distorted and will have an effect on turbine's performance. Regarding the free power turbine, since it is at the engine's outlet its degradation level will not be comparable with the compressor's or the compressor-turbine's degradation.

5.3.1.1 Compressor fouling

Compressor degradation is simulated by Turbomatch through degradation scaling factors, which correspond to pressure ratio degradation, non-dimensional mass flow degradation and isentropic efficiency degradation. These scaling factors have been applied at different degrees to simulate different levels of fouling degradation. Moreover, they have been simulated jointly and severally in order to observe the influence of each of them. As a result, it has been found that the isentropic efficiency degradation causes the greatest impact above all the degradation factors, and that the difference between the degradation of the isentropic efficiency and the degradation of all the deterioration factors together is minor. Although, this could be unexpected the same trends were obtained in [26].

Figure 5-10 to Figure 5-12 represent the performance of the gas engine at constant fuel flow under deteriorated operation. Essentially, when the compressor is operating under fouling conditions, the salt present in the air deposits on the compressor surface reducing the space between blades and hindering the air's path. Consequently, the inlet mass flow drops drastically, as it can be seen in Figure 5-10 for a 5% degradation there is a reduction of 2.75% in the inlet mass flow.

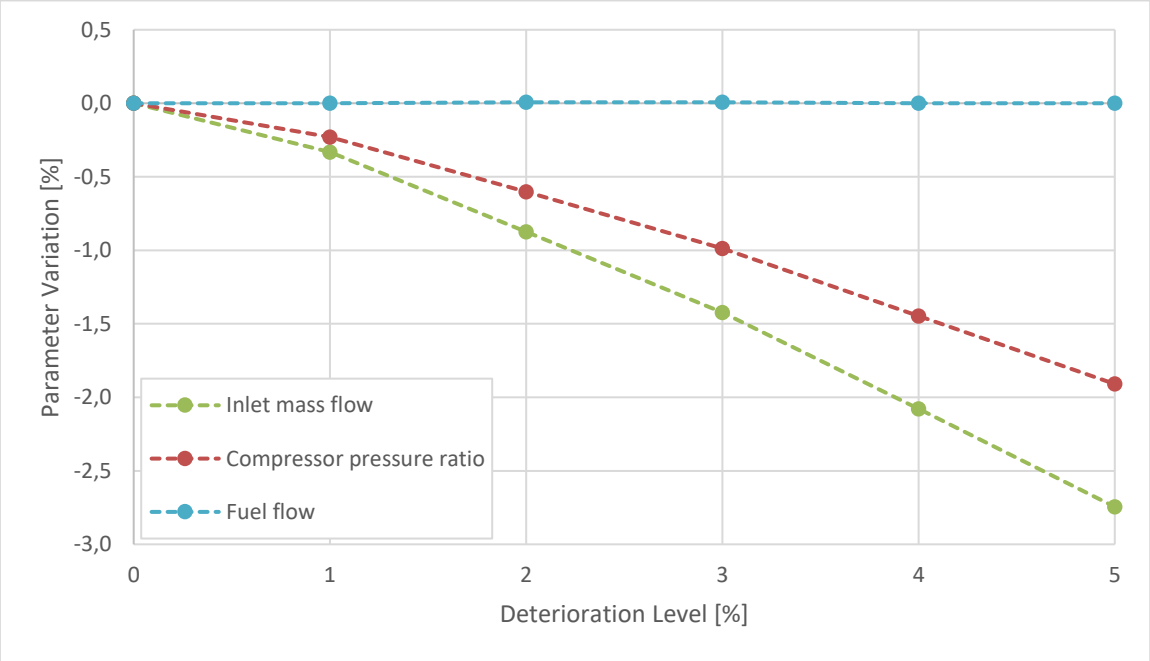

Figure 5-10. Degradation of the gas engine's performance due to fouling

As a result of compressor isentropic efficiency degradation, there is a reduction of the pressure ratio. However, since the reduction in the efficiency is higher than the reduction of the pressure ratio, according to equation (5-5) the temperature at the outlet of the compressor must increase.

$$\eta_{comp} = \frac{T'_{out} - T_{in}}{T_{out} - T_{in}} = \frac{\frac{T'_{out}}{T_{in}} - 1}{\frac{T_{out}}{T_{in}} - 1} = \frac{\left(\frac{p_{out}}{p_{in}}\right)^{\frac{\gamma-1}{\gamma}} - 1}{\frac{T_{out}}{T_{in}} - 1} = \frac{(PR)^{\frac{\gamma-1}{\gamma}} - 1}{\frac{T_{out}}{T_{in}} - 1} \quad \textbf{(5-5)}$$

For a 5% degradation, there is a reduction of 1.91% in the pressure ratio, whereas the isentropic efficiency experiments a reduction of 2.89%. Consequently, the

outlet temperature of the compressor rises leading to higher TET, since the simulations have been run for a constant fuel flow.

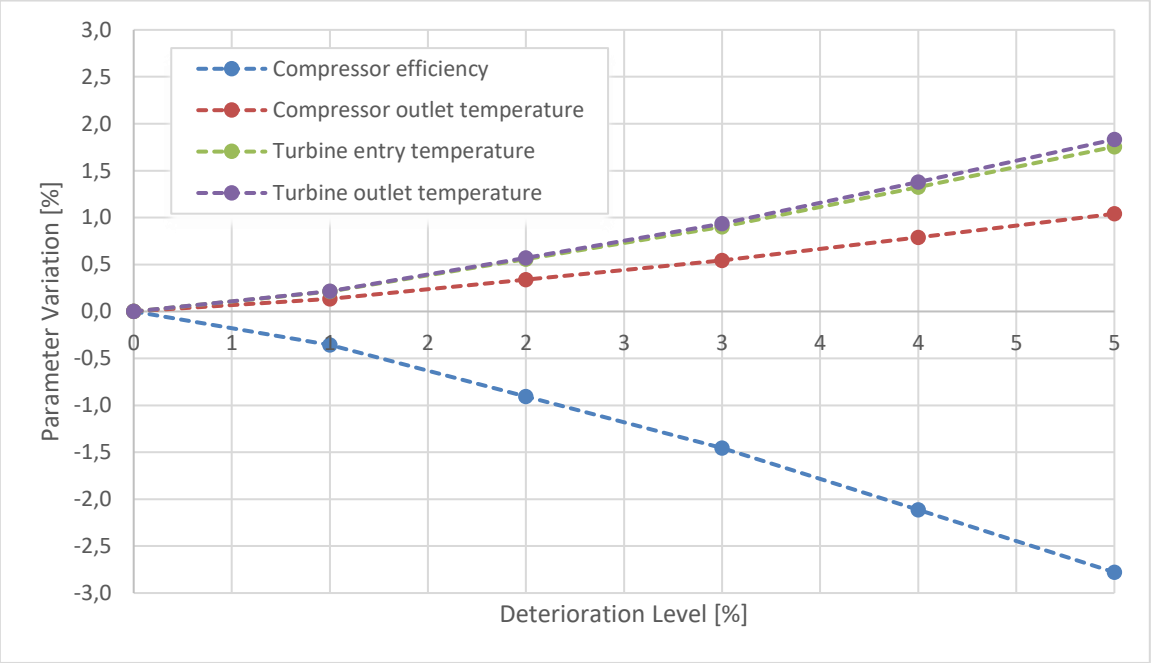

Figure 5-11. Degradation of the compressor efficiency and compressor and turbine temperatures

Moreover, in Figure 5-11 can be appreciated that the turbine entry temperature and the turbine exhaust temperature present the same growth rate. Nevertheless, as degradation progresses, a slight difference appears between them due to the mass flow reduction. When the inlet mass flow decreases, the amount of air for cooling decreases as well, ending with less available air to cool and higher exhaust temperatures.

The degradation of the compressor influences over the turbine's performance deteriorating its pressure ratio and efficiency, but in a lower degree. In the same way, the temperature variation across the turbine increases slightly and although it leads to higher power outputs, the mass flow reduction strongly deteriorates the resulting power output. For a 5% of degradation a reduction of 2.75% in the mass flow means a reduction of 1.72% in the power output.

Regarding the specific fuel consumption, which is the ratio between the fuel flow and the power output, since the fuel flow remains constant the SFC will degrade in the same way as the power output but inversely proportional. Thermal efficiency experiments the same behaviour, however in this case it is defined as the ratio between the power output and the heat input. As it can be appreciated in Figure 5-12 the heat input does not vary with degradation, as mass flow decreases the temperature increment through the combustor rises keeping the heat input constant. Thereby the power output controls the behaviour of the thermal efficiency. Finally, for a 5% of degradation the power output experiments a deterioration of 1.72%, the specific fuel consumption of 1.75% and the thermal efficiency of 1.71%.

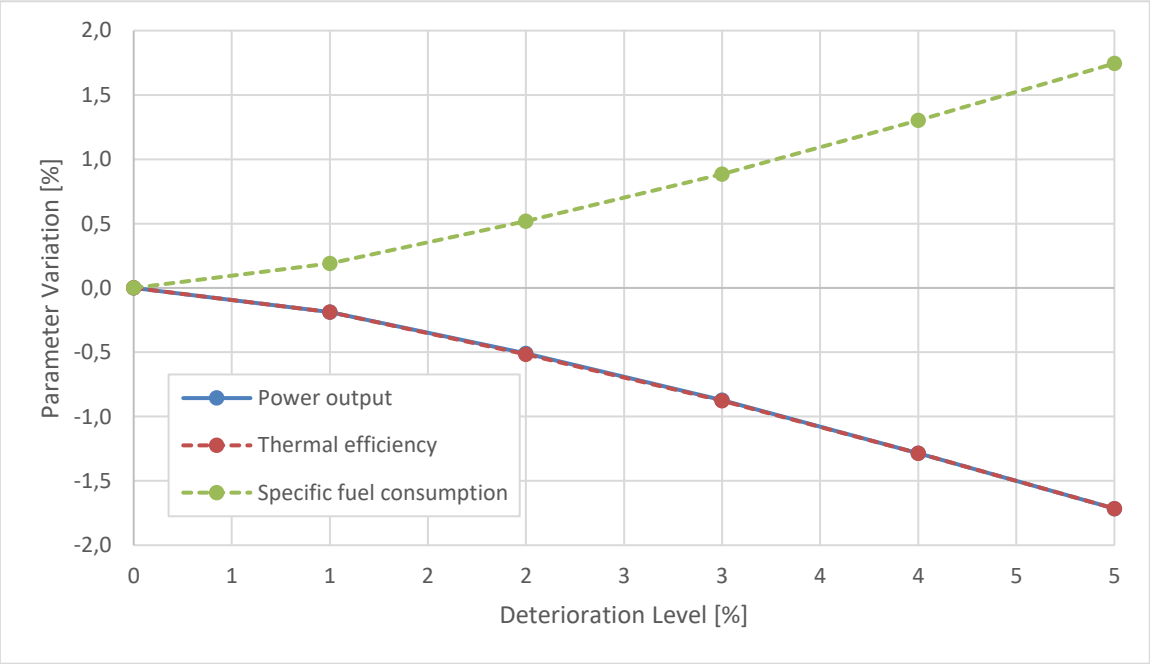

Figure 5-12. Degradation of the power output, thermal efficiency and specific fuel consumption due to compressor fouling

5.3.1.2 Turbine erosion

As in the compressor deterioration, the turbine deterioration has been simulated through degradation scaling factors, such as the non-dimensional mass flow degradation and the isentropic efficiency degradation. These scaling factors have been applied at different degrees to simulate different levels of fouling degradation. Moreover, they have been simulated jointly and severally in order to

observe the influence of each of them. And again, the influence of the thermal efficiency degradation has shown the greatest impact on the turbine deterioration.

Figure 5-13 represents the performance of the gas engine at constant fuel flow under erosion deterioration. The impact of the particles, present in the fuel-air mixture that goes through the turbine, provoke a material loss that distorts the blade profile surface deteriorating the expansion process and therefore, reducing the pressure ratio across the turbine. Moreover, the material removal increases the available area, allowing a higher mass flow. For instance, a degradation of 5% due to erosion, represents a 0.53% increase of the mass flow.

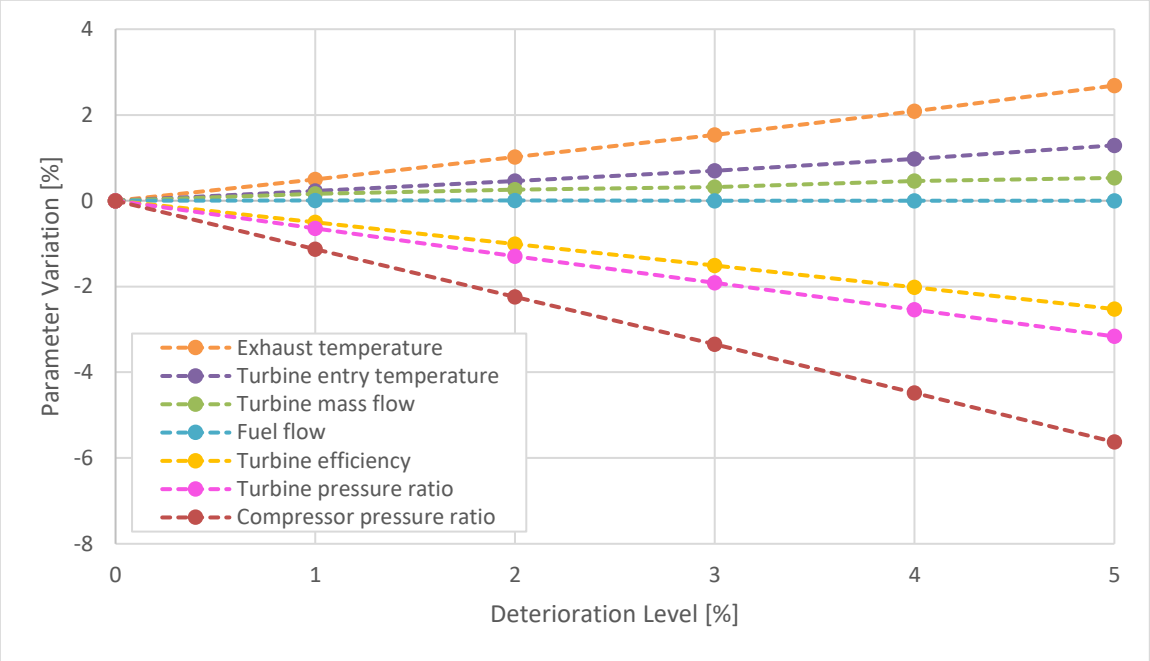

Figure 5-13. Variation of different engine parameters due to turbine erosion

The degradation of the turbine's performance is reflected by a 2.53% drop in the isentropic efficiency and a drop of 3.16% in the pressure ratio for a 5% degradation of the turbine. This leads to higher temperatures at the outlet of the turbine as degradation progresses, since the expansion ability of the turbine is decreasing. It can be justified by means of equation (5-6), where the reduction of the pressure ratio leads to an increase of the term on the right, and since the efficiency has been reduced due to the erosion, the temperature ratio must increase in order to verify the equation. Therefore, the temperature at the outlet

of the turbine must experiment a higher increase than the entry temperature as degradation progresses.

$$\eta_{turb} = \frac{T_{in} - T_{out}}{T_{in} - T'_{out}} = \frac{1 - \frac{T_{out}}{T_{in}}}{1 - \frac{T'_{out}}{T_{in}}} = \frac{1 - \frac{T_{out}}{T_{in}}}{1 - \left(\frac{p_{out}}{p_{in}}\right)^{\frac{\gamma-1}{\gamma}}} = \frac{1 - \frac{T_{out}}{T_{in}}}{1 - \left(\frac{1}{PR}\right)^{\frac{\gamma-1}{\gamma}}} \quad \textbf{(5-6)}$$

Figure 5-13, shows how the parameters above-mentioned react to turbine erosion. As the turbine degrades the work that drives the compressor reduces, and so the work that the compressor transmits to the fluid. As the ambient temperature remains constant, a reduction in the compressor work will lead to a reduction of the compressor outlet temperature and since the fuel flow is constant for the present simulation, lower TET will be reached. In addition, compressor pressure ratio will experience a deterioration as can be expected. For instance, a 5% degradation means a compressor pressure ratio reduction of 5.63% whereas the turbine pressure ratio reduction is 3.16%.

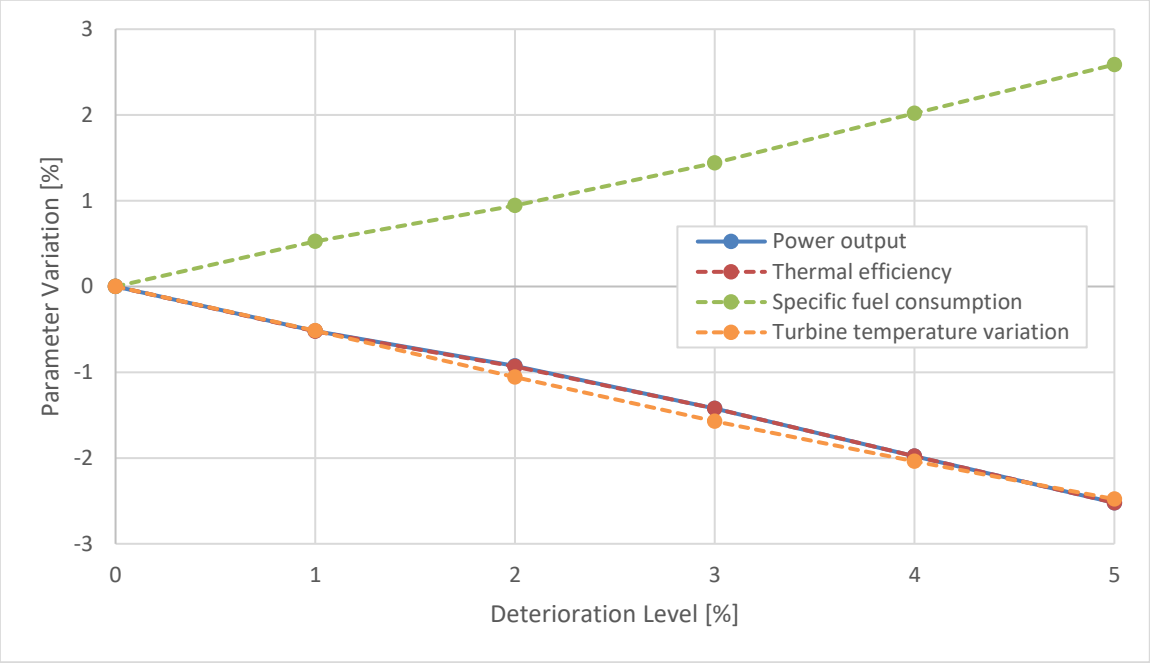

Figure 5-14. Degradation of the power output, thermal efficiency and specific fuel consumption due to turbine erosion

Figure 5-14 shows the detrimental impact caused by erosion on the power output, thermal efficiency and specific fuel consumption. For a 5% degradation, the

power output and the thermal efficiency decrease around 2.52%, and the specific fuel consumption increases around 2.59%. As in compressor fouling, thermal efficiency and specific fuel consumption depend completely on the power output behaviour. In this case, the power deterioration is due to the reduction of the temperature variation across the free power turbine, even if the mass flow has increased, it is not enough to compensate the temperature reduction along the turbine. Meanwhile, the mass flow across the turbine experiments a rise of 0.53% for 5% degradation, the temperature variation is decreased by a 2.48%.

5.3.2 Overall degradation effect

Herein it is presented the performance deterioration of the gas engine when it operates with a fouled compressor together with an eroded turbine and a certain power setting is required. The results are plotted for different levels of degradation when a power output of 25 MW is demanded.

From the results obtained with Turbormatch it can be appreciated that the combination of both effects results in a reduction of the mass flow ingested by the engine. For instance, a degradation of 5% means a reduction of 5.59% and as degradation progresses to 10% this reduction becomes into 11.72%. The mass flow is proportional to the power output and in order to supply the required power, the compressor must rotate faster to increase the amount of gasses expanded by the turbine. The rotational speed of the compressor rises by increasing the fuel flow, then for higher levels of degradation a higher fuel flow will be required. It can be seen how from a 5% to 10% of deterioration the fuel flow increases from 4.13% to 8.80%. In addition, the performance of compressor and turbine worsens with the presence of fouling and erosion, reducing the pressure ratio across both components, above all compressor pressure ratio. For a 5% degradation, the compressor pressure ratio experiences a reduction of 7.74% whereas the turbine pressure ratio 5.62%. Consequently, lower power is delivered and additional fuel is required in order to maintain the desired power setting. Since higher fuel flow is injected, the temperature at combustor exit will experience a significant rise. And this will lead to higher temperatures at turbine's exit. Moreover, since the turbine is degraded the expansion ability will be lower,

which at the same time will contribute in the turbine outlet temperature rise. And this is the reason why the turbine outlet temperature increases faster than the turbine inlet temperature as degradation progresses. For a 5% degradation, the inlet temperature experiments a rise of 4.60% and the outlet temperature of 6.63%, whereas for a 10% degradation the corresponding temperature increases are 10.16% and 14.33% according to the run simulations.

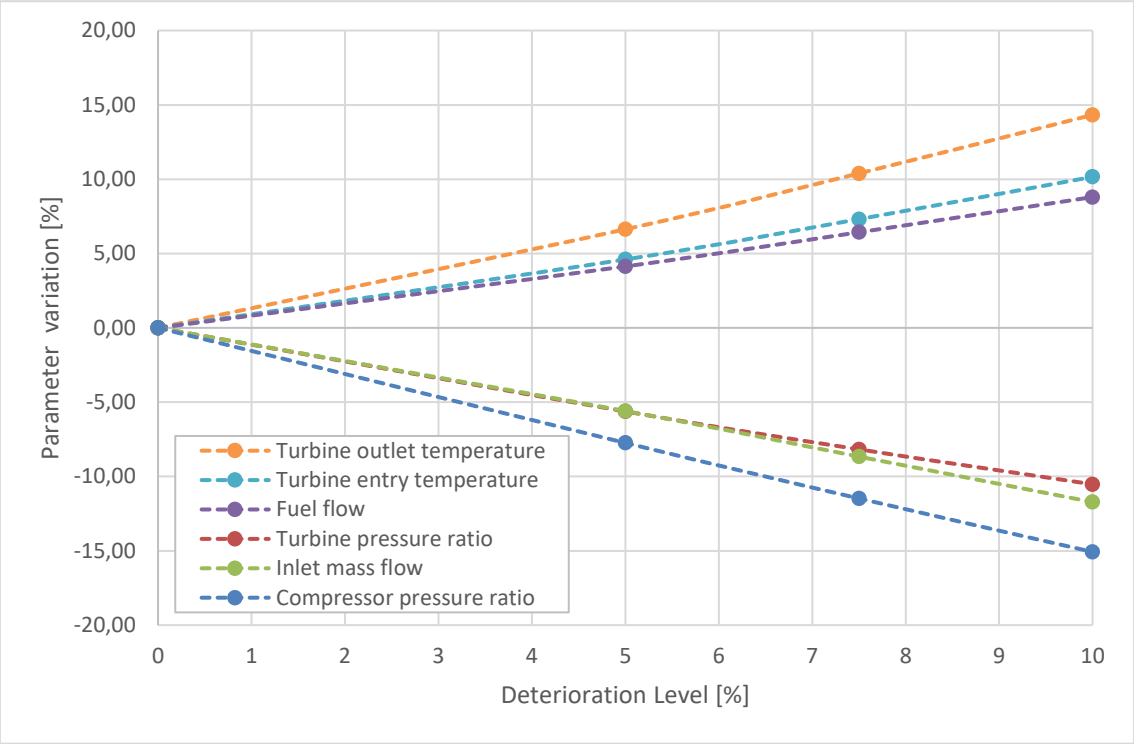

Figure 5-15. Engine parameters evolution as a function of the degradation for a constant power output of 25 MW

Finally, thermal efficiency and specific fuel consumption are represented in Figure 5-16 as degradation progresses. By reason of the factors above-mentioned, it can be appreciated how these parameters deteriorate in order to reach a certain power output. For instance, a 5% degradation leads to a 4.23% reduction in the thermal efficiency and a rise of 3.91% in the specific fuel consumption. For higher levels of deterioration, such as 10%, these parameters reach a value of 8.57% and 7.39%.

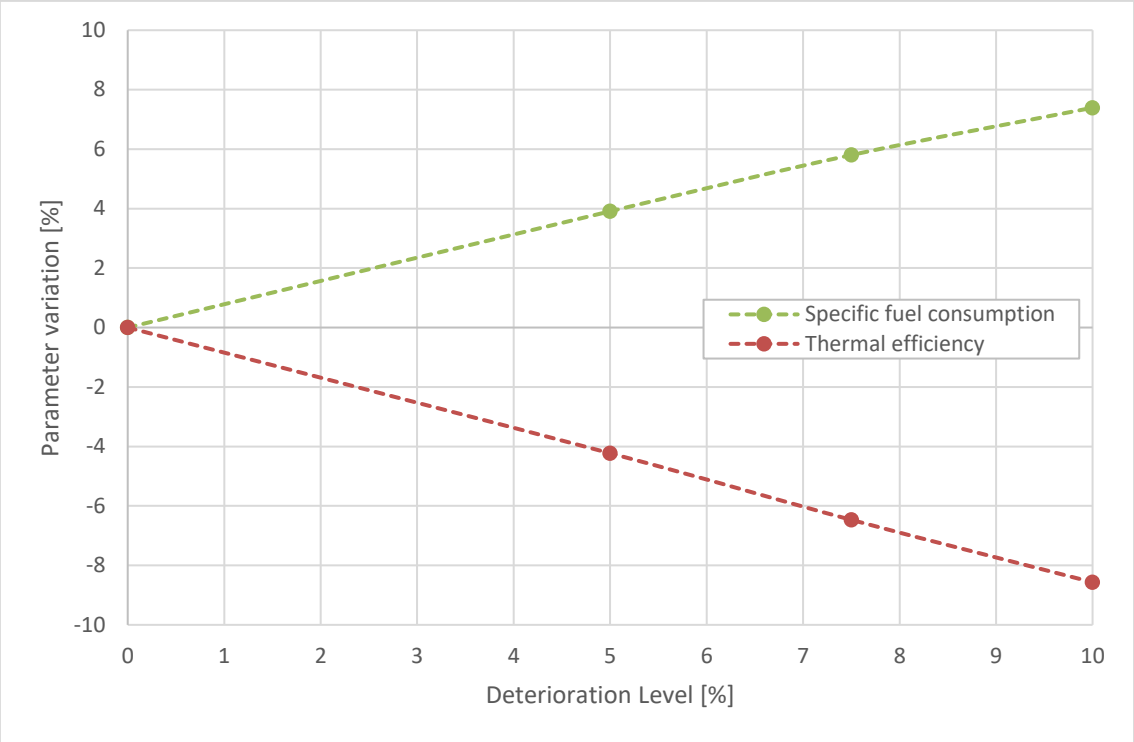

Figure 5-16. Thermal efficiency and specific fuel consumption evolution as a function of the degradation for a constant power output of 25 MW

With the purpose of showing the quantitative variation of the gas turbine engine performance parameters, a sample of three different power outputs: 10 MW, 15 MW and 25 MW is exhibited in Table 5-4,

Table 5-5 and Table 5-6.

Table 5-4. Engine performance for different degradation levels when the demanded power output is 10 MW

10 MW	Clean	Deteriorated			Deviation from clean performance		
Deterioration Level	0.0%	5.0%	7.5%	10.0%	5.0%	7.5%	10.0%
Inlet Mass Flow (kg/s)	49.60	46.71	45.31	43.88	-5.83	-8.65	-11.54
Fuel Flow (kg/s)	0.735	0.777	0.799	0.823	5.77	8.79	12.03
Compressor Pressure Ratio (-)	11.32	10.44	10.04	9.65	-7.78	-11.33	-14.76
Turbine Pressure Ratio (-)	3.75	3.52	3.42	3.31	-6.09	-8.92	-11.69
TET (K)	1208.6	1269.0	1303.1	1341.7	4.99	7.81	11.01
EGT (K)	876.2	939.5	974.5	1013.6	7.22	11.22	15.68
Thermal Efficiency (-)	0.315	0.298	0.290	0.281	-5.33	-8.00	-10.73
SFC (kg/kWh)	0.267	0.282	0.290	0.298	5.54	8.50	11.63

Table 5-5. Engine performance for different degradation levels when the demanded power output is 15 MW

15 MW	Clean	Deteriorated			Deviation from clean performance		
Deterioration Level	0.0%	5.0%	7.5%	10.0%	5.0%	7.5%	10.0%
Inlet Mass Flow (kg/s)	57.99	54.84	53.32	51.76	-5.43	-8.05	-10.74
Fuel Flow (kg/s)	0.994	1.043	1.070	1.097	4.94	7.59	10.39
Compressor Pressure Ratio (-)	13.79	12.75	12.27	11.82	-7.55	-11.00	-14.32
Turbine Pressure Ratio (-)	3.75	3.53	3.43	3.33	-5.94	-8.67	-11.30
TET (K)	1311.6	1375.1	1411.6	1451.7	4.84	7.62	10.68
EGT (K)	953.4	1020.1	1057.3	1097.9	6.99	10.90	15.16
Thermal Efficiency (-)	0.351	0.335	0.327	0.319	-4.60	-6.92	-9.26
SFC (kg/kWh)	.237	0.248	0.254	0.260	4.65	7.19	9.95

Table 5-6. Engine performance for different degradation levels when the demanded power output is 25 MW

25 MW	Clean	Deteriorated			Deviation from clean performance		
Deterioration Level	0.0%	5.0%	7.5%	10.0%	5.0%	7.5%	10.0%
Inlet Mass Flow (kg/s)	70.87	66.91	64.73	62.57	-5.59	-8.66	-11.72
Fuel Flow (kg/s)	1.513	1.575	1.610	1.646	4.13	6.43	8.80
Compressor Pressure Ratio (-)	18.03	16.63	15.96	15.31	-7.74	-11.48	-15.07
Turbine Pressure Ratio (-)	3.75	3.54	3.44	3.35	-5.62	-8.17	-10.52
TET (K)	1517.6	1587.5	1628.6	1671.8	4.60	7.31	10.16
EGT (K)	1107.8	1181.3	1222.9	1266.5	6.63	10.39	14.33
Thermal Efficiency (-)	0.383	0.367	0.359	0.350	-4.23	-6.47	-8.57
SFC (kg/kWh)	0.219	0.227	0.232	0.235	3.91	5.80	7.39

5.3.3 Degradation effect on the marine propulsion plant

Following the same approach as in the ambient temperature study, the maximum power output will be defined by the maximum turbine entry temperature admissible. Since TET increases with the engine degradation, at a certain point, when the maximum TET is reached, the control system stops increasing the fuel flow and effectively the propulsion system starts losing power. In order to study this effect over the propulsion plant performance a TET of 1535 K has been assumed as the maximum temperature that inlet turbine material can bear.

Table 5-7 presents for the maximum power output attainable due to degradation, the reached vessel's speed and the thermal efficiency and specific fuel consumption penalties caused by engine deterioration.

Table 5-7. Engine's maximum performance as degradation progresses

Deterioration	Maximum Power (MW)	Power Loss (MW)	Variation (%)	Speed (knots)	Speed Loss (knots)	Variation (%)
Clean	25,851	0	0	28,57	0	0
5%	23,096	2,755	10,66	27,79	0,78	2,74
7,50%	21,714	4,136	16,00	27,37	1,20	4,21
10%	20,345	5,506	21,30	26,93	1,64	5,74

Deterioration	Thermal Efficiency (-)	Thermal Eff. Loss (-)	Variation (%)	SFC (kg/kWh)	SFC loss (kg/kWh)	Variation (%)
Clean	0,384	0	0	0,218	0	0,00
5%	0,363	0,021	5,47	0,231	0,014	6,31
7,50%	0,352	0,033	8,47	0,239	0,021	9,84
10%	0,340	0,045	11,59	0,247	0,030	13,63

In the same way as the ambient temperature effect, as degradation progresses the power loss increases deteriorating the engine's performance. Nevertheless, the speed reduction is negligible due to the propeller's curve law shape. (see section 4) As it can be appreciated a 10% degradation means a power loss of 21.30%, whereas for the same degradation the speed reduction is 5.74%, a bit less than 2 knots. Regarding the engine performance, thermal efficiency reducedes11.59% and the specific fuel consumption increases a 13.63%.

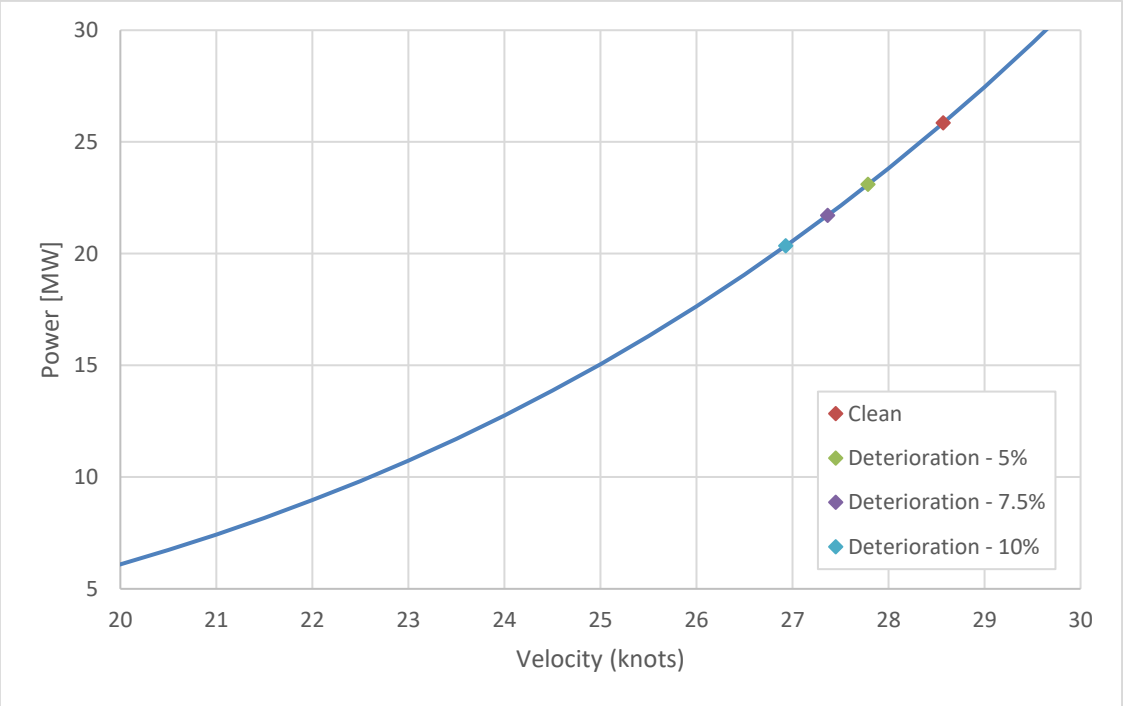

Figure 5-17. Maximum power supplied by the gas engine over propeller's law for different levels of degradation

Figure 5-17 shows graphically the maximum power and speed attainable, when the maximum TET is reached as a consequence of the engine's degradation. Although this power limitation barely modifies the vessel speed ranges for the second operational mode, the fuel consumption loss due to engine's degradation is significant and leads to the following idea:

Under engine degradation conditions, when the vessel is sailing at a speed close to the change mode speed, around 21 knots, it could be worthy to reduce vessel's speed in order to use the diesel engines, instead of the gas turbine, and save some fuel, considering that the diesel engines are not affected by the ambient temperature. Depending on the circumstances, the reduction in speed may not be a problem and from an economical point of view it seems interesting.

In order to give an idea of the possible fuel savings, in Table 5-8 it is presented the specific fuel consumption for the first operational mode, when the prime movers are the diesel engines, and for the second operational mode, when the prime mover is the gas engine. As it can be seen below the specific fuel consumption increases as degradation progresses for the gas engine mode.

Whereas the specific fuel consumption of the diesel engine remains constant since it has been neglected the diesel deterioration in order to simplify the analysis.

Table 5-8. Fuel savings due to the use of different operational modes as degradation progresses

	Diesel Engines	Gas Turbine	Speed Loss (%)
Speed (knots)	20	21	4.76
Deterioration	SFC (g/kWh)	SFC (g/kWh)	Fuel Savings (%)
Clean	218.87	293.87	34.27
5.0%	218.87	314.35	43.63
7.5%	218.87	324.97	48.48
10.0%	218.87	336.29	53.65

In spite of the speed loss due to the operating mode change, from the gas turbine utilization to the diesel engine, the fuel savings are sufficient remarkable, between 35% and 54% depending on the degradation level. Besides, the gas engine is not working at design point or close to it, which worsens its consumption.

5.4 Ambient temperature and engine degradation combined effect on the marine propulsion plant

With the purpose of completing the study of the temperature and degradation influence on the gas turbine operating mode, both effects have been simulated simultaneously. The assessment of the damage caused by these combined effects over the power plant operation can be carried out by means of the charts plotted in Figure 5-18 and Figure 5-19. Where the thermal efficiency and the specific fuel consumption have been represented as a function of the vessel's speed for different ambient temperatures and degradation levels. Every temperature has been plotted for different degradation levels and for visual understanding reasons, only three ambient temperatures and four degradation levels have been represented. The selected temperatures are -10°C, 15°C and

40°C, whereas the degradation levels are 0%, 5%, 7.5% and 10%. In addition, the power required for a particular speed has been plotted with a red line.

A great facet of these charts is the swiftness with which is possible to obtain valuable information, such as the fuel consumption, for a given vessel’s speed depending on the climatic and engine conditions.

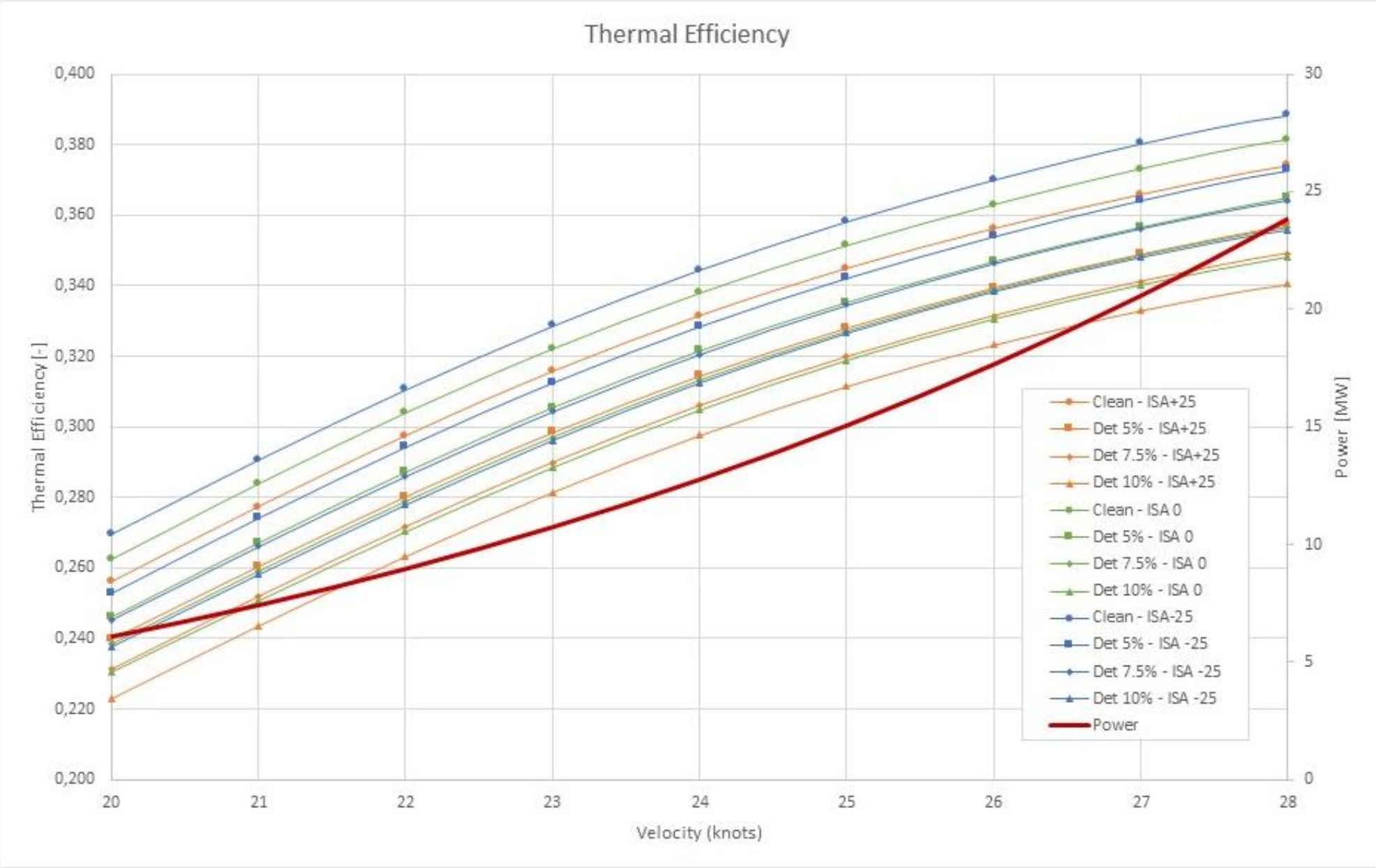

Figure 5-18. Thermal efficiency as a function of the ambient temperature and the engine's degradation for the whole gas turbine speed range

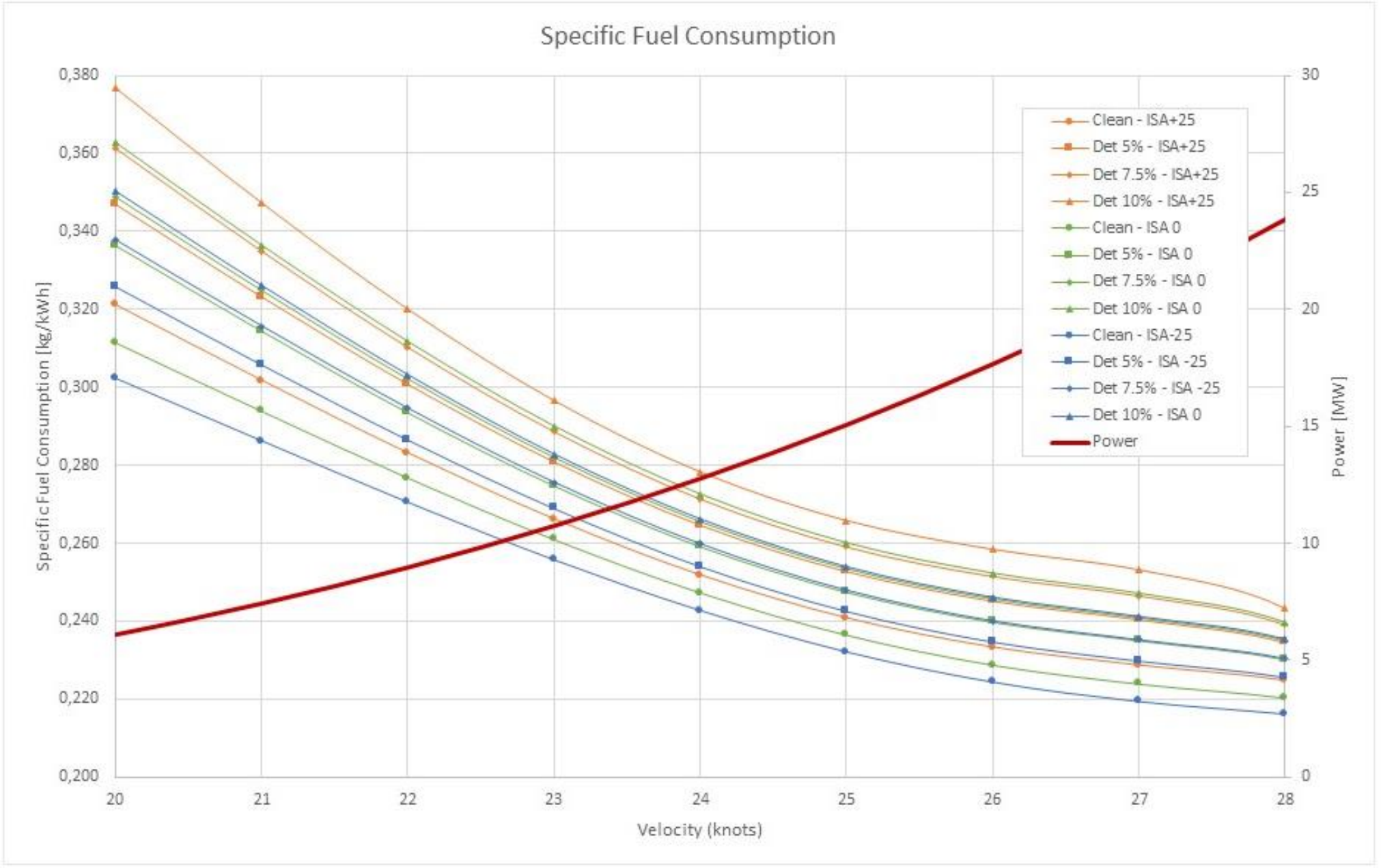

Figure 5-19. Specific fuel consumption as a function of the ambient temperature and the engine's degradation for the whole gas turbine speed range

5.5 Simulation of a vessel's operating profile

As an exhibition of the developed tool potential, a vessel operating profile is analysed. The tool calculates the fuel consumed by the CODAG configuration taking into account the ambient temperature influence, as well as, the degradation state of the gas turbine. The vessel's speed is used to calculate the required power than the prime movers must supply. Depending on the ambient temperature and the degradation state of the engine the fuel consumption will be modified according to the operational mode. For the example given below, zero degradation has been applied.

For the case studied the following hypothesis has been assumed:

- For each cycle the ambient temperature, the degradation level of the engine and the speed remain constant. Therefore, just steady states are considered.

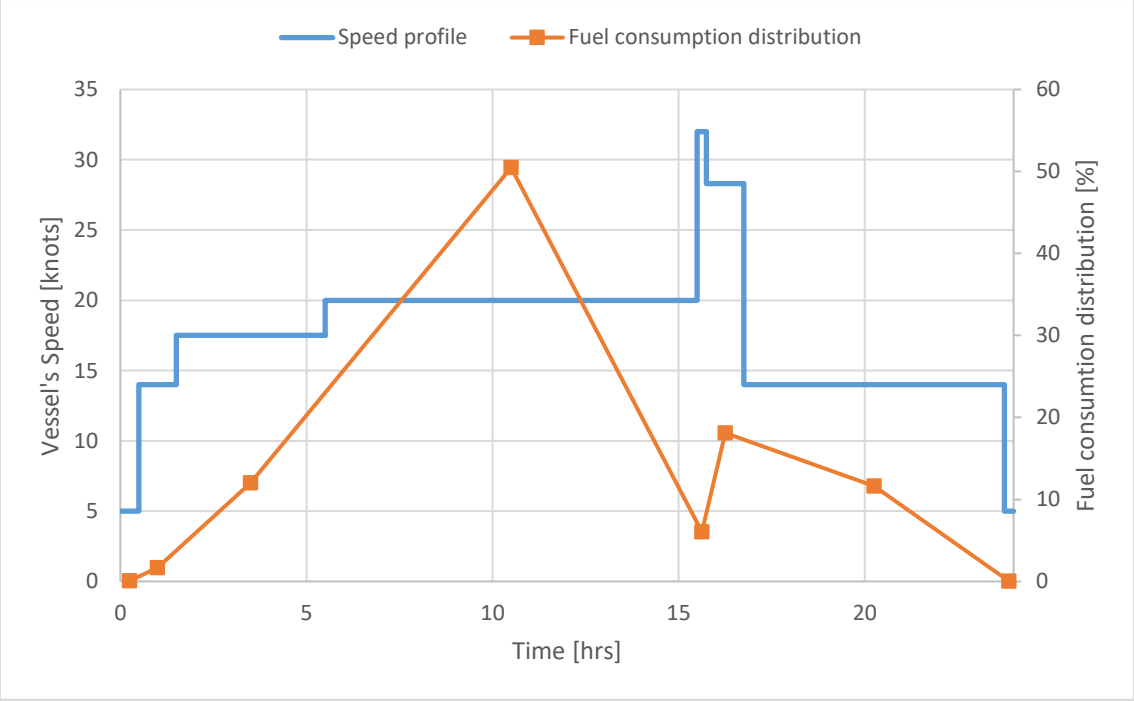

Figure 5-20. Typical warship operating profile and fuel consumption distribution

Table 5-9. Typical warship operating profile

Cycle	Temperature (K)	Duration (min)	Velocity (knots)	Distance (km)	Operating mode	Power (MW)	Fuel consumption (tons)
1	15	30	5,0	4,630	Diesel engines	0,120	0,022
2	15	60	14,0	25,928	Diesel engines	2,124	0,488
3	15	240	17,5	129,640	Diesel engines	4,343	3,533
4	15	600	20,0	370,400	Diesel engines	6,750	14,840
5	-10	15	32,0	14,816	CODAG	32,425	1,775
6	-10	60	28,3	52,412	Gas turbine	24,726	5,328
7	-10	420	14,0	181,496	Diesel engines	2,124	3,413
8	-10	15	5,0	2,315	Diesel engines	0,120	0,011

Table 5-9 show the characteristics of each cycle belonging to a typical warship operating profile. In addition, Figure 5-20 displays the fuel consumption of each cycle. As it can be seen, the tool is able to estimate the fuel necessary to complete a particular mission. For this particular case, the time weighted average of the fuel consumption is 8.03 tons, for a mean power mission of 5.62 MW at a mean speed of 17.59 knots.

6 CONCLUSIONS AND RECOMENDATIONS

The work executed throughout this thesis can be divided into two main parts, the development of a CODAG model and the assessment of the performance of a particular CODAG configuration using the built model.

The requirement of developing the tool emerges from the necessity of determining the power and the torque that the prime movers must supply to the shaft, in order to produce the demanded thrust and therefore, the speed that commands the operating profile of the vessel.

First of all, after selecting a specific ship suitable for a CODAG configuration, it has been calculated the resistance that the ship experiments when is moving at a certain velocity. The resistance module has been elaborated applying different methods used by naval architects. Once the resistance is known, a series of losses due to the propeller performance, the interaction between the hull and the propeller or the transmission of the power through the shaft and reduction gears must be taken into consideration. After obtaining the power and the rotational speed, at which the prime movers must operate in order to achieve the desired speed, a suitable engine must be chosen. Depending on the operating mode, which in turn depends on the vessel's speed, the selected prime mover will change.

The next objective was to match the selected engines and the propeller. Knowing that both type of engines rotate at higher rotational speeds than a propeller is capable, the use of reduction gears become essential. Since the ship designer has some freedom in selecting the gear reduction ratio, this propeller matching problem was solved by selecting a ratio that allowed the best rpm for both engine and propeller. For the gas turbine matching, some difficulties were found since the software used, Turbomatch, works with relative rotational speeds that depend on the temperature at the inlet of the free power turbine. Therefore, an iterative process was developed in order to obtain the fuel consumption for different rotational speeds when a specific power output is demanded. However, the rotational speed of the gas turbine cannot be directly related to the rotational speed of the shaft that drives the propeller, for the reason above mentioned.

Regarding the second part of the project, once the demanded power for a certain speed is known an assessment of the propulsion system performance has been carried out. The effects of ambient temperature on the gas turbine performance have been analysed. In addition to the degradation of the gas engine performance due to the deterioration caused by compressor fouling and turbine erosion. From both studies, it has been obtained a similar conclusion. Although, either the increase of ambient temperature or the increase of the degradation level, deteriorate the performance of the gas turbine operational mode, the

consequences over the speed are negligible. The reason for this, is the shape of the propeller's law curve as it has been explained in the results and discussion chapter. Nevertheless, when the turbine performs under such unfavourable conditions, there is a significantly increase in the specific fuel consumption and a great deterioration of the thermal efficiency, as expected. One possible solution, when the gas engine is working under these conditions, is to change the operational mode from the gas turbine to the diesel engines mode. Although lower speeds are reached the fuel savings compensate this loss.

Finally, a demonstration of the developed tool has been performed in order to show its potential to optimise the performance of vessels with a CODAG propulsion system. Depending on the vessel requirements, the optimization could be among a wide range of possibilities. Also, different CODAG configurations, such as adding another gas turbine, or removing one diesel engines can be analysed.

6.1 Recommendations

One of the difficulties of developing a tool from scratch, is to fix some limits in order to establish a solid base. Later on, it can be enhanced, by improving the precision of the models or by adding another feature that makes the tool more faithful to reality. Below a list of recommendations is left for future work.

- Development of a diesel engine model, instead of using an engine's performance chart, so as to adapt the tool for different types of diesel engines and to accelerate the results processing.
- Study of the gearbox loss and development of a better model in order to refine the level of accuracy of the results.
- Integration of a controllable pitch propeller model, so as to widen the propulsion system possibilities that the tool is capable to analyse.
- In the degradation study, regarding the compressor fouling it could be add the possibility of incorporating periodic recoverable actions, such as compressor online washing, in order to estimate the real degradation that a marine gas turbine engine experiences.
- Although the most influential degradation mechanisms for marine gas turbine have been taken into consideration, adding other types of degradation it would increase the reliability of the results.
- Study of the deterioration factors that influence on the diesel engine performance, so as to incorporate them and obtain more realistic results.
- Take advantage of the built tool that exhibits a great potential to optimise the performance of vessels with a CODAG propulsion system. Depending on the vessel requirements, the optimization could be among a wide range of possibilities. Also, different CODAG configurations, such as adding another gas turbine, or removing one diesel engines can be analysed, as well as other kind of combined propulsion systems.

REFERENCES

[1] H. F. Ohmayer, «Propulsion System Choices for modern Naval Vessels,» de *Application Center Governmental Naval*, Washington, November 8, 2012.

[2] P. B., F. Hoppe y M. Heger, «Combined Marine Propulsion Systems: Optimization and Validation by Simulation,» *AGMA Technical Paper,* October 2012.

[3] D. Woodyard, Pounder's Marine Diesel Engines and Gas Turbines, Elsevier, Ninth edition 2009.

[4] GE Aviation, «GE Aviation Marine Engines,» 2017. [Online]. Available: https://www.geaviation.com/marine/engines/military/lm500-engine. [Last access: 2017 June 21].

[5] MAN Diesel & Turbo, «32/40 Four-stroke diesel engine,» 2017. [On line]. Available: http://marine.man.eu/four-stroke/engines/32-40. [Last access: 21 June 2017].

[6] Rolls Royce, «MT 30 Marine Gas Turbine Engine,» 2017. [Online]. Available: https://www.rolls-royce.com/products-and-services/marine/product-finder/gas-turbines-and-gensets/gas-turbines/mt30-marine-gas-turbine.aspx#section-product-search. [Last access: 2017 June 21].

[7] WÄRTSILÄ, «WÄRTSILÄ 46F,» 2017. [Online]. Available: https://www.wartsila.com/products/marine-oil-gas/engines-generating-sets/diesel-engines/wartsila-46f. [Last access: 2017 June 21].

[8] C. Meher-Homji, Chaker, M. y Motiwala, H., «Gas Turbine Performance Deterioration,» de *Proceedings of the 30th Turbomachinery Symposium. , (pp. 139-176)*, Texas A & M University, Texas, 2001.

[9] R. Kurz y K. Brun, «Degradation in Gas Turbine Systems,» de *Journal of Engineering for Gas Turbines and Power, Vol. 123*, January 2001.

[10] G. H. Badeer, «GE Aeroderivative Gas Turbines - Design and Operating Features,» GE Power Systems, GER-3695E.

[11] GE Aviation, «LM2500 Marine Gas Turbine,» Data sheet , 2017.

[12] J. Babicz, WÄRTSILA Encyclopedia of Ship Technology, WÄRTSILA Coorporation, 2015.

[13] E. V. Lewis, Principles of Naval Architecture, Jersey City: The Society of Naval Architects and Marine Engineers, First edition 1988.

[14] «Type 45 Daring Class Destroyer - Naval Technology,» 28 February 2017. [Online]. Available: http://www.naval-technology.com/projects/horizon/. [Last access: 15 March 2017].

[15] M. D. &. Turbo, «Basic Principles of Ship Propulsion,» 2011.

[16] K. U. Hollenbach, «Estimating Resistance and Propulsion for Single-Screw and Twin-Screw Ships,» Ship Technology Research Vol.45, 1998.

[17] «Performance, Propulsion 1978 ITTC Performance Prediction Method,» de *International Towing Tank Conference*, Prediction, Special Committee for Powering Performance, 2008.

[18] J. H. a. G. Mennen, «An Approximate Power Prediction Method,» de *International Shipbuilding Progress, Volume 31, Number 363*, October 1978.

[19] E. Zini, «Resistenza al moto,» Universita degli Studi di Genova Scoula Politecnica, 2014-2015.

[20] J. Holtrop, «A Statistical Re-analysis of Resistance and Propulsion,» de *International Shipbuilding Progress, Vol.31, Part 363, pp 272-276*, July 1984.

[21] E. Tsoudis, «Technoeconomic Environmental and Risk Analysis of Marine Gas Turbine Power Plants,» PhD Thesis, School of Engineering, July 2008.

[22] S. T. D. H. A.F.Molland, Ship Resistance and Propulsion: Practical Estimation of Ship Propulsive Power, Cambridge University Press, 2011.

[23] M. Oosterveld y P. Oossanen, «Further Computer Analysed Data of the Wageningen B-Screw Series,» de *International Ship Building Progress, Vol. 22, Part 251, pp 251-262,*, July 1975.

[24] H. W. Kohler, «Diesel and gas turbines - a techno-economical comparison,» de *HSB International*, September 1999.

[25] M. A. A. F. H. K. Majid Rezazadeh Reyhani, «Turbine Blade Temperature Calculation and Life Estimation - a Sensitivity Analysis,» Propulsion and Power Research, University of Tehran, Iran, 2013.

[26] A. Zwebek y P.Pilidis, «Degradation Effects on Combined Cycle Power Plant Performance. Part I: Gas Turbine Cycle Component Degradation Effects,» *Department of Power Engineering and Propulsion, School of Engineering,* vol. Cranfield University.

[27] S. Koussis, «Propulsion System for a Cruise Liner - a CODAG System,» M.Sc Thesis, School of Engineering Department of Power Engineering and Propulsion, August 2001.

APPENDICES

Appendix A

A.1 Resistance coefficients

	'mean'			'minimum'	
	single-screw		twin-screw	single-screw	twin-screw
	design draft	ballast draft		design draft	
$a1$	-0.3382	-0.7139	-0.2748	-0.3382	-0.2748
$a2$	0.8086	0.2558	0.5747	0.8086	0.5747
$a3$	-6.0258	-1.1606	-6.7610	-6.0258	-6.7610
$a4$	-3.5632	0.4534	-4.3834	-3.5632	-4.3834
$a5$	9.4405	11.222	8.8158	0	0
$a6$	0.0146	0.4524	-0.1418	0	0
$a7$	0	0	-0.1258	0	0
$a8$	0	0	0.0481	0	0
$a9$	0	0	0.1699	0	0
$a10$	0	0	0.0728	0	0
b_{11}	-0.57424	-1.50162	-5.34750	-0.91424	3.27279
b_{12}	13.3893	12.9678	55.6532	13.3893	-44.1138
b_{13}	90.5960	-36.7985	-114.905	90.5960	171.692
b_{21}	4.6614	5.55536	19.2714	4.6614	-11.5012
b_{22}	-39.721	-45.8815	-192.388	-39.721	166.559
b_{23}	-351.483	121.820	388.333	-351.483	-644.456
b_{31}	-1.14215	-4.33571	-14.3571	-1.14215	12.4626
b_{32}	-12.3296	36.0782	142.738	-12.3296	-179.505
b_{33}	459.254	-85.3741	-254.762	459.254	680.921
c_1	$F_n/F_{n,\text{krit}}$	$10C_B(F_n/F_{n,\text{krit}}-1)$	$F_n/F_{n,\text{krit}}$	0	0
d_1	0.854	0.032	0.897	0	0
d_2	-1.228	0.803	-1.457	0	0
d_3	0.497	-0.739	0.767	0	0
e_1	2.1701	1.9994	1.8319	0	0
e_2	-0.1602	-0.1446	-0.1237	0	0
f_1	0.17	0.15	0.16	0.17	0.14
f_2	0.20	0.10	0.24	0.20	0
f_3	0.60	0.50	0.60	0.60	0
g_1	0.642	0.42	0.50	0.614	0.952
g_2	-0.635	-0.20	0.66	-0.717	-1.406
g_3	0.150	0	0.50	0.261	0.643
h_1	1.204	1.194	1.206		
ship length L [m]	42.0...205.0	50.2...224.8	30.6...206.8	42.0...205.0	30.6...206.8
$L/\nabla^{1/3}$	4.49...6.01	5.45...7.05	4.41...7.27	4.49...6.01	4.41...7.27
C_B	0.60...0.83	0.56...0.79	0.51...0.78	0.60...0.83	0.51...0.78
L/B	4.71...7.11	4.95...6.62	3.96...7.13	4.71...7.11	3.96...7.13
B/T	1.99...4.00	2.97...6.12	2.31...6.11	1.99...4.00	2.31...6.11
L_{os}/L_{wl}	1.00...1.05	1.00...1.05	1.00...1.05	1.00...1.05	1.00...1.05
L_{wl}/L	1.00...1.06	0.95...1.00	1.00...1.07	1.00...1.06	1.00...1.07
D_P/T	0.43...0.84	0.66...1.05	0.50...0.86	0.43...0.84	0.50...0.86

A-1. Resistance coefficients [16]

A.2 Wageningen B-series polynomials

C_T	s	t	u	v	C_Q	s	t	u	v
0.0088	0	0	0	0	0.00379	0	0	0	0
-0.2046	1	0	0	0	0.00887	2	0	0	0
0.16635	0	1	0	0	-0.0322	1	1	0	0
0.15811	0	2	0	0	0.00345	0	2	0	0
-0.1476	2	0	1	0	-0.0409	0	1	1	0
-0.4815	1	1	1	0	-0.108	1	1	1	0
0.41544	0	2	1	0	-0.0885	2	1	1	0
0.0144	0	0	0	1	0.18856	0	2	1	0
-0.053	2	0	0	1	-0.0037	1	0	0	1
0.01435	0	1	0	1	0.00514	0	1	0	1
0.06068	1	1	0	1	0.02094	1	1	0	1
-0.0126	0	0	1	1	0.00474	2	1	0	1
0.01097	1	0	1	1	-0.0072	2	0	1	1
-0.1337	0	3	0	0	0.00438	1	1	1	1
0.00638	0	6	0	0	-0.0269	0	2	1	1
-0.0013	2	6	0	0	0.05581	3	0	1	0
0.1685	3	0	1	0	0.01619	0	3	1	0
-0.0507	0	0	2	0	0.00318	1	3	1	0
0.08546	2	0	2	0	0.0159	0	0	2	0
-0.0504	3	0	2	0	0.04717	1	0	2	0
0.01047	1	6	2	0	0.01963	3	0	2	0
-0.0065	2	6	2	0	-0.0503	0	1	2	0
-0.0084	0	3	0	1	-0.0301	3	1	2	0
0.01684	1	3	0	1	0.04171	2	2	2	0
-0.001	3	3	0	1	-0.0398	0	3	2	0
-0.0318	0	3	1	1	-0.0035	0	6	2	0
0.0186	1	0	2	1	-0.0107	3	0	0	1
-0.0041	0	2	2	1	0.00111	3	3	0	1
-0.0006	0	0	0	2	-0.0003	0	6	0	1
-0.005	1	0	0	2	0.0036	3	0	1	1
0.0026	2	0	0	2	-0.0014	0	6	1	1
-0.0006	3	0	0	2	-0.0038	1	0	2	1
-0.0016	1	2	0	2	0.01268	0	2	2	1
-0.0003	1	6	0	2	-0.0032	2	3	2	1
0.00012	2	6	0	2	0.00334	0	6	2	1
0.00069	0	0	1	2	-0.0018	1	1	0	2
0.00422	0	3	1	2	0.00011	3	2	0	2
5.7E-05	3	6	1	2	-3E-05	3	6	0	2
-0.0015	0	3	2	2	0.00027	1	0	1	2
					0.00083	2	0	1	2
					0.00155	0	2	1	2
					0.0003	0	6	1	2
					-0.0002	0	0	2	2
					-0.0004	0	3	2	2
					8.7E-05	3	3	2	2
					-0.0005	0	6	2	2
					5.5E-05	1	6	2	2

A-2. Wageningen B-series polynomials [23]

Appendix B

B.1 Turbomatch Input file – design point

```
Single spool turboprop with power turbine
_____________________________________________________
////
OD SI KE VA FP
-1
-1
INTAKE  S1,2       D1-6            R200
COMPRE  S2,3       D7-18           R205     V7    V8
PREMAS  S3,10,4    D19-22
BURNER  S4,5       D23-30          R215
MIXEES  S5,10,6
TURBIN  S6,7       D31-45                   V32
TURBIN  S7,8       D46-60                   V47   V50
NOZCON  S8,9,1     D61,62          R220
PERFOR  S1,0,0     D46,64-66,220,200,215
CODEND

DATA ITEMS ////
1 0.             ! INTAKE: Altitude [m]
2 0.               ! Deviation from ISA temperature [K]
3 0.0              ! Mach number
4 0.9951           ! Pressure recovery, according to USAF
5 0.               ! Deviation from ISA pressure [atm]
6 0.               ! Relative humidity [%]

7 0.85           ! COMPRESSOR - FAN: Z = (R-R[choke])/(R[surge]-R[choke]) (if =-1. the default value 0.85 is invoked)
8 1.               ! Relative rotational speed PCN
9 18.              ! DP Pressure ratio
10 0.90            ! isentropic efficiency
11 0.              ! Error selection
12 5.              ! Compressor Map Number
13 1.              ! Shaft number
14 1.              ! Scaling factor of Pressure Ratio - Degradation factor
15 1.              ! Scaling factor of Non-D Mass Flow - Degradation factor
16 1.              ! Scaling factor of ETAc is (Compressor isentropic efficiency) - Degradation factor
17 0.03            ! Effective component volume [m^3]
18 0.              ! Stator angle (VSV) relative to DP

19 0.1           ! PREMAS: LAMDA W Cooling bypass (Wout/Win)
20 0.              ! DELTA W
21 1.              ! LAMBDA P
22 0.              ! DELTA P

23 0.065         ! COMBUSTOR: Pressure loss (=Total pressure loss/Inlet total pressure)
24 0.998           ! Combustion efficiency
25 -1              ! Fuel flow (If -1. is given the TET must be determined in the station vector
26 0.              ! (>0) Water flow [kg s-1 or lb s-1] or (<0) Water to air ratio
27 288.            ! Temperature of water stream [K]
28 0.              ! Phase of water (0=liquid, 1=vapour)
29 1.              ! Scaling factor of ETAb (combustion efficiency) - Degradation factor
30 0.05            ! Effective component volume [m^3]

31 0.            ! COMPRESSOR TURBINE: Auxiliary or power output [W]
32 -1              ! Relative non-dimensional massflow W/Wmax (if = -1, value 0.8 is invoked)
33 -1              ! Relative non-rimensional speed CN (if = -1, value 0.6 is invoked)
34 0.87            ! Design isentropic efficiency
35 -1.             ! Relative non-dimensional speed PCN (= -1 for compressor turbine)
36 1.              ! Shaft Number (for power turbine, the value "0." is used)
37 5.              ! Turbine map umber
38 -1.             ! Power law index "n" (POWER = PCN^n) If = -1, power is assumed to be a constant
39 1.              ! Scaling factor of TF (non-D inlet mass flow) - Degradation factor
40 1.              ! Scaling factor of DH (enthalpy change) - Degradation factor
41 1.              ! Scaling factor of ETAc is (Turbine isentropic efficiency) - Degradation factor
42 200.            ! Rotor rotational speed [RPS]
43 15.             ! Rotor moment of inertia [kg.m^2]
44 0.05            ! Effective component volume [m^3]
45 0.              ! NGV angle, relative to D.P.
```

```
31 0.            ! COMPRESSOR TURBINE: Auxiliary or power output [W]
32 -1              ! Relative non-dimensional massflow W/Wmax (if = -1, value 0.8 is invoked)
33 -1              ! Relative non-rimensional speed CN (if = -1, value 0.6 is invoked)
34 0.87            ! Design isentropic efficiency
35 -1.             ! Relative non-dimensional speed PCN (= -1 for compressor turbine)
36 1.              ! Shaft Number (for power turbine, the value "0." is used)
37 5.              ! Turbine map umber
38 -1.             ! Power law index "n" (POWER = PCN^n) If = -1, power is assumed to be a constant
39 1.              ! Scaling factor of TF (non-D inlet mass flow) - Degradation factor
40 1.              ! Scaling factor of DH (enthalpy change) - Degradation factor
41 1.              ! Scaling factor of ETAc is (Turbine isentropic efficiency) - Degradation factor
42 200.            ! Rotor rotational speed [RPS]
43 15.             ! Rotor moment of inertia [kg.m^2]
44 0.05            ! Effective component volume [m^3]
45 0.              ! NGV angle, relative to D.P.

46 -1.05             ! POWER TURBINE: Auxiliary or power output [W]
47 0.89            ! Relative non-dimensional massflow W/Wmax (if = -1, value 0.8 is invoked)
48 0.68            ! Relative non-rimensional speed CN (if = -1, value 0.6 is invoked)
49 0.89            ! Design isentropic efficiency
50 1.              ! Relative non-dimensional speed PCN (= -1 for compressor turbine)
51 0.              ! Shaft Number (for power turbine, the value "0." is used)
52 5.              ! Turbine map umber
53 1000            ! Power law index "n" (POWER = PCN^n) If = -1, power is assumed to be a constant
54 1.              ! Scaling factor of TF (non-D inlet mass flow) - Degradation factor
55 1.              ! Scaling factor of DH (enthalpy change) - Degradation factor
56 1.              ! Scaling factor of ETAc is (Turbine isentropic efficiency) - Degradation factor
57 200.            ! Rotor rotational speed [RPS]
58 20.             ! Rotor moment of inertia [kg.m^2]
59 0.15            ! Effective component volume [m^3]
60 0.              ! NGV angle, relative to D.P.

61 -1.           ! CONVERGENT NOZZLE: Swich set (= "1" if exit area "floats"
                   !                             = "-1" if exit area is fixed)
62 1.              ! Scaling factor

64 22000000.00     ! ENGINE RESULTS: Propeller efficiency (= -1 for turbojet/turbofan)
65 0.              ! Scaling index ("1" = scalling needed, "0" = no scaling)
66 0.              ! Required DP net thrust(Turbojet,turbofan) or shaft power (Turboprop.turboshaft)
                   ! = 0 if Scaling index = 0


-1
1 2 70.86           ! item 2 at station 1 = Mass flow(kg/s)
5 6 1509.5
-1
25 1.6
-1
-1
25 1.4
-1
-1
25 1.2
-1
-1
25 1.0
-1
-1
25 0.8
-1
-1
25 0.6
-1
-1
25 0.4
-1
-1
-3
```